IN SILICO ANALYSIS OF ZEBRAFISH LEPTIN-A KNOCKDOWN GENE EXPRESSION DATA REVEALS ENRICHMENT FOR METABOLIC AND DEVELOPMENTAL PATHWAYS INCLUDING MORPHOLINO ARTIFACTS

A Thesis

Presented to

The Graduate Faculty of The University of Akron

In Partial Fulfillment

of the Requirements for the Degree

Master of Science

Matthew Tuttle

May, 2017

IN SILICO ANALYSIS OF ZEBRAFISH LEPTIN-A KNOCKDOWN GENE EXPRESSION DATA REVEALS ENRICHMENT FOR METABOLIC AND DEVELOPMENTAL PATHWAYS INCLUDING MORPHOLINO ARTIFACTS

Matthew Tuttle

Thesis

Approved:

_____
Faculty Advisor
Dr. Richard Londraville

_____
Faculty Reader
Dr. Qin Liu

_____
Faculty Reader
Dr. Joel Duff

_____
Department Chair
Dr. Stephen Weeks

Accepted:

_____
Dean of the College
Dr. John Green

_____
Dean of the Graduate School
Dr. Chand Midha

_____
Date

ABSTRACT

Mammalian leptin (*LEP*) is a pleiotropic peptide hormone best characterized for its roles related to obesity and diabetes. However, the molecular function of the leptin signal transduction pathway in non-mammals is less clear. Comparative studies that address leptin signaling in non-model organisms are integral components of the leptin phylogenetic history, and there is little evidence addressing the functional disparities between the teleost leptin paralogues and mammalian leptins. To demarcate genes and biochemical pathways regulated by leptin signaling in developing zebrafish, microarray gene expression data were generated with total RNA isolated at 48 hours post fertilization from leptin-a morpholino oligonucleotide "knockdown", recombinant leptin-a "rescue", and wild type embryos. Expression estimates were computed for 26,046 genes across 16 microarray samples. Differentially expressed genes (DEG), (KEGG) pathways, and Gene Ontologies (GO) were evaluated for three contrasts (Morphant:Control, Rescue:Morphant, Rescue:Control).

Signaling pathways that respond to leptin-a knockdown and rescue are analogous to gene targets of the mammalian *LEP* system ("GnRH", "MAPK", "Adipocytokine", "Phosphatidylinositol", "mTOR", "ErbB", "FoxO", and "Notch"). A subset of differentially expressed transcription factors in leptin-a morphants are homologous to putative regulators of *LEP* expression in mammals (*cebpb*, *creb5*, *fosl1a,*

mybl1, pax5, pou3f1, pparg, stat1a). "Neuroactive ligand-receptor interaction" as well as cAMP-responsive hormone signaling pathways responded to leptin-a. Consistent with leptin-a as an endocrine regulator, agouti-related peptide-2 (*agrp2*), cocaine-and-amphetamine-related-transcript (*LOC557301*), gonadotropin-releasing hormone 2 (*gnrh2*), and melanocortin receptor 5a (*mc5ra*) were dysregulated in rescue embryos. Further, "Notch signaling" and "Spinal cord/CNS development" were enriched in morphants whereas rescue arrays were comparable to wild type expression. Together with upregulated odorant receptors and "G-protein signaling" in rescue embryos, these data signify that embryonic leptin-a serves a pleiotropic role in zebrafish sensory system development and neurogenesis, endocrine physiology, and lipid signaling. "p53 signaling", "Ribosome biogenesis", and "mRNA surveillance pathway" were over-represented in leptin-a morphants including components of the RNA-induced-silencing-complex (protein argonaute-1-like (*LOC570775*)) which is consistent with activation of RNA interference pathways. Collations between the leptin-a knockdown dataset and un-related morpholino expression data suggest that "p53 signaling" and "Phototransduction" are ubiquitous responses to morpholino knockdown. However, additional molecular and biochemical analyses are needed to validate these assertions.

ACKNOWLEDGEMENTS

1. The Choose Ohio First for Bioinformatics Scholarship provided by the Ohio Board of Reagents.
2. The experiments described in this thesis were supported by NIH 2R15DK079282-02 to Richard Londraville and Qin Liu.

TABLE OF CONTENTS

LIST OF TABLES

Table

LIST OF FIGURES

Figure

CHAPTER I

THE LEPTIN SIGNAL TRANSDUCTION PATHWAY

INTRODUCTION

Immunoblotting bony fish blood, brain, heart, and liver tissue homogenates with a polyclonal antibody against mouse leptin served as preliminary evidence describing leptin expression in fishes [Johnson et al., 2000]. The first fish leptin, *Takifugu rubripes*, was characterized in 2005 after the mouse *ob* locus was cloned [Zhang et al., 1994; Kurokawa et al., 2005]. Comparative leptin studies give insight into human leptin function which plays a significant role in obesity and diabetes [Zhang et al., 1994], sexual development [Elias and Purohit 2013], immune response [Lord et al., 1998], bone growth [Zhou et al., 2014], and pregnancy [Tessier et al., 2013]. In addition to mammals [Zhang et al., 1994] and fishes [Johnson et al., 2000; Kurokawa et al., 2005], leptin orthologues have also been characterized in amphibians [Crespi and Denver 2006], birds [Prokop et al., 2014], as well as reptiles [Paolucci et al., 2001]. Each taxon displays variable degrees of leptin expression and tissue distribution [Copeland et al., 2011; Prokop et al., 2012].

Zebrafish are a popular research model. They have a well-annotated genome, transparent and external embryogenesis, rapid maturation, high fecundity, curated mutant and transgenic lines, small body size, and low maintenance costs [Bradford et al., 2011]. Zebrafish are model organisms for a growing number of human diseases including Alzheimer's as well as metabolic disorders [reviewed: Newman et al., 2011; Seth et al., 2013]. Both the human and zebrafish genomes share a syntenic relationship, and an estimated 70% of human genes have a zebrafish orthologue [Barbazuk et al., 2000; Howe et al., 2013]. Mammalian leptins have been best characterized for their association with morbid obesity and diabetes but how the pleiotropic features of the leptin signal transduction pathway are represented in comparative systems is an area of active research.

MAMMALIAN LEPTIN

Human leptin, a 16 kD pleiotropic peptide hormone, functions as an anorectic adipose-derived signaling molecule that binds to leptin receptor, abundantly expressed in the hypothalamus, where signal transduction alters gene expression in the neuroendocrine system, hypothalamic-pituitary-adrenal, and hypothalamic-pituitary-ovarian axes [Ghilardi et al., 1996; reviewed: Cervero et al., 2006; Malendowicz et al., 2007]. Mammalian leptin is secreted primarily from adipocytes in proportion to white adipose tissue (WAT) mass; this confers lipid availability among peripheral tissues to the central nervous system [Campfield et al., 1995]. Leptin receptor is expressed in many human tissues including: brain, heart, placenta, lung, kidney, thymus, muscle, spleen,

pancreas, prostate, testes, ovaries, colon, and adipose [Kielar et al., 1998]. In mouse and human, secreted leptin is bound to serum proteins, and obese individuals exhibit elevated circulating free (unbound)-leptin [Houseknecht et al., 1996; Lahlou et al., 2000]. Neuron-specific silencing of murine leptin receptor long isoform (*Ob-Rb*) results in a negative correlation between receptor expression and obesity. There is no correlation between the incidence of obesity and hepatic *Ob-Rb* disruption which indicates different roles for the leptin signal transduction pathway between peripheral tissues and the CNS [Cohen et al., 2001].

The 2.4 Å crystal structure of recombinant human E100W leptin is a 167 residue four-helix bundle stabilized by a single disulfide bridge (Cys^{96} – Cys^{146}); its structure is homologous to class-I long chain helical cytokines. The asymmetric unit forms a hexagonal space group that packs as a monomer in solution [PDB: 1AX8; Zhang et al., 1997]. Examples of class-I long chain helical cytokines are: leukemia inhibitory factor (*LIF*), oncostatin-M (*OSM*), ciliary neurotrophic factor (CNF), interleukin-6 (*IL-6*), interleukin-11 (*IL-11*), and cardiotrophin-1 (CT-1) [Huising et al., 2006]. Class-I long chain cytokine folds are stabilized by a series of hydrophobic interactions and intramolecular hydrogen bonds between main chain atoms surrounding the core. Family members generally share a single disulfide bond linking the C-termini of helices C+D, although some members lack this feature as is the case of IL-6 [Rozwarski et al., 1996]. Despite robust differences in primary sequence among family members, class-I long chain helical cytokines share a structural orientation: an "(A) up, (B) up, (C) down, (D) down" antiparallel four-helix bundle. Long chain members are distinguishable from

their short chain cytokine counterparts by length (x > 150 residues) and, in many cases, an additional 5th short helix in a connecting loop of adjacently packed helices of the bundle [reviewed: Boulay et al., 2003 and Huising et al., 2006].

LEPTIN IN DISEASE

Clinical approaches to restore leptin sensitivity may have therapeutic value. Dysregulation of the leptin signal transduction pathway is extensively linked to early-onset and morbid obesity [Zhang et al., 1994; Tartaglia et al., 1995; Chen et al., 1996; Lee et al., 1996], breast and gastric cancers [Ishikawa et al., 2004 and 2006], impaired sexual development and pregnancy [Farooqi et al., 2007; Malendowicz et al., 2007], as well as immune disease [for review see La Cava et al., 2004; DeRosa et al., 2007]. Leptin ($ob^{-/-}$) and leptin receptor ($db^{-/-}$) mice are disease models for morbid obesity and type II diabetes, respectively [Coleman 1973 and 1978; reviewed: Wang et al., 2014]. $ob^{-/-}$ and $db^{-/-}$ genotypes drive expression of truncated leptin or leptin receptor gene products [Chen et al., 1996; Lee et al., 1996]. Homozygous autosomal recessive nonsense and missense mutations in human leptin or leptin receptor are rare inborn errors of metabolism which exhibit familial patterns of inheritance, however, at least one case of a leptin receptor compound heterozygote ($lepr^{+/-, -/+}$) has been reported [Montague et al., 1997; Clément et al., 1998; Strobel et al., 1998; Farooqi et al., 1999 and 2002 and 2007]. These individuals are normal birthweight but suffer from early-onset and morbid obesity, hypogonadotropic hypogonadism, hyperphagia, compromised immune response, as well as endocrine, pituitary, and thyroid dysfunction [Swerdloff et al., 1976;

Zhang et al., 1994; Tartaglia et al., 1995; Chua et al., 1996; Lord et al., 1998; Rau et al., 1999; Gibson 2004].

In wild type mammals, serum leptin is generally correlated with adipose mass and obese individuals exhibit higher levels of circulating leptin [Halaas et al., 1995; Maffei et al., 1995; Considine et al., 1996]. Heterozygous $ob^{+/-}$ and $db^{+/-}$ rats exhibit substantially higher body fat percentage than wild type littermates. $ob^{+/-}$ rat genotypes have reduced serum leptin concentrations in contrast to $db^{+/-}$ rats which display elevated leptin titers relative to wild type littermates [Chung et al., 1998]. Directed point mutations of granulocyte-macrophage colony stimulating factor (*GMCSF*), another class-I cytokine, reduced granulocyte-macrophage colony stimulating factor receptor (*GMCSFR*) signaling (as measured by cell proliferation assay) by inhibiting ligand-receptor conjugation [Rozwarski et al., 1996]. These findings indicate that genetic variation in Class-I cytokines, or Class-I cytokine receptors, are risk factors for disease.

The molecular basis for the $ob^{-/-}$ and $db^{-/-}$ disease states differ; both genotypes suffer from symptoms including early-onset obesity, hyperphagia, and disrupted beta cell physiology [Coleman 1978]. $ob^{-/-}$ rodents exhibit null serum leptin, beta cell hypertrophy, increased insulin secretion, and hyperglycemia. Hallmarks of $db^{-/-}$ genotypes are: chronic elevation of serum leptin, beta cell atrophy, hypoinsulinemia, severe hyperglycemia, and reduced lifespan. Beta cell physiology can be normalized in $ob^{-/-}$, but not $db^{-/-}$ genotypes [Coleman 1973 and 1978]. Intraperitoneal leptin injection promotes weight loss as well as reduced food intake in wild type mice. $ob^{-/-}$ mice lost

30% of their body weight while *db*$^{-/-}$ elicited no response to clinical leptin intervention [Halaas et al., 1995]. Leptin therapy in human *lep*$^{-/-}$, but not *lepr*$^{-/-}$, congenital deficiency mirrors the normalizing effects of exogenous leptin in the *ob*$^{-/-}$ mouse [Campfield et al., 1995; Pelleymounter et al., 1995; Heymsfield et al., 1999; Farooqi et al., 1999 and 2002; Gibson et al., 2004; Licinio et al., 2004]. As a consequence, functional annotations for leptin and leptin receptor are primarily derived from *ob*$^{-/-}$ and *db*$^{-/-}$ rodents as well as human case studies [Montague et al., 1997; Strobel et al., 1998; Farooqi et al., 2007]. Positional cloning of the *ob* and *db* loci intensified biomedical research related to the inherent genetics of human metabolism, and there is broad interest in characterizing the biochemical, structural, and molecular components of the leptin signal transduction pathway [Zhang et al., 1994; Tartaglia et al., 1995].

Leptin resistance, a form of non-congenital human obesity, is generally characterized by four biomarkers including: hyperleptinemia, defective autophagy, inflammation, and ER stress. These factors lead to impairment of leptin transport, leptin receptor signaling, and intracellular leptin receptor trafficking to/from the plasma membrane, endosome, and golgi. Decreased localization of leptin receptor at the plasma membrane is also thought to be a marked contributor of leptin resistance [reviewed: Zhou and Rui 2013]; leptin-receptor-overlapping-transcript (*LEPROT*), or endospanin, may be important to the localization of leptin receptor at the plasma membrane. Importantly, immunostaining of P-STAT3 in the arcuate nucleus is reduced in mouse diet-induced obesity indicating that leptin resistance may be attributed to decreased sensitivity to the hormone in the CNS [Munzberg et al., 2004].

LEPTIN RECEPTOR

Leptin receptor is homologous to the class-I cytokine receptor family which includes the glycoprotein 130 (*gp130*) receptor subunit of the IL-6 receptor, granulocyte macrophage colony stimulating factor receptor (*GMCSFR*), and leukemia inhibitory factor receptor (*LIFR*) [Bazan 1990; Tartaglia et al., 1995]. These members are single-transmembrane-spanning receptors that lack intrinsic kinase activity. Class-I cytokines act on tissue-specific class-I cytokine receptors which regulate gene transcription through potentiation of JAK/STAT intracellular signaling cascades [Darnell et al., 1994; Vaisse et al., 1996; reviewed: Tartaglia 1997]. Structural data of the leptin receptor is derived from a 1.95 Å crystallographic model of recombinant human leptin receptor ectodomain in complex with a leptin-displacing antibody [PDB: 3V6O; Carpenter et. al, 2012]. However, this does not unanimously represent the physiologically competent ligand-bound signaling complex as high resolution structural elucidation of full-length leptin and receptor conjugation remains elusive.

At least six protein coding isoforms of human and murine leptin receptor have been characterized. All isoforms vary in cytoplasmic domain length and tissue distribution while each shares the first N-terminal 805 residues [Chen et al., 1996; Lee et al., 1996]. The mammalian leptin receptor long isoform (*Ob-Rb*) primarily acts through the JAK2/STAT3 axis on specific neurons (e.g. those which express agouti-related protein and proopiomelanocortin) throughout the brain [Håkansson et al., 1998; Håkansson and Meister 1998; Elmquist el al., 1998; Gong et al., 2007]. Notably, $ob^{-/-}$ and $db^{-/-}$ mammals

are deficient in activation of hypothalamus STAT pathways [Ghilardi et al., 1996]. The human genome encodes 4 JAK and 7 STAT members, and class-I cytokine receptor family members exhibit selectivity in their JAK/STAT utilization [reviewed in: Boulay et al., 2003].

Ob-Rb encodes the largest protein of all leptin receptor isoforms which contains 302 cytoplasmic residues harboring Box 1 - 3 motifs, or critical tyrosine residues obligate for JAK/STAT interactions [Bahrenberg et al., 2003]. Notably, Ob-Rb is highly expressed in the (human) hypothalamus, and serves as the only STAT-3 signaling-competent leptin receptor isoform. The Box 1, 2, and/or 3 motifs are absent in some truncated leptin receptor isoforms as well as $db^{-/-}$ genotypes. Leptin receptor stimulation of STAT3, but not STAT5, is dependent on the Box3 motif in hepatoma cells [Baumann et al., 1996; White et al., 1997]. Stimulation of Ob-Rb augments phosphorylation of STAT3, STAT5, MAPK, IRS-1, and ERK2 in Chinese hamster ovary (CHO) cells; overexpression of JAK1 or JAK2 increases this association [Bjorbaek et al., 1997]. The absolute functions of the truncated *lepr* isoforms have not been characterized; preliminary studies suggest that the short isoforms function as mediators of leptin transport across tissue barriers [reviewed: Zhang et al., 2005; reviewed: Schulz and Widmaier 2006]. *In vitro* heterodimerization between soluble leptin receptor isoforms does not occur [Devos et al., 1997] suggesting that regulation of leptin signaling is, in part, levered by ligand transport between tissue systems.

LEPTIN SIGNALING

Stimulation of the leptin receptor regulates STAT3, STAT5, and STAT1 intracellular signaling cascades [Baumann et al., 1996; White et al., 1997; Gong et al., 2007]. Ob-Rb is purportedly localized at the plasma membrane in a dimeric orientation. Binding of leptin to the dimerized receptors (2:2) induces a conformational change which recruits cytosolic Janus kinases to the receptor Box 1 and Box 2 motifs. This structural arrangement places receptor-bound JAK's in a bioenergetically favorable orientation which leads to transphosphorylation of each kinase which, in turn, primes autophosphorylation of receptor tyrosine (P-Tyr) residues. P-Tyr residues on the cytosolic segment of leptin receptor then function as active sites that interact with the SH2 domains of STAT family members. Receptor-bound STAT's are phosphorylated by receptor-associated JAK's leading to homo- or hetero- dimerization of two P-STAT's. Finally, P-STAT dimers translocate to the nucleus which then regulates gene transcription of STAT-responsive promoters [White et al., 1997; Prokop et al., 2014].

Leptin signaling is tied to adaptive immune function; the long and short isoforms of leptin receptor are constitutively expressed by natural killer (NK) cells. $db^{-/-}$ mice NK cells feature downregulation of the P-STAT1/P-STAT3 signaling axes as well as reduced expression of *IL-2* (interleukin-2) and *IFNr* (interferon production regulator) [Zhao et al., 2003]. Leptin signaling also mediates T-regulatory lymphocyte (naïve, memory, regulatory T-cell) proliferation and cytokine secretion [reviewed by Hasenkrug 2007]. A leptin antagonist reversed hyporesponsiveness and anergy in $CD4^+$ and $CD25^+$ regulatory T cells *in vitro* [De Rosa et al., 2007]. Additionally, leptin treatment in starved mice normalized cytokine release from Th1 and Th2 cells [Lord et al., 1998]. These studies

suggest leptin signaling is a candidate pathway that could serve as one point of crosstalk between nutritional state and immune response.

Elements of the leptin signal transduction pathway are present at the earliest stages of mammalian life. Leptin receptors are expressed in human oocytes as well as follicular cells [Cioffi et al., 1997]. Additionally, leptin signaling regulates implantation of the embryo in the endometrium [Yang et al., 2006]. Anti-leptin and anti-STAT-3 immunofluorescence demonstrated that both proteins are expressed and differentially localized in preimplantation stage human and mouse embryos. Both polar bodies were derived from regions of oocytes displaying strong leptin/STAT3 immunofluorescence [Antczak and Blerkom 1997]. The spatial orientation of polar bodies relative to the recently fertilized embryo is thought to delimit animal-vegetal axis specification in murine blastocysts [Gardner 1997]. In most instances, two-cell stage leptin/STAT-3 immunofluorescence is greater in one of the two blastomeres. Segregation between outer blastomeres displaying strong leptin/STAT3 immunofluorescence and inner blastomeres featuring reduced or absent signal intensities are evident by the morula stage [Antczak and Blerkom 1997]. Notably, these developmental studies show that leptin expression precludes terminal adipocyte differentiation in mammals. This suggests leptin plays a facultative role in embryogenesis which is distinct from its function as an adipokine (in mammals).

COMPARATIVE LEPTIN

The zebrafish genome harbors as many as 36 Class-I helical cytokine receptor family members including leptin receptor [Liongue and Ward 2007]. In addition to leptin, fishes express orthologous members of cytokine families including IFN-I (interferon type I), IFN-II (interferon type-II), IL (interleukins), chemokines, and TNF (tumor necrosis factor) [reviewed: Savan and Sakai 2006]. The presence of two disparate teleost leptin paralogues, refractory to a teleost genome duplication event [Jaillon et al., 2004; Gorissen et al., 2009], has complicated comparative interpretations drawn from the zebrafish model with respect to the human leptin signal transduction pathway. Further, it is unknown if the regulatory factors that govern expression of the leptin system in bony fishes are also maintained in mammals. In addition to zebrafish [Gorissen et al., 2009], leptin paralogues (*lepa, lepb*) have been characterized in many bony fishes including bass [Won et al., 2012], carp [Tang et al., 2013], goldfish [Tinoco et al., 2012], medaka [Kurokawa and Murushita 2009], salmon [Rønnestad et al., 2010], grouper [Zhang et al., 2013], rainbow trout, brown trout, and Arctic char [Angotzi et al., 2013]. The zebrafish genome has only one copy of *lepr,* however, there are two *lepr* copies in species of eel and salmon [Liu et al., 2010; Morini et al., 2015; Angotzi et al., 2016].

The zebrafish leptin paralogues share little amino acid sequence homology with human leptin or one another [Gorissen et al., 2009]. *In silico* structural modeling of non-mammal leptins adopt the class-I cytokine four-helix fold illustrated by the X-ray crystal structure of human leptin suggesting that the leptin structure is conserved between lower and higher vertebrates [Zhang et al., 1997; Gorissen et al., 2009; Kurokawa and

Murashita 2009; Crespi and Denver 2006; Angotzi et al., 2013; Prokop et al., 2012 and 2014]. Structural modeling of the activated leptin receptor complex follows 2:2 stoichiometry, however, a 2:4 hexameric complex has also been reported [Mistrik et al., 2004; Peelman et al., 2006]. Molecular dynamics simulations show that leptin-a exhibits higher binding energy than does leptin-b to the leptin receptor. Additionally, the leptin binding site is conserved between fish and mammal leptin receptors [Prokop et al., 2012]. The zebrafish leptin receptor features more hydrophobic residues at the ligand-receptor interface than human, and discrepancies in the number of hydrophobic contacts are likely contributors to leptin receptor conjugation at alternative concentration gradients or biochemical conditions [Prokop et al., 2012].

X. laevis recombinant leptin (RxLEP) injections accelerated prometamorphic *S. hammondii* (tadpole) hind-limb morphogenesis but did not affect feeding behavior or body size. Intracerebroventricular RxLEP injections induce an anorectic response among mid-prometamorphosis frogs; a stage of development characterized by the advent of fat bodies [Crespi and Denver 2006]. Zebrafish leptin-a mRNA is present at the single cell stage, and leptin receptor expression is evident in the notochord by 24 hpf and brain at 5 days post fertilization (dpf) [Liu et al., 2010 and 2012]. Zebrafish *lepb* is expressed in response to tissue regeneration [Kong et al., 2016] while leptin-a mitigates beta cell physiology and glucose homeostasis [Michel et al., 2016] but neither paralog has been demonstrated to regulate adiposity. In contrast to mammals, leptin-a and leptin-b expression has not been validated in zebrafish adipocytes. The liver is generally an abundant reservoir of leptin expression in many fishes, chicken (although this has been

disputed), and frogs [Gorissen et al., 2009; Kurokawa and Murushita 2009; Taouis et al., 1998; Crespi and Denver 2006]. Interestingly, leptin is expressed in *Salmo salar* adipocytes *in vitro*, and this result was supported by immunostaining of rainbow trout leptin in visceral adipose tissue (VAT) [Pfundt et al., 2009; Vegusdal et al., 2003]. Comparatively, the human and zebrafish leptins vary in sequence content as well as tissue distribution. Zebrafish leptin-a and leptin-b are co-expressed in brain, heart, gut, liver, ovary, spleen, and gills [Gorissen et al., 2009], however, the nature of this coexpression is unresolved. Why do zebrafish coexpress the leptin paralogues in many of the same tissues, and why do bony fish maintain two (functional) copies of leptin? Zebrafish leptin and leptin receptor knockouts, or teleost analogs of $ob^{-/-}$ and $db^{-/-}$ rodents, can serve as comparative models representing congenital leptin deficiency in lower vertebrates.

The role(s) of leptin signaling in zebrafish developmental physiology are not well defined. ENU (N-ethyl-N-nitrosourea) mutagenesis in medaka and zebrafish *lepr* have manifested lines of fish harboring a truncated (nonsense) leptin receptor at alternative loci (5' of the extracellular ligand binding domain in medaka; 3' of the cytoplasmic Box1 motif in zebrafish). Discrepancies between medaka and zebrafish leptin receptor deficiency are evident, and neither phenotype directly corresponds to the morbid $db^{-/-}$ mouse. Adult $lepr^{-/-}$ medaka exhibit hyperphagia, increases in visceral fat depots, upregulation of neuropeptide Ya and agouti related protein, as well as downregulation of proopiomelanocortin-1 mRNA's [Chisada et al., 2014]. In contrast, zebrafish $lepr^{sa1508/sa1508}$, $lepr^{CRISPR-/-}$, and $lepa^{CRISPR-/-}$ feature alterations in beta cell physiology

including upregulation of insulin-a as well as hepatic mRNA's that regulate endogenous glucose production. *lepr*$^{sa1508/sa1508}$ adults exhibit negligible differences in adiposity, body size, and feeding behavior; there was no difference in fertility relative to controls [Michel et al., 2016]. Initially, these findings may suggest divergent roles for leptin signaling among ray-finned fishes. Comparatively, the ligand binding domain of the zebrafish *lepr*$^{sa1508/sa1508}$ genotype, and the truncated ligand binding domain in *lepr*$^{-/-}$ medaka suggest that the two are not directly comparable molecular models representing leptin receptor deficiency in ray-finned fishes because the (soluble) leptin receptor ligand binding domain may facilitate leptin transport or clearance. CRISPR Cas9 targeted disruption 5' of the zebrafish *lepr* ligand binding domain, or conversely, directly 3' of the medaka *lepr* Box1 motif may substantiate or disprove the differences in leptin action between zebrafish and medaka.

MORPHOLINO OLIGONUCLEOTIDES

Structurally, antisense morpholino oligonucleotides (MO) are short (~25 mer), chemically-modified nucleic acids with alternative morpholine ring in place of the native deoxyribose and ribose moieties present in DNA and RNA, respectively [Summerton and Weller 1997]. Uncharged phosphodiamorate linkages between morpholino nucleotides juxtapose the negatively charged phosphodiester backbones of native DNA/RNA. These structural rearrangements confer resistance to RNase H nucleolytic cleavage, and the uncharged MO backbone inhibits off-target electrostatic interactions during delivery and diffusion [Summerton 1999]. MO's have been primarily implemented to disrupt

translational processing of a target mRNA in developing *Xenopus* and *Danio rerio in vivo* [Heasman et al., 2000; Nasevicius and Ekker 2000]. MO's are generally directed against the translation initiation site of a "sense strand" mRNA sequence as described here [Figure 3.1]. Alternatively, mRNA transport, maturation, and processing can be manipulated by directing MO's against precursor mRNA intron:exon boundaries [Kloosterman et al., 2007]. Gene knockdown is catalyzed by complementary Watson-Crick base-pairing between antisense MO and target sense-strand mRNA which sterically excludes the ribosome from executing translation [Summerton 2007]. Notably, MO "gene knockdown" refers to reduced target protein synthesis or disrupted mRNA processing through these mechanisms.

MICROARRAYS

Eukaryotic gene expression is controlled by transcriptional machinery, mRNA processing and transport, post translational modification, and epigenetic factors. The transcriptome generally pertains to the complete spectrum of RNA species expressed in a biological sample at one reference point in time (e.g. 48 hours post fertilization). Microarrays are high-throughput technologies that test hypotheses directly related to genomics and transcriptomics. One application of these platforms interrogates mRNA expression as a means to distinguish which genes are over- or under- represented in a particular treatment relative to a reference sample; this process is referred to as a gene set enrichment analysis (GSEA) [Subramanian et al., 2005]. Microarrays may also probe for genetic variants such as copy number variations (CNV), single nucleotide

polymorphisms (SNP), translocations, InDels, and epigenetic modifications which are oftentimes marked contributors to the prevalence of various cancers and disease [Rays et al., 1996; Consoli et al., 2002]. One facet of computational biology seeks to establish analytical pipelines for the identification of novel biomarkers, molecular signatures, and functional enrichment represented by complex (polygenic) human diseases [Rhodes et al., 2004; Weinstein et al., 2013].

Microarrays are small silicon flow cells studded with millions of oligonucleotide probes. Each probe represents a fragment of a known sequence complementary to an mRNA or EST [Schena et al., 1995]. Microarray probe designs are built from species-specific reference assemblies which contain genome-wide annotation data. Microarray platforms are designed for model and non-model organisms by a number of manufacturers that differ in probe design, chip geometries, quality control, and hybridization protocols [Hochreiter et al., 2006]. Within this context, the process of normalization describes the excision of non-biological variability within the dataset (ex. cross hybridization) which generally improves the accuracy of results [Wu and Irizarry 2004].

Expression microarrays are molecular technologies adapted to qualitatively and semi-quantitatively define all actively transcribed regions of the genome using a single experiment. Quantifying differences in mRNA expression levels for target genes (over/under representation relative to the normal) is one application of microarrays related to human health (disease diagnosis, progression and prognosis, therapy) [Schena

et al., 1996; Pollack et al., 2002; Antonell et al., 2013]. *In silico* analyses of gene expression data provide high-throughput alternatives to wet-lab experimental techniques (qPCR, Northern Blot). Microarray datasets often require an independently validated measure of gene expression due to a number of drawbacks including cross-hybridization and background normalization. Quantitative real-time PCR (qPCR) is generally coupled with microarray datasets as a means to experimentally validate expression measures for a subset of candidate genes distinguished as differentially expressed (between two groups of samples) using *in silico* methods [Brazma et al., 2001].

A canonical approach to expression microarray investigations begins with RNA extraction from test (*lepa* knockdown, rescue) and control (wild type) samples. RNA extraction is followed by labeled, or biotinylated, cDNA synthesis. cDNA is then washed over a microchip containing millions of gene-specific oligonucleotide probes to which complementary base stacking interactions between target cDNA and probe emit a fluorescent signal that is detected, quantified, and recorded by a digital camera or imaging system. In this manner, target RNA species can be characterized both qualitatively and semi-quantitatively lending to many applications of gene expression based research efforts. Comparative analyses of probe-level signal intensities between test and control arrays provide insight into over/under representation of expression levels for target genes or transcripts relative to the reference sample [Schena et al., 1995].

Microarrays have limitations including signal saturation, signal to noise calibration, hybridization - amplification - labeling biases, and probe requirements for known sequence data. Microarrays do not calculate absolute quantities of RNA species in a sample. Rather, they provide a robust, but relative, quantitative measurement of RNA's expressed at the time of extraction. Affymetrix microarray platforms control for nonspecific cDNA:probe hybridization (cross hybridization) with QA/QC control "spike-in's" which are designed to interrogate hybridization and labeling accuracy of the cDNA when processed on the chip [Burden 2008]. The control probes measure non-specific photometric intensity from which background can be estimated and subtracted from gene-level probes [Irizarry et al., 2006]. As an example, "Spike-ins" are (biotinylated) labeled cDNA's for housekeeping genes (i.e. actin, GAPDH); these are added to the chip hybridization mixture in serial dilutions (Affymetrix@GeneAtlas; Affymetrix; Santa Clara, CA). In a simple sense, these controls work by adding a known amount of substrate "spike-in X" that, in the absence of error, generates a photometric value of "Y". Actin spike-in is added at a lower concentration than GAPDH spike-in; hence actin is expected to have a lower (relative) probe cell intensity. Subsequently, GAPDH is added at a lower concentration than CreX. After normalization, resulting expression values for the Affymetrix spike in's should be estimated as Actin < GAPDH < CreX [Figures 3.4 – 3.5]. Results that disagree with this hierarchy of QA spike-in intensities suggest inaccuracy and/or imprecision of the resultant expression data across the series of arrays.

CHAPTER II

MATERIALS AND METHODS

ANIMAL CARE

All zebrafish and associated animal procedures were maintained in The University of Akron's (UA) department of biology animal vivarium which were reviewed and approved by the UA Institutional Animal Care and Use Committee (IACUC) protocol # 14-07-9-LFD. Zebrafish were purchased from Aquatic Tropicals (Bonita Springs, FL). All zebrafish were bred in house and maintained in an aquatic fish housing system at: temperature 28.5˚C, 13:11h light/dark, and ammonia < 0.01 ppm. Embryonic life staging, animal caretaking, diet, and husbandry approaches were in reference to *The Zebrafish Book* [Westerfield 1995]. All tank water was prepared in a water dechlorination system supplemented with Stress Coat (API Fishcare; Chalfont, PA). Adult fish were kept in equal tank densities; breeding arrangements were set to accommodate eight adult females with four adult males in 4L fish tanks heated to 28.5˚C also containing marbles and artificial plants. Age of embryo was quantified as hours post fertilization (hpf). Clutches of fertilized embryos were serially collected, cleaned, and segregated from adults directly after spawning (~ 0.25 hpf). Embryos were raised in sterile incubators (28.5^{o}C) using tank water supplemented with 10^{-5} % (w/v) methylene

blue fungicide (Sigma Aldrich; St. Louis, MO) until reaching the larval stages of development (0 - 5 days post fertilization). Juvenile zebrafish were transported from 28.5^{o}C incubators to aquatic fish housing systems at 30 days of age where they were maintained throughout adulthood.

MICROINJECTION

Microinjection of *lepa* morpholino oligonucleotide "knockdown" and recombinant *lepa* protein "rescue" was emulated as described in [Liu et al., 2012]. Embryos (1 - 2 cell stage), visible by light microscopy on live feed camera, were mounted on 1% agarose injection plates supplemented with 0.05% (w/v) methylene blue (Sigma Aldrich; St. Louis, MO). 2 nL of 0.4 mM leptinA antisense morpholino oligonucleotides (5'-TTG AGC GGA GAG CTG GAA AAC GCA T -3'), reconstituted in Daneau buffer ([58 mM NaCl, 0.7 mM KCl, 0.4 mM MgSO4, 0.6 mM Ca(NO3)2, 5.0 mM HEPES pH 7.6]) (Gene Tools; Philomath, OR), were delivered into the blastomeres(s) of 1 – 2 cell stage zebrafish embryos (x < 0.75 hpf) using a Narishije MI300 gas pressurized microinjector (Narishije; East Meadow, NY). "Rescue" injections were prepared with 30 µM recombinant zebrafish *lepa* protein stock solution (50 mM Tris, pH 8.0, > 90% pure; GenScript; Piscataway; New Jersey) mixed (1:1) with 0.4 mM *lepa* morpholino oligonucleotides directed against the translation initiation sequence of leptin-a (Gene Tools; Philomath, OR). Clutches of embryos were developed to 48 hours post fertilization (hpf) then sacrificed for RNA isolation.

RNA ISOLATION

Five dechorionated embryos were pooled together for each replicate (n = 8 wild type, n = 4 knockdown, n = 4 rescue) then manually homogenized at 48 hours post fertilization (hpf). Total RNA was isolated with Trizol reagent (Thermo Fisher Scientific; Waltham, MA), DNase treated with the Turbo-DNA-free kit (Ambion; Santa Clara, CA), washed using the RNeasy MinElute cleanup kit (Qiagen; Hilden, Germany), then eluted in RNase free water. RNA integrity (RIN) was assessed with an Agilent 2100 Electrophoretic Bioanalyzer (Agilent; Santa Clara, CA). RNA was quantified using a Qubit 2.0 Fluorimeter (Thermo Fisher Scientific; Waltham, MA). Equal amounts (1 ug) of high quality total RNA [8.0 ≤ RIN], [260 : 280 < 1.9 - 2.2], [260 : 230 < 1.9 - 2.2] were processed using single-channel Affymetrix Zebrafish 1.1 ST whole-transcriptome gene array strips (Affymetrix; Santa Clara, CA). cDNA library preparation, labeling, and microarray processing followed the manufacturer guidelines for the Affymetrix GeneAtlas system (Affymetrix; Santa Clara, CA). cDNA library preparation and microarray processing were performed by the University of Michigan's Core Facility. Microarrays were processed in five separate batches; scan dates are listed in Supporting Information.

MICROARRAY PROCESSING

(.CEL) files, containing raw probe cell intensities from each microarray, were placed into "R" v3.3.2 statistical environment [R Core Team 2013] fitted with Bioconductor v3.4 [Gentlemen et al., 2004] and associated plugins. Using a supervised approach, the default RMA algorithm [Bolstad et al., 2003; Irizarry et al., 2003 (a) and

(b)] was applied to n = 16 (.CEL) files in '*oligo*' v1.36.1 [Carvalho and Irizaray 2010] using "core" probeset summarization. "Core" summarization is a method that generates expression estimates from concatenation of probes with identical sequence content into probesets using all ~1.2 million probes on the microarray. Probesets represent "safely annotated" genes from the reference assembly which generally refer to those which have been described in some experimental or functional context. In other words, annotations for these gene products were not inferred from sequence similarity or homology-based computational predictions. Affymetrix probeset ID's were mapped to their respective annotations from the Zv9 reference assembly with '*affycoretools*' [MacDonald 2008]; annotations for each probeset were obtained from '*pd.zebgene.1.1.st*' and '*org.Dr.eg.db*' [Pages et al., 2008; Pages et al., 2009; Carvalho et al., 2015; Carlson et al., 2016].

Probesets that did not contain *Danio rerio* gene symbol or transcript identifiers were filtered from the expression set prior to performing the moderated t-test. These probesets included Affx "Poly-A" and "Hybridization" spike-in controls, "rescue" probesets, as well as antigenomic controls; it should be noted that these control probesets were components of the raw (.CEL) dataset to which the RMA algorithm was applied for signal normalization. Affx "Main" probesets on each array were retained for differential expression analyses. Probesets with identical gene symbol identifiers, or multiplicate probesets (ex. different probesets that map to the same gene but interrogate different sequences along the length of that target gene; common among genes with splice variants or isoforms), were also filtered from the analysis following

RMA normalization, however, one multiplicate probeset (with the highest expression value) was retained to represent the target gene's expression measure.

Differentially expressed genes (DEG) were filtered for three contrasts using a '*limma*' v3.28.21 [Ritchie et al., 2015] moderated t-test, or linear model analysis, on each gene independently across the series of arrays. This method also calculates standard error for each gene using empirical Bayesian methods (eBayes) [Smyth 2004]. An intensity-dependent trend was used to adjust prior variances generated from the linear fit for each gene (lmFit) [Smyth and McCarthy]. To identify differentially expressed pathways and functional enrichment that respond to leptin-a, the resulting MArrayLM object, which contains a vector of Entrez gene identifiers returned from each linear coefficient, was passed with the goana/topGO and kegga/topKEGG functions at FDR < 0.01 [Smyth and Hu]. KEGG pathway and GO enrichment tables were generated for all three coefficients, separately [Tables 3.1 – 3.3 and Tables 6.2 – 6.4].

113 differentially expressed transcription factors and their corresponding moderated test statistics were manually extracted from the leptin-a morphant:control comparison in the MArrayLM object then parsed into .csv format. Available Entrez gene identifiers from 113 differentially expressed transcription factors were mapped to *Danio rerio* biological process gene ontologies using the PANTHER database (pantherdb.org/) followed by Bonferroni p.value correction (P < 0.01). Transcription factor enrichment results are presented in Table 3.4.

QPCR

To validate expression estimates generated from the microarray dataset, relative expression levels for 96 transcripts in 48 hpf zebrafish embryos (n = 2 *lepa* MO knockdown, n = 2 *lepa* rescue, and n = 2 wild type) were analyzed via RT^2 Signal Transduction Pathway Finder qPCR Arrays (Qiagen; Hilden, Germany). The RT^2 qPCR array was run in duplicate using batch-matched pools of homogenized embryonic RNA for each condition. Microinjections and RNA isolation were reiterated as detailed above. Each qPCR array was prepared with RNA derived from clutches of five homogenized embryos at 48 hpf. Equal amounts of quality assured total RNA for each condition were reverse transcribed along with null template, null primer, and null reverse transcriptase (RT) controls using qScript Flex cDNA Synthesis Kit (Quanta Bio; Beverly, MA; cat. # 95049-025) and oligo dT primers. cDNA synthesis was cycled at: 22°C 5min, 42°C 30 min, 85°C 5 min then held at 4°C. cDNA was precipitated from the RT reaction using 3M Sodium Acetate and 100% EtOH, frozen for one hour, and 3x washed in 100%, 90%, and 80% EtOH (12,000 RPM, 15 minutes) before resuspension in nuclease free water.

Primer sequences used for qPCR amplification of the 96 transcripts can be found in the manufacturer catalogue (PAZF-014Z) along with the 5 reference/housekeeping genes to which expression was normalized (*acta1b, b2m, hprt1, nono, rpl13a*). Cycling was performed in an AppliedBiosciences 7300 Real Time Cycler (Applied Biosciences; Foster City, CA); cDNA samples were prepared with RT^2 SYBR Green qPCR Master Mix (Cat. # 330529; Qiagen; Hilden, Germany). Fold changes (*lepa* morphant – control; *lepa* rescue – control) were calculated using the delta delta Ct method [Pfaffl 2001] in the

Qiagen Gene Globe data analysis web portal (Qiagen; Hilden, Germany). To validate microarray expression estimates, DEG identified from the microarray dataset were compared to fold changes experimentally determined with qPCR for two contrasts (morphant : control, rescue : control) [Figures 3.14 – 3.15]. The qPCR clustergram was generated from hierarchical clustering (average linkage, Euclidean distance) of all DEG in group #1 (*lepa* morphant) or group #2 (*lepa* rescue) relative to control [Figure 3.16].

CHAPTER III

RESULTS

PROJECT OVERVIEW

The zebrafish pharyngula refers to the transient developmental stage (24 – 48 hpf) characterized by body-axis straightening (angle between trunk/head), circulatory system formation, pigmentation, and the advent of fin development [Kimmel et al., 1995]. Zebrafish leptin-a knockdown adversely effects 48 hpf development, and embryos "rescued" with recombinant leptin-a (rLEPA) reflect wild type morphology [Liu et al., 2012]. Here, embryonic leptin signaling was reduced using morpholino oligonucleotides directed against the *lepa* sense strand translation initiation sequence (5'-TTGAGCGGAGAGCTGGAAAACGCAT-3') [Figure 3.1] as in [Liu et al., 2012]. Expression microarrays were used to investigate candidate genes and cellular pathways that respond to leptin-a knockdown and recombinant leptin-a (rLEPA) rescue.

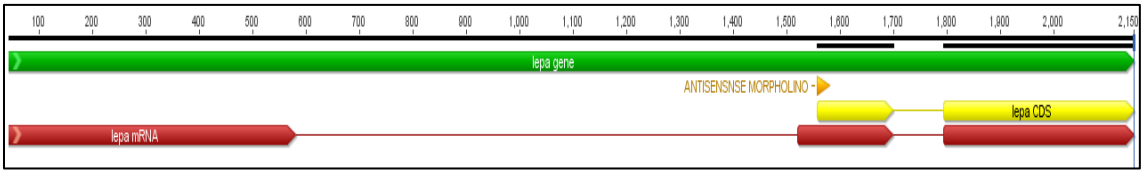

Figure 3.1: Zebrafish *lepa* (ENSDARG00000091085). DNA 2,150 bp (green), mRNA (red), and CDS (yellow); morpholino oligonucleotide target sequence (gold). [5'->3']

Total RNA was isolated at 48 hpf from zebrafish embryos. "Morphants" were microinjected in the 1 – 2 cell stage of development with *lepa* antisense morpholino oligonucleotides, and commensurable "rescue" injections were performed using a 1:1 mixture of both *lepa* morpholino oligonucleotides and recombinant leptin (rLEPA). Sixteen single-channel expression microarray samples (n=8 wild type, n=4 morphant, n=4 rescue) were prepared using total RNA derived from five-embryo homogenates per replicate [Figure 3.2]. cDNA libraries were prepared at the University of Michigan's Core Facility; libraries were processed on Affymetrix 1.1 ST Zebrafish Gene Array Strips (Affymetrix; Santa Clara, CA; n = 16) in correspondence with the Affymetrix GeneAtlas guidelines (Affymetrix; Santa Clara, CA).

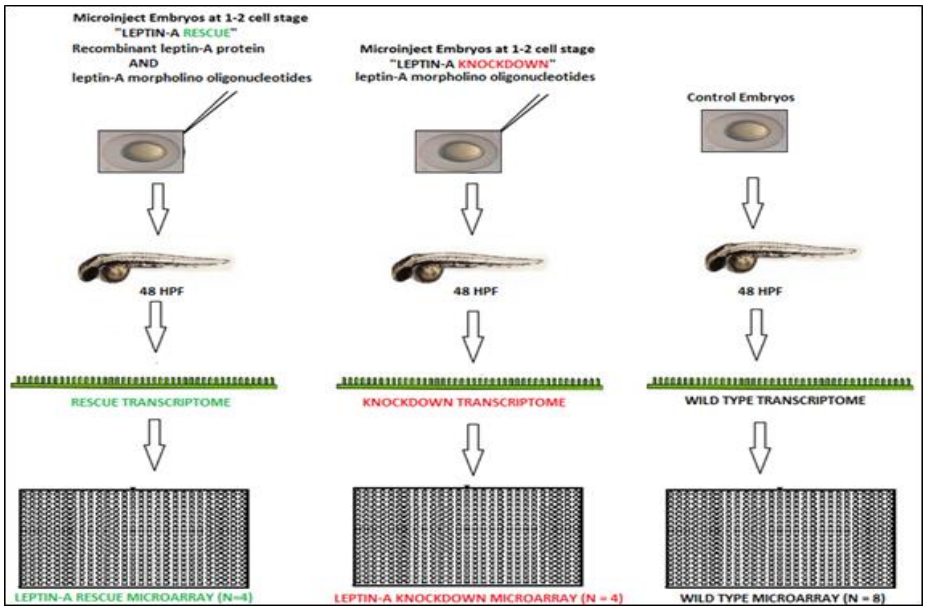

Figure 3.2: Microarray workflow.

To generate expression estimates for each probeset (gene) on the microarray platform, robust Multichip Average (RMA) background correction, quantile

normalization, and median polish probeset summarization were applied to ~1.2 million raw probe cell intensities (.CEL) produced from each microarray sample (n = 16) [Figure 3.3] [Bolstad et al., 2003; Irizarry et al., 2003 (a) and (b)]. RMA-normalized $\log_2$ signal intensities served as gene expression estimates for "core" probesets which refer to "safely annotated" genes that have, at minimum, a corresponding EST or cDNA database identifier. Putative transcripts that have been predicted from sequence similarity or homology-based approaches are not included in "core" probeset (transcript) annotations. Expression measures for each gene on the microarray platform were produced from RMA-normalization of probeset photometric signal intensities.

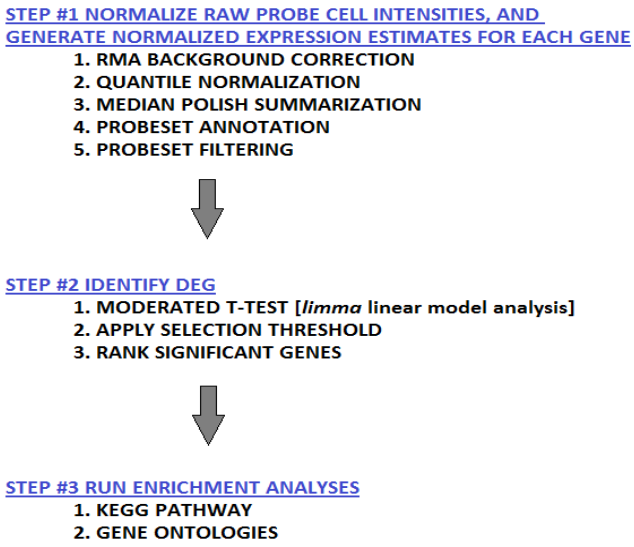

Figure 3.3: Computational workflow.

The *'pd.zebgene.1.1.st'* annotation package [Carvalho 2015] contains mapping information between Affymetrix probeset ID's and *Danio rerio* transcript identifiers using annotations provided by the Zv9 (*Danio rerio*) reference assembly. Probesets that

map to the same gene symbol identifier but vary in sequence content, or multiplicate probesets, were filtered from the analysis prior to the moderated t-test. Only one multiplicate probeset, with the highest log expression, was retained for estimating expression of each gene. All control probesets ("rescue", "antigenomic", "Affx"), as well as additional probesets that did not contain gene symbol identifiers, were filtered from the analysis before the moderated t-test. A total of 75,212 "core" probesets on each microarray platform were reduced to 26,046 gene-wise probesets after filtering. Each of the 26,046 gene-wise probesets represents an expression measure for one gene, exclusively.

QUALITY ASSURANCE

Figure 3.4 illustrates quality assurance measures describing all probeset signal intensities (gene expression estimates) across the series of microarray samples (n = 16). Two factors of variance were considered: treatment [left panel] and scan date [right panel] [Figure 3.4]. In the box and whisker plot, the area spanning between the upper and lower quartiles are colored for each array sample; outliers are indicated by dashed lines [Figure 3.4 – Bottom]. Unexpectedly, the median intensity value for each array, indicated by a notch, was inconsistent both within and between treatments. Lower and upper quartiles of the box and whisker plot segregated between two groups of arrays with the following scan dates: [#1: 5/12/2012, 4/23/2014] and [#2: 7/16/2013, 9/7/2012, 3/6/2013]. The boxplot indicates that the lower (median assigned to the smallest 50% of values) and upper (median assigned to the highest 50% of values)

quartiles were most similar between microarray samples that share one scan date as opposed to samples that share a treatment [Figure 3.4 - bottom].

Differences in median intensity between arrays with alternative scan dates are also evident in the density plot [Figure 3.4 - Top]. Log_2 expression signal (x-axis) is plotted vs. empirical density (y-axis; normalized to a scale of one) for all probesets on each microarray. One subset of samples, containing a mixture of wild type and *lepa* morphant arrays, has two "humps", or split-means, centered at intensities near 3 and 7. The remaining group of samples, containing a mixture of *lepa* morphant, rescue, and control arrays, has one peak, or single mean, near a signal intensity of 6. The signal histogram shows that the group of arrays scanned on 9/7/2012, 3/6/2013, and 7/16/2013 share similar signal distributions as opposed to those scanned on 7/6/2014 and 4/23/2014. The empirical densities of the former group have an alternative signal distribution than the latter group scanned on 5/12/2012 and 4/23/2014 [Figure 3.4 - Top]. Referring to the arrays processed on 5/12/2012 and 4/23/2014, the single peak indicates that ~25% of all probesets have a log expression value near 6. In contrast, the other group of microarray samples (with two means - 9/7/2012, 3/6/2013, 7/16/2013) has ~17% of all log expression values near 2.5 while another ~15% of probesets have a expression signal near 7. Notably, the two "humps" may be characteristic of signal saturation during microarray processing, and arrays processed on 9/7/2012, 3/6/2013, and 7/16/2013 (two humps) did not contain any "rescue" treated embryos. In summary, variation in expression estimates between microarray samples was strongly tied to treatment (e.g. leptin-a knockdown and rescue) but was also obscured by batch

effects including: unknown background genetics of zebrafish, alternative breeding clutches of adult fish, and varying efficiencies of RNA isolation as well as microarray processing between replicates from five separate batches.

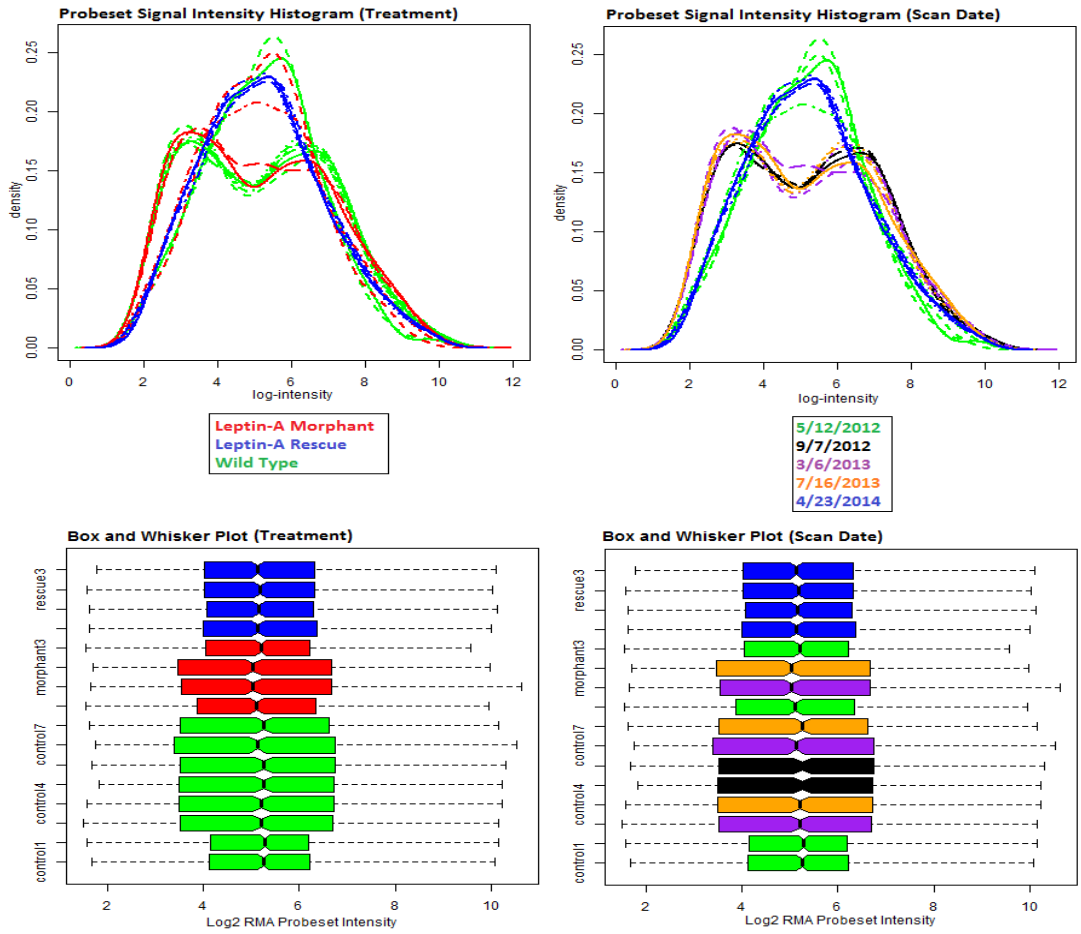

Figure 3.4: Top – Signal Intensity Histogram. Bottom – Box and whisker plots. Plots illustrate the distribution of probeset signal intensities between microarrays. [Left – Microarrays are colored by treatment]. [Right – Microarrays are colored by scan date].

Affymetrix "spike-in" metrics were quality assessed in Expression Console v1.0 (Affymetrix; Santa Clara, CA). All microarrays passed 'hybridization' but not 'Poly-A' thresholds hinting that the precision of cDNA library labeling was inconsistent between

microarray samples from separate processing dates [Figures 3.5 – 3.6]. In spite of the Affx Poly-A spike-in's not meeting desired thresholds (*thr* > *phe* > *lys* > *dap*), no microarray samples were aborted from the study. Indications taken from QA/QC metrics suggest that the distribution of probeset photometric signal intensities were most similar between samples sharing one scan date. Gene expression estimates and corresponding p.values may be skewed by inaccurate signal estimation for the same genes (probesets) across replicates of arrays, and this may have also been a causative factor in Affx "Poly-A spike-in" control failure [Figure 3.6]. Breeding with random combinations of adult zebrafish that stem from a line(s) of unknown background genetics likely impacted similarity measures between/among groups processed from separate clutches as did inherent differences in experimental efficiency throughout RNA extraction and microarray processing from 2012 – 2014. Microarrays processed with embryos derived from the same batch, or scan date, are more similar in expression features to one another as opposed to embryos from separate clutches.

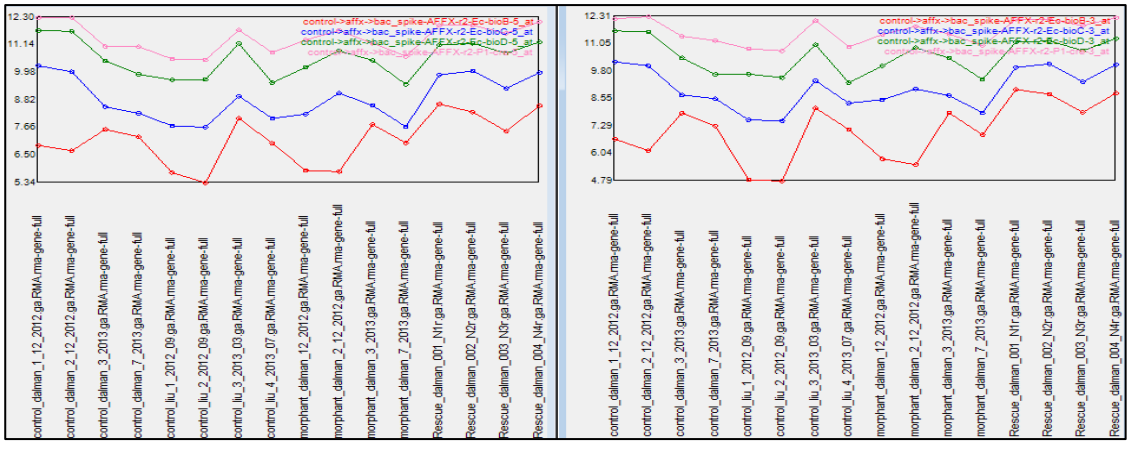

Figure 3.5: Affx 'hybridization' thresholds. Passed thresholds. (CreX > bioD > bioC > bioB)

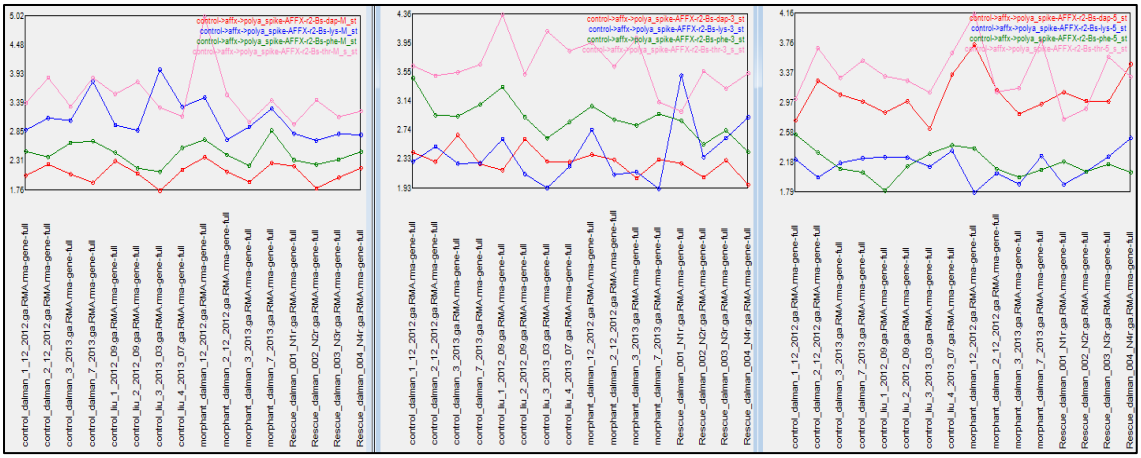

Figure 3.6: Affx 'Poly-A' thresholds. Did not pass for all arrays. (thr > phe > lys > dap)

A multivariate, or principle component analysis (PCA), was used to probe for correlated variables between gene expression, scan date, and treatment across the series of arrays (n = 16) [Figure 3.7]. Each point on the scatterplot represents one microarray sample distributed along the first two principle components, or greatest features of variation. Points, or microarray samples, that are oriented close together in the scatterplot indicate more similar variable features to one another as opposed to those with more distant coordinates. The first two principle components contributed to 31.66% (19.59% and 12.07%) of signal variation in the dataset; microarray samples are colored by treatment (left panel) versus scan date (right panel) [Figure 3.7].

Rescue arrays are the most distinct cluster, as measured by average linkage/Euclidean distance. All four leptin-a rescue samples shared one scan date and also belonged to the same treatment. Subsequently, the smallest margin of signal variation was expected among rescue embryos (relative to the remaining 12 samples). A group of six of wild type arrays, spanning three separate scan dates, also formed a

distinct cluster while two of the remaining wild type arrays were segregated from the faction of six wild types [Figure 3.7 - left]. These two control arrays clustered nearest two of the four morphant arrays, and this cluster of four arrays shared a common scan date [Figure 3.7]. Taken together, the PCA supports results presented in Figure 3.4; there is a significant degree of similarity in signal variation between microarray samples related to both treatment (expected) and batch effects (unexpected). Importantly, each treatment formed its own cluster, and there were no clusters containing members from different treatments [Figure 3.7 – left panel].

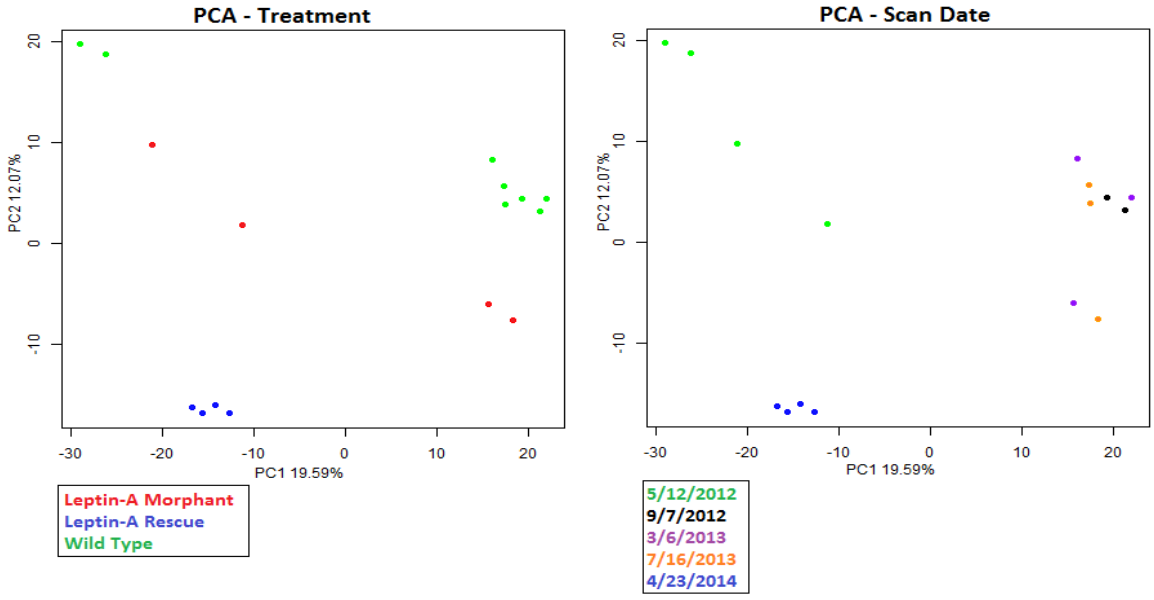

Figure 3.7: Principle Component Analysis. Each point represents one microarray.

DIFFERENTIALLY EXPRESSED GENES

After normalization and filtering raw (.CEL) probe cell intensities from sixteen single-channel expression microarrays, normalized $\log_2$ intensities for each probeset were compared between treatments using the '*limma*' linear model analysis for three

contrasts: (1) leptin-a morphant : control (2) leptin-a rescue : leptin-a morphant (3) leptin-a rescue : control. This model applies a linear least-squares fit to the RMA-normalized $\log_2$ intensities for individual probesets across the series of arrays (n = 16) [Smyth 2004; Ritchie et al., 2015]. This statistical test probes for genes with reliable differences in expression estimates between two groups of samples. In short, this model performs a moderated t-test on each row of the expression matrix (generated during RMA output) for each contrast, separately. Due to performing a large number of t-tests, p.values from each linear coefficient, or comparison between two groups of samples, in the moderated t-test were adjusted with the Benjamini and Hochberg (BH) post-hoc test which controls for false discovery rate (FDR), or type-I error (incorrectly reject a true null hypothesis) [Benjamini and Hochberg 1995]. P.values obtained from each comparison in the gene-wise (*limma*) linear model analysis were adjusted separately [Smyth 2004; Ritchie et al., 2015].

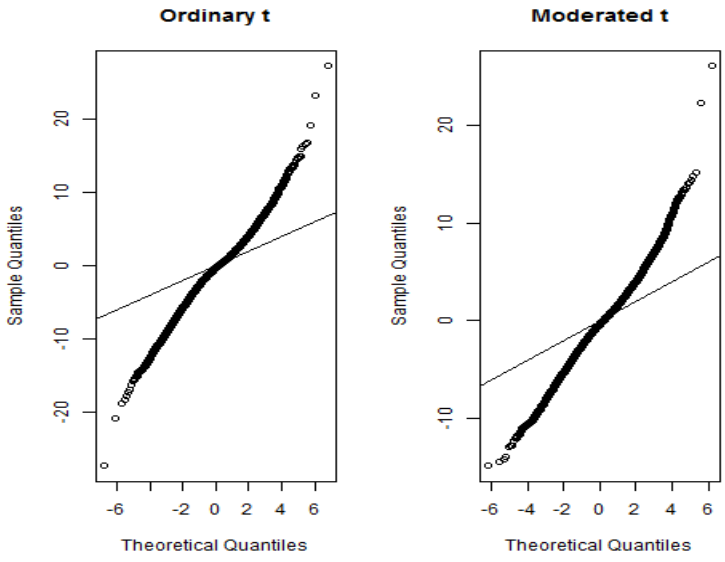

Figure 3.8: Q-Q Plot. Each point represents one probeset (gene).

The normalizing effects of the *limma* moderated t-test, which shrinks signal variation in probeset expression towards a common value [Smyth 2004], are illustrated by the Q-Q plot [Figure 3.8]. The left panel shows the t-score distribution from an unmoderated t-test where adjustments for prior variances were not made. In the moderated t-test (right panel), the theoretical and sample quantiles (t-scores plotted for each probeset) are reduced in absolute value relative to the unmoderated t-test (left panel), a less stringent analysis. The diagonal illustrates $R^2 = 1.0$, or a 1 to 1 relationship between the observed (Y) and expected (X) distributions of probeset t-scores. Gene expression estimates that fall on the slope of the Q-Q plot are expected to follow a normal distribution, or are not differentially expressed, between groups of samples. In contrast, genes distant from the slope have irregularly distributed (non-normal) expression estimates between treatments; these are generally referred to as differentially expressed. If 0 genes were differentially expressed in any comparison, all points would fall on the diagonal. The plot illustrates that many genes have widely variable expression measures, or do not follow a normal distribution in terms of their relative expression, between control, knockdown, and rescue embryos.

From a universe containing 26,046 genes, DEG were filtered using arbitrary selection criteria: adjusted p.value < 0.01 and $\log_2$ fold-change < -0.5 or > 0.5 [Figure 3.9]. 1,461 genes, or 5.6% of the 26,046 filtered probesets, were differentially expressed in the morphant:control contrast (40.0% or 585 upregulated; 60.0% or 876 downregulated). 5,105 genes (19.6% of the 26,046 probesets) were differentially expressed (30.7% or 1,567 upregulated; 69.3% or 3,538 downregulated) in the

rescue:control contrast. Analysis of the leptin-a rescue:morphant contrast returned 1,714 DEG (27.9% or 479 upregulated; 72.1% or 1,235 downregulated), or 6.6% of the 26,046 gene-level probesets. There were 43 of the same genes (0.0017%) differentially expressed in all three comparisons while 19,987 genes (76.7 %) were not differentially expressed between any two groups. In total, 6,059 genes (23.3%) were significant in at least one of three comparisons. There were more downregulated DEG than upregulated in all three contrasts [Figure 3.9 – 3.10].

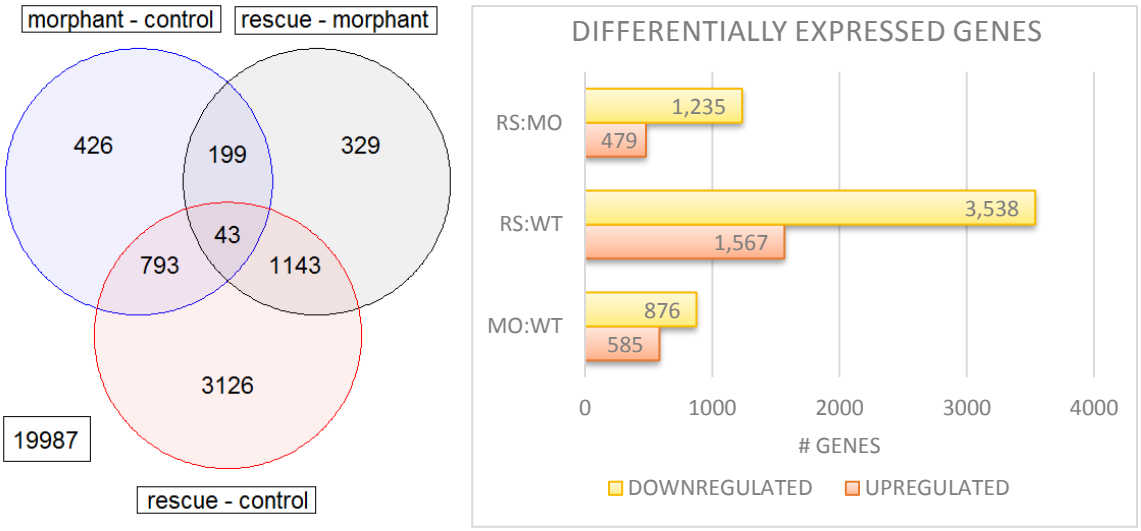

Figure 3.9: Left - Venn Diagram. DEG in each comparison: fold change < -0.5 or > 0.5 and adjusted p.value < 0.01. Right – bar chart of DEG in all contrasts.

Volcano plots illustrate the distribution of all genes on the array platform as a function of fold change (x) and log odds ratio (y) between two groups of samples where each point represents one probeset; the distribution of DEG between each comparison was plotted separately [Figure 3.10]. The top-50 probeset gene symbols, sorted by highest log odds ratio, are highlighted where a high log odds ratio is comparable to a

low (significant) p.value. Colored axes in each plot represent the significance and fold-change thresholds for selecting DEG from the moderated t-test: Benjamini and Hochberg adjusted P.value < 0.01 and $\log_2$ fold change < -0.5 or > 0.5.

Mean-Average (MA) plots illustrate the relationship between normalized photometric intensity (average log expression) and fold change for each probeset on the array when comparing two groups of samples [Figure 3.10]. The colored axes indicate the fold change < -0.5 or > 0.5 cutoffs for selecting DEG, and adjusted p.value is not incorporated into these plots. The relationship between probeset fold change and photometric intensity was assessed for each contrast, separately. Genes with fold change > 0.5 or < -0.5 in the morphant:control contrast [top panel] were evenly distributed between log intensities of 4 and 9. Downregulated genes (fold change < -0.5) in the rescue : control contrast [bottom panel] were clustered between expression values of 5 to 8; upregulated genes (fold change > 0.5) ranged between low intensities spanning 2 to 5. Upregulated genes in the morphant : rescue contrast [middle panel] were packed between intensities of 4 to 8 while downregulated genes clustered between (low) signal intensities of 2 and 4. The MA plots illustrate intensity-specific effects on fold change in the rescue:morphant [middle panel] and rescue:control [bottom panel] contrasts which have more comparable MA distributions to one another as opposed to the morphant:control [top panel] comparison. Genes with (low) expression estimates ranging from $2 < x < 4.5$ tended to be upregulated, and genes spanning average log expression signals of $5 < x < 8$ were generally downregulated [Figure 3.10 – middle, bottom panels].

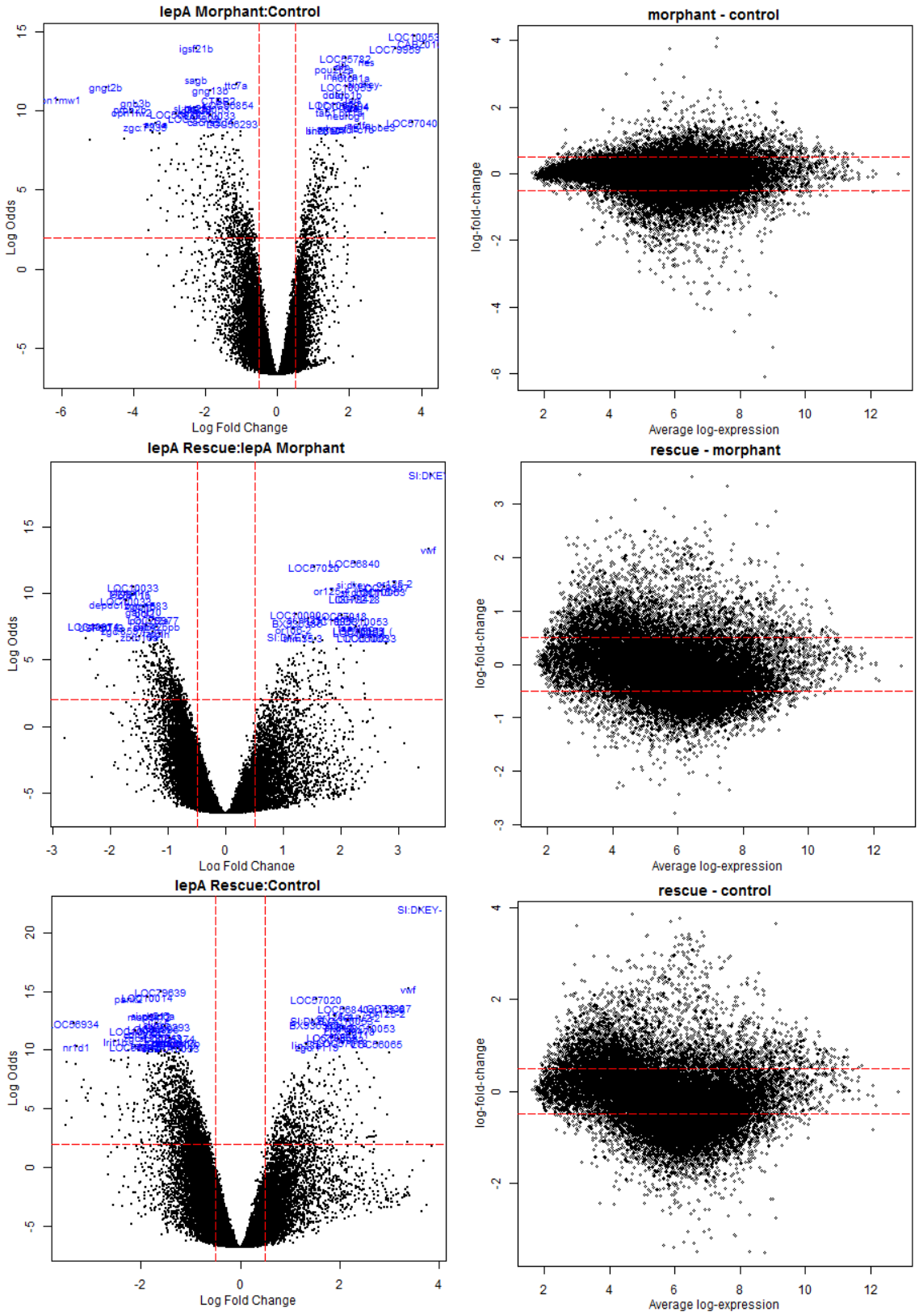

Figure 3.10: Left - Volcano Plots. Right - MA plots. Each dot represents one probeset.

Expression estimates from the top-50 DEG in each contrast, sorted by lowest adjusted p.value, were clustered (average linkage, Euclidean distance measures) to illustrate expression patterns between genes and microarray samples [Figures 3.11 – 3.13]. Both rows (genes) and columns (microarray samples) were clustered. Genes displayed in the heatmaps are color-scaled by log expression signal, or probeset intensity. Transcription factors are indicated using purple dots adjacent to the corresponding gene symbols of each heatmap. A red color scale indicates the target gene was highly expressed while green indicates low expression for a gene. Microarray samples clustered according to treatment in all three comparisons as expected. The heatmaps also reinforce quality assurance measures from Figure 3.4. In all comparisons, control1/control2 aligned nearest to morphant1/morphant4, and these four arrays share one scan date [Figures 3.4 and 3.11 – 3.13; Table 6.1]. Importantly, notch-related genes (orange rectangles) showed reciprocal expression patterns compared to phototransduction related genes (blue rectangles) for each group of samples [Figure 3.11]. Three transcription factors also shared similar expression patterns between each group of samples (*foxn4, neuog1, pou2f2a*) [Figure 3.11] indicating that these genes may be coregulated, and this may provide a link between notch signaling and phototransduction [Figure 3.11].

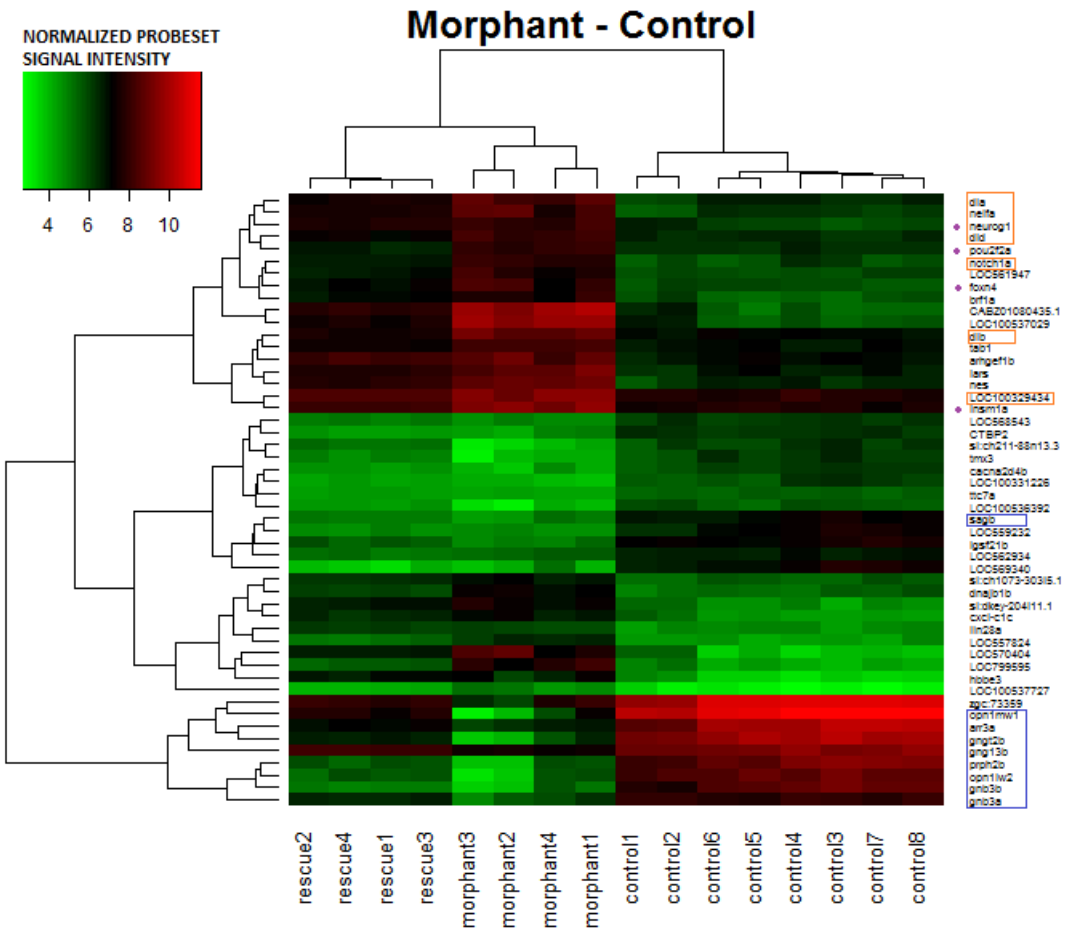

Figure 3.11: Heatmap of the top-50 DEG in the morphant : control contrast sorted by lowest adjusted p.value. Notch signaling genes are indicated in orange rectangles; phototransduction genes are indicated by blue rectangles.

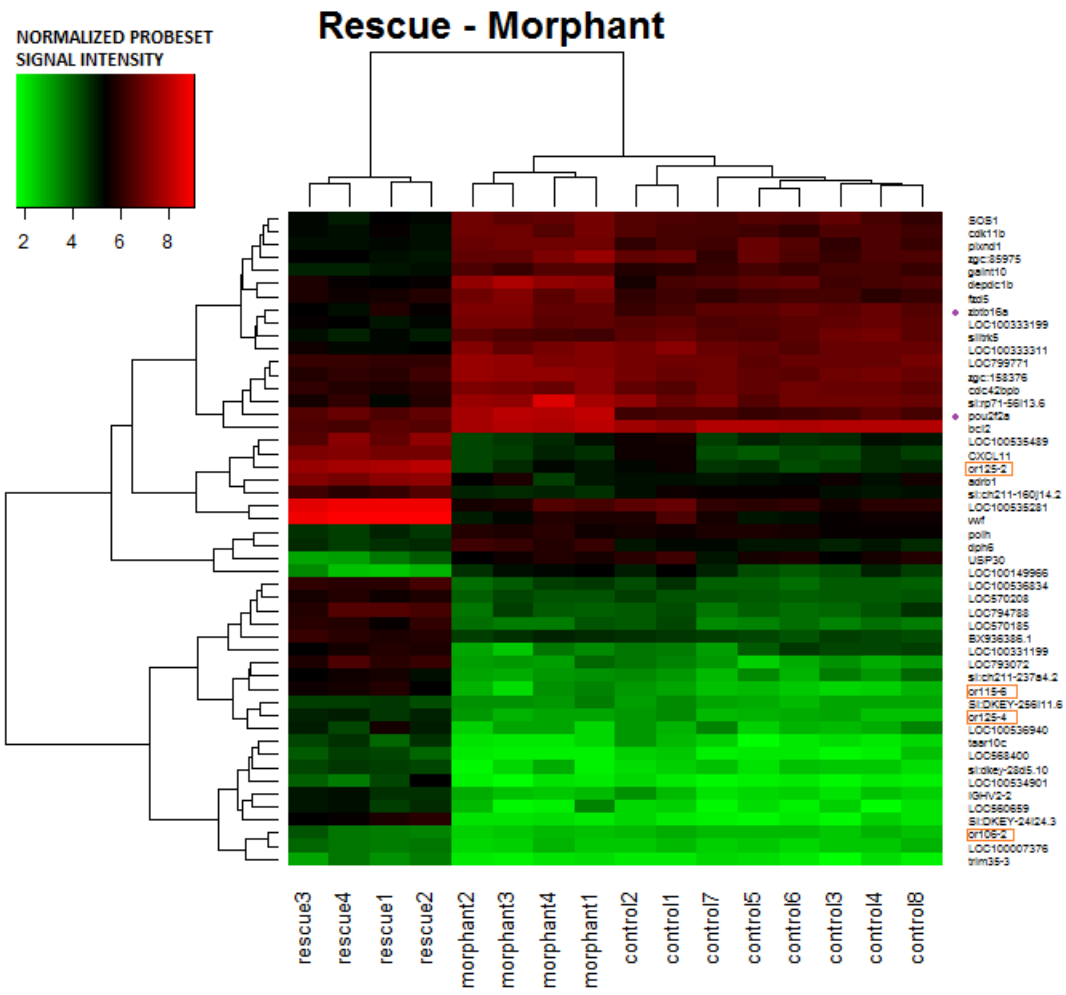

Figure 3.12: Heatmap of the top-50 DEG in the rescue : morphant contrast sorted by lowest adjusted p.value. Olfactory (odorant) receptors are depicted in orange rectangles.

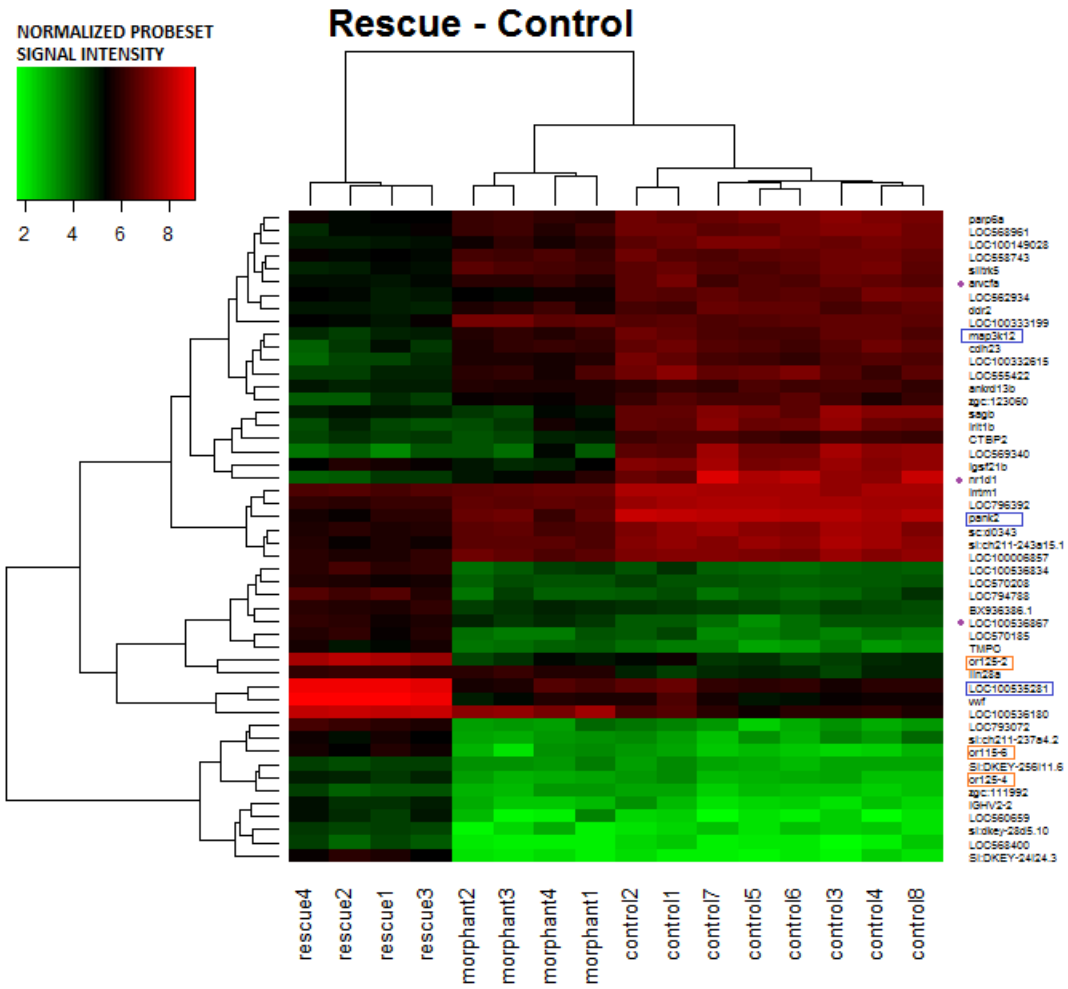

Figure 3.13: Heatmap of the top-50 DEG in the rescue : control contrast sorted by lowest adjusted p.value. Olfactory (odorant) receptors are shown in orange rectangles; intracellular kinases are indicated by blue rectangles.

QPCR VALIDATION

Qiagen Zebrafish RT^2 qPCR Signal Transduction Profiling Arrays (Qiagen; Hilden, Germany) were used to validate differentially expressed genes (DEG) called from the microarray dataset. This qPCR array quantifies expression for a total of 96 transcripts which includes 5 reference and 7 control genes. The qPCR array was run in duplicate, and RNA was prepared from age-matched, not batch-matched (to microarray samples), 48 hpf embryos which may explain some discrepancies between expression estimates of qPCR versus microarray. Expression for an assortment of 84 transcripts (not including reference/control samples) from qPCR analysis was compared to microarray expression estimates for 26,046 genes. Fold changes for the genes selected from the microarray morphant:control and rescue:control contrasts were compared to fold changes experimentally determined with qPCR [Figures 3.14 – 3.15]. A dendogram (unsupervised hierarchical clustering) was generated using expression measures for all DEG identified by qPCR analysis [Figure 3.16]. qPCR analysis identified dysregulation of *notch1b*, *jag1b*, *wnt1b*, *wisp1a*, and *her6* which agrees with enrichment for "Notch signaling in the microarray dataset [Table 3.1 – 3.2; Figure 3.16]. From the qPCR dataset, *stat1a* was downregulated in morphant arrays which corresponds well to reduced leptin signaling as *jak2a*/*jak2b* were downregulated in the microarray dataset. Together, these findings may link *lepa*, *jak2a*, and *stat1a* to the same signaling cascade.

Thirteen transcription factors were differentially expressed in the qPCR clustergram: *arnt, atf4b1, atf4b2, csf1a, gata3, bmp2b, bmp4, fosl1a, her6, myca, mycb,*

nfixa, ppardb, and *stat1a* [Figure 3.16]. Four of these transcription factors (*gata3*, *ppardb, bmp4, fosl1a*) have human homologues or related family members that play roles in adipogenesis. *fosl1a* was differentially expressed in both the qPCR and microarray datasets [Figures 3.14 – 3.15]; a related transcription factor, *FOSL2* of the c-Fos transcription factor family, induces leptin expression in human and rodent adipocytes [Wrann et al., 2014]. *GATA3* is also a transcriptional regulator of mammalian adipogenesis [Tong et al., 2000]. By way of qPCR, *gata3* expression was upregulated (logFC = 2.0) in leptin-a morphants and downregulated in rescue embryos (logFC = -1.02). However, *gata3* was not among significant genes in any contrast from the microarray dataset. cAMP responsive element binding protein-like 2 (*crebl2*) was downregulated in leptin-a rescue embryos (-1.05 logFC); human *CREB2* participates in adipogenesis through transcriptional regulation of *CREB1*. In leptin-a rescue embryos, dysregulation of *arnt* was identified from both qPCR and microarray analyses [Figure 3.14]. Interestingly, human *ARNT* is a subunit of the HIF-1α bHLH transcription factor, and *in vivo* promoter analysis shows that hypoxia inducible factor-1α binds an enhancer element of the zebrafish *lepa* promoter [Chu et al., 2010].

15 total DEG from the microarray analysis were probed using qPCR [Figures 3.14 – 3.15]. 6 of these genes (6/15, or 40.0%) were transcription factors: *arnt, atf4b1, fosl1a, myca, mycb,* and *nfixa*. However, expression for only three (20.0%) of the transcripts (*cdkn1a, fosl1a*, and *nfixa*) tested with qPCR were differentially expressed in both the rescue:control and morphant:control microarray contrasts [Figures 3.14 – 3.15]. Relative expression for 11 leptin-a morphant DEG called from the microarray

dataset were measured on the qPCR array [Figure 3.15]. Fold changes for two of these genes (*cdkn1a, wnt3a*) disagreed between qPCR and microarray expression estimates in terms of relative expression (up versus downregulated relative to control). 8 DEG called from the leptin-a rescue microarray comparison (relative to control) were tested with qPCR. Fold changes for 4 of these genes (*bcl2, cdkn1a, fosl1a, nfixa*) disagreed between qPCR and microarray expression estimates [Figure 3.14]. 50% (4 / 8) of DEG in the rescue:control contrast [Figure 3.14] compared to 80% (8 / 10) of DEG in the morphant:control comparison were validated with qPCR [Figure 3.15]. These results show a slight degree of disagreement between *in silico* and experimental estimation of gene expression.

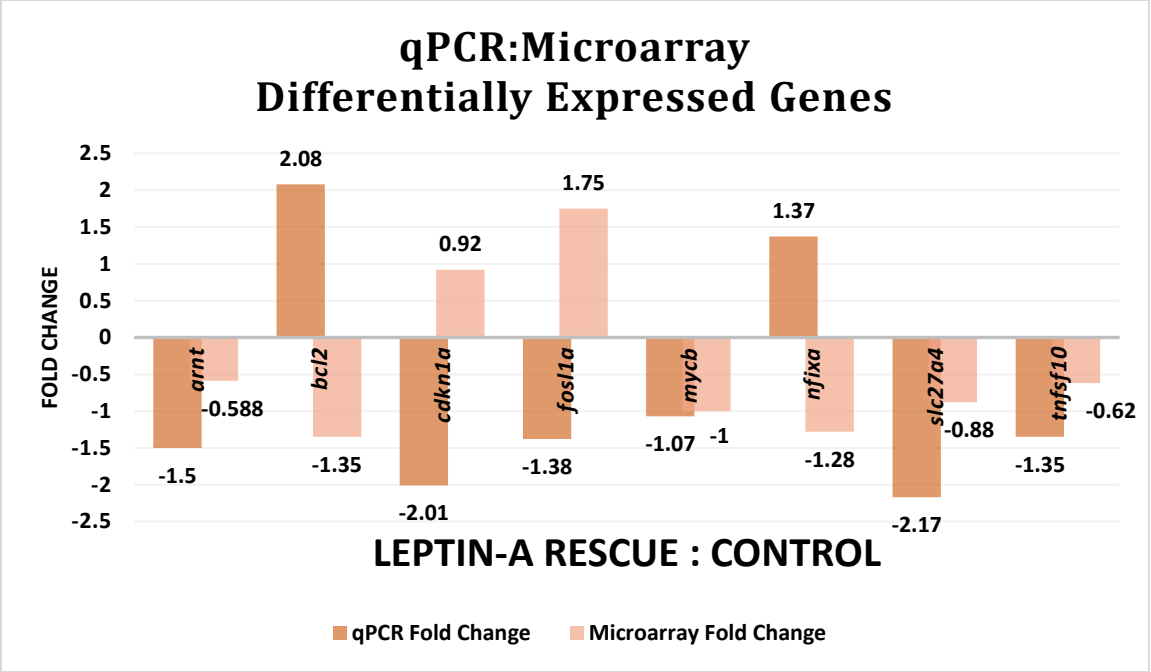

Figure 3.14: Comparison of fold changes between microarray and qPCR using the leptin-a rescue and control comparison.

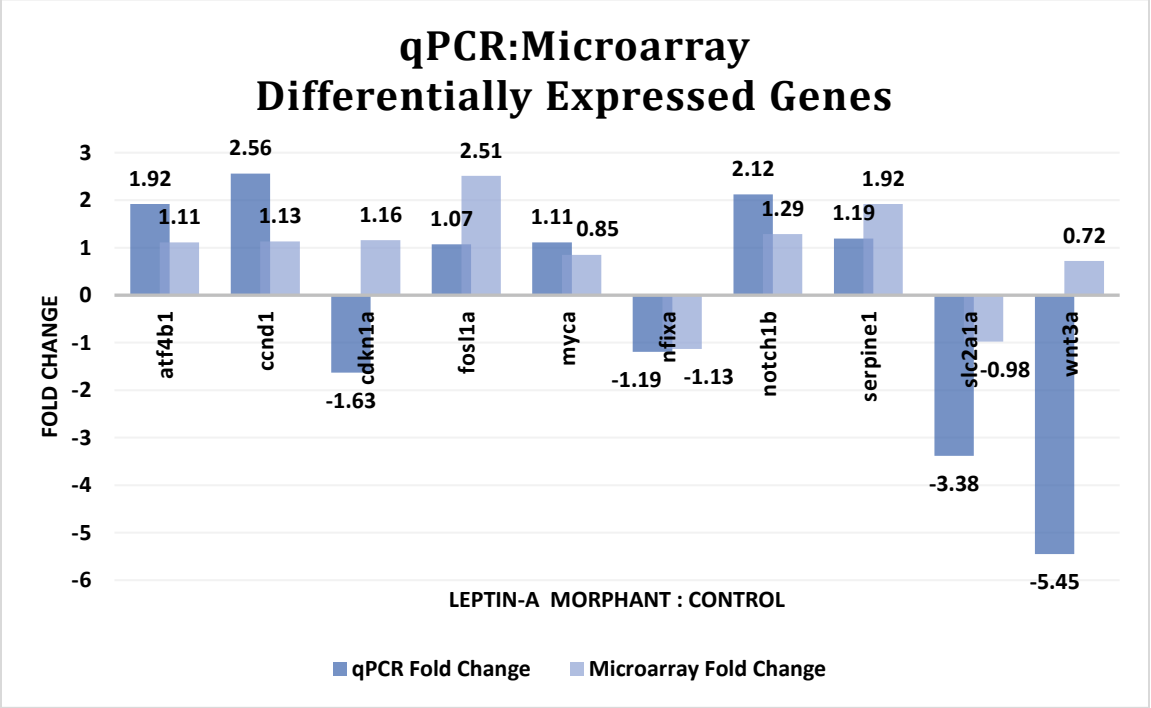

Figure 3.15: Comparison of fold changes between microarray and qPCR using the leptin-a morphant and control comparison.

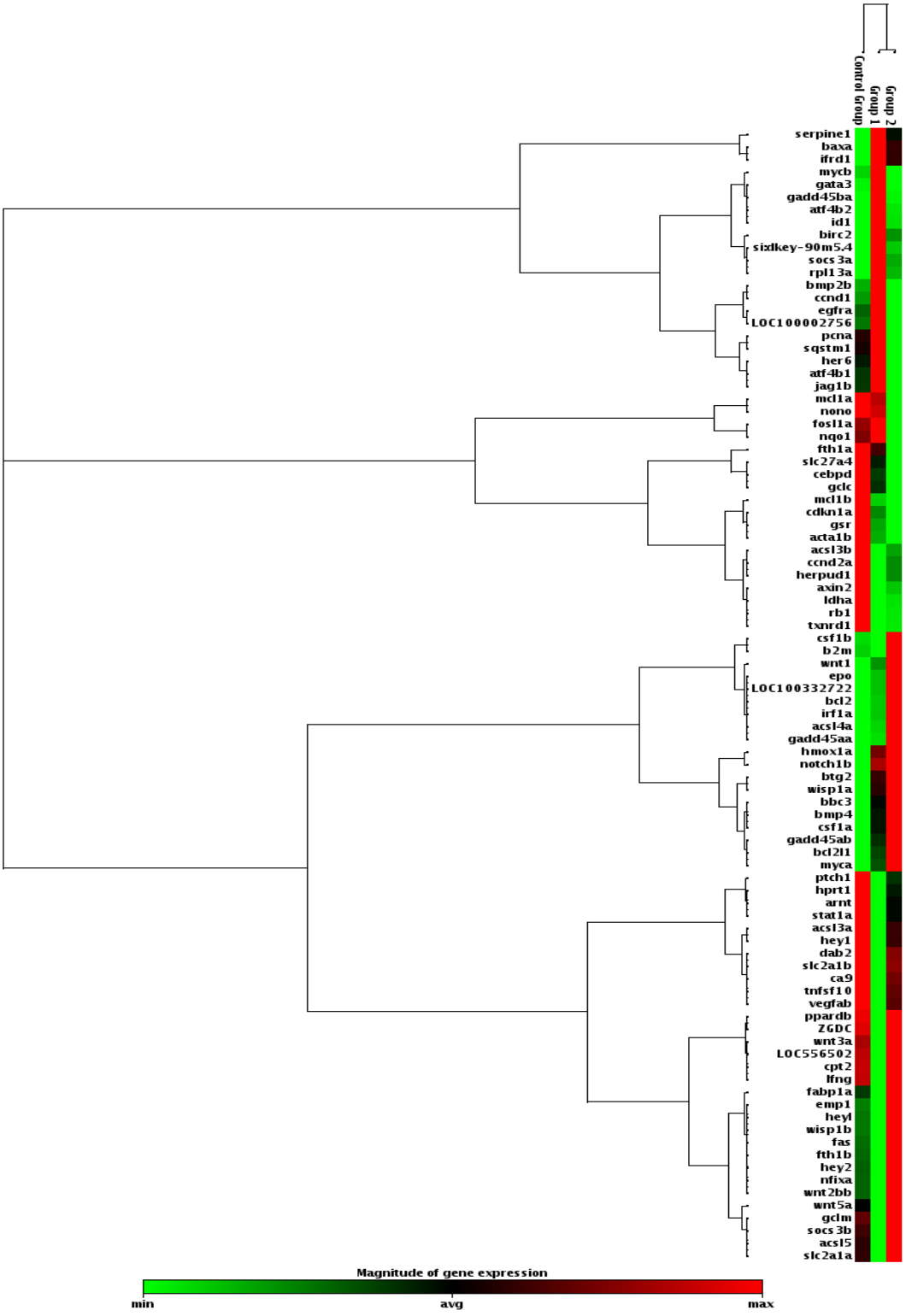

Figure 3.16: Quantitative PCR clustergram (Group 1 = leptin-a morpholino knockdown; Group 2 = leptin-a rescue). (green = low relative expression, red = high expression)

KEGG AND GO ENRICHMENT ANALYSES

Kyoto Encyclopedia of Genes and Genomes (KEGG) and Gene Ontology (GO) are curated databases populated with information describing molecular interaction networks which describe cellular pathways and biochemical processes that correspond to functionally related genes [Ashburner et al. 2000; Ogata et al., 1999]. Entrez gene identifiers were extracted from all differentially expressed probesets ($P < 0.01$, fold change < -0.5 and > 0.5) for three comparisons [Figure 3.9]. DEG Entrez gene identifiers from each contrast were mapped to the *Danio rerio* KEGG and GO databases separately, and results ($P < 0.01$) are displayed in Tables 3.1 – 3.3 as well as Tables 6.2 – 6.4, respectively. Table 3.1, complemented by Table 6.2, depicts biochemical pathways and GO terms enriched in leptin-a morphants relative to control arrays ($P < 0.01$). Many coregulated genes that responded to *lepa* knockdown were related to neuron function ("Phototransduction", "GnRH signaling", "Neuroactive ligand-receptor interaction", "Calcium signaling"). KEGG pathways involved in transcriptional and translational processing ("RNA metabolic process", "Ribosome biogenesis in eukaryotes", "RNA transport", "Amino acyl tRNA biosynthesis", "mRNA surveillance pathway", "RNA polymerase", "spliceosome", "mTOR") were also dysregulated in *lepa* morphants. Upregulation of protein-like-argonaute-1 (*LOC570775*) in leptin-a morphants (1.17 logFC) is consistent with activation of the RNAi pathway, and this was also evident in the rescue:morphant comparison [Table 3.2] where protein-like-argonaute-1 was downregulated in rescue arrays (relative to morphants, -1.05 logFC). Interestingly,

protein-like-argonaute-1 was not differentially expressed in the leptin-a rescue:control dataset.

A subset of all pathways returned from the analysis are consistent with gene targets comparable to the mammalian leptin signal transduction pathway ("GnRH signaling", "Phosphatidyl inositol signaling", "Notch signaling", "Metabolic pathways", "FoxO signaling", "MAPK", "Adipocytokine signaling"). KEGG enrichment for "Adrenergic signaling in cardiomyocytes" and "Vascular smooth muscle contraction" corresponds well to the leptin-a knockdown phenotype (pericardial edema) and functional data (decreased metabolic rate) [Liu et al., 2012; Dalman et al., 2013] [Table 3.1]. "Melanogenesis" was enriched in morphant arrays [Table 3.1] and it was also enriched in rescue arrays relative to morphants [Table 3.2] which may suggest a "rescue" of this pathway (decreased pigmentation in leptin-a morphant embryos, pigmentation in rescue embryos was comparable to control) [Liu et al., 2012]. Notably, pathways linked to nitrogen metabolism also responded to leptin-a knockdown (purine/pyrimidine and tryptophan metabolism [Table 3.1]) as well as leptin-a rescue ("Folate", "Glycosphingolipid" and "Glycosaminoglycan" biosynthesis [Tables 3.2 - 3.3]).

KEGG pathways in Table 3.3, complemented by GO terms in Table 6.4, represent enrichment analyses generated from the leptin-a rescue:control contrast ($P < 0.01$). Similarly, KEGG pathways in Table 3.2 are complemented by GO terms in Table 6.3 which describe enrichment in leptin-a rescue (relative to morphant) embryos. Consistent with leptin signaling in mammals, adipocytokine signaling was enriched in

the rescue:morphant contrast [Table 3.2]. All 5 DEG (*jak2a, jak2b, mapk8a, ppargc1a, nfkbie*) were downregulated in rescue arrays (relative to morphants). Adipocytokine signaling was not enriched in the other two comparisons (morphant:control, rescue:control). In the morphant:control contrast, *lepa* and *lepr* were upregulated while adiponectin receptor 2 (*adipor2*) and acetyl Co-A carboxylase beta (*acacb*) were downregulated. Most notably, 13 DEG in the rescue:control contrast were involved in adipocytokine signaling, β-oxidation/fatty acid biosynthesis, and/or PPAR signaling. Downregulated adipocytokine signaling genes from the rescue:control comparison includes AMP-activated kinase (*prkaa2*), Janus kinases (*jak2a, jak2b*), mitogen activated protein kinase (*mapk4, mapk7, mapk10*), acetyl Co-A carboxylase (*acacb*), acetyl-CoA synthetase (*acsbg2*), v-akt oncogene (*akt21*), adiponectin receptor (*adipor2*), PPAR transcriptional coactivator (*ppargc1a*), as well as an NFKα b-cell transcription factor (*nfkbiab*). Upregulated adipocytokine signaling genes extracted from the rescue:control comparison included leptin-b (*lepb*) and glucose-6-phosphatase (*gc6pcb*). Notably, zebrafish development requires mobilization of lipid from the yolk to developing cells, and these enrichment analyses ("Adipocytokine signaling", "Arachidonic acid metabolism", "Glycerophospholipid metabolism") show that leptin-a may participate in embryonic lipid signaling.

KEGG Pathway	Leptin-a Morphant : Control	N	Up	Dwn	P.Up	P.Dwn
path:dre04080	Neuroactive ligand-receptor interaction	313	2	33	0.837059	3.67E-19
path:dre04744	Phototransduction	35	0	15	1	6.09E-19
path:dre03008	Ribosome biogenesis in eukaryotes	63	13	0	4.66E-14	1
path:dre04020	Calcium signaling pathway	216	0	21	1	9.12E-12
path:dre03013	RNA transport	143	15	0	1.44E-11	1
path:dre04330	Notch signaling pathway	46	9	1	7.35E-10	0.503899
path:dre00230	Purine metabolism	165	4	13	0.090157	1.18E-06
path:dre04912	GnRH signaling pathway	107	1	10	0.671048	4.6E-06
path:dre04270	Vascular smooth muscle contraction	114	1	10	0.694249	8.15E-06
path:dre04261	Adrenergic signaling in cardiomyocytes	155	1	11	0.800989	2.17E-05
path:dre00970	Aminoacyl-tRNA biosynthesis	34	5	0	2.3E-05	1
path:dre04514	Cell adhesion molecules (CAMs)	107	1	9	0.671048	3.28E-05
path:dre04114	Oocyte meiosis	125	3	9	0.13772	0.000111
path:dre04310	Wnt signaling pathway	144	8	4	0.000114	0.172981
path:dre03015	mRNA surveillance pathway	76	6	0	0.000125	1
path:dre04115	p53 signaling pathway	62	5	1	0.000425	0.611526
path:dre04916	Melanogenesis	122	5	8	0.008392	0.000506
path:dre04540	Gap junction	107	0	7	1	0.001151
path:dre04530	Tight junction	139	4	8	0.054937	0.001193
path:dre00830	Retinol metabolism	32	1	4	0.282014	0.001291
path:dre04110	Cell cycle	118	6	0	0.001335	1
path:dre01100	Metabolic pathways	1086	11	29	0.568442	0.001575
path:dre04150	mTOR signaling pathway	166	7	3	0.001589	0.459469
path:dre04070	Phosphatidylinositol signaling system	88	0	6	1	0.002101
path:dre03020	RNA polymerase	27	3	0	0.002585	1

path:dre00380	Tryptophan metabolism	39	0	4	1	0.002722
path:dre04320	Dorso-ventral axis formation	28	3	0	0.002874	1
path:dre04623	Cytosolic DNA-sensing pathway	36	3	1	0.005902	0.422082
path:dre03040	Spliceosome	116	5	0	0.006814	1
path:dre03460	Fanconi anemia pathway	40	3	0	0.007928	1
path:dre00983	Drug metabolism - other enzymes	28	0	3	1	0.008375
path:dre04060	Cytokine-cytokine receptor interaction	127	5	2	0.009888	0.574452

Table 3.1: KEGG pathways (FDR < 0.01) in the leptin-a morphant : control contrast.

KEGG Pathway	Leptin-a Rescue : Leptin-a Morphant	N	Up	Dwn	P.Up	P.Dwn
path:dre04330	Notch signaling pathway	46	0	12	1	1.41E-11
path:dre04350	TGF-beta signaling pathway	92	0	11	1	5.76E-07
path:dre04080	Neuroactive ligand-receptor interaction	313	9	3	1.07E-06	0.91709
path:dre04672	Intestinal immune network for IgA production	31	4	0	3.98E-06	1
path:dre04310	Wnt signaling pathway	144	0	12	1	8.4E-06
path:dre03013	RNA transport	143	0	11	1	4.25E-05
path:dre04145	Phagosome	121	5	2	6.34E-05	0.631808
path:dre04320	Dorso-ventral axis formation	28	0	5	1	0.000113
path:dre04010	MAPK signaling pathway	257	0	14	1	0.000175
path:dre04068	FoxO signaling pathway	145	2	10	0.093659	0.000235
path:dre04520	Adherens junction	72	0	7	1	0.000261
path:dre04144	Endocytosis	273	2	14	0.253326	0.000325
path:dre04110	Cell cycle	118	0	8	1	0.001108

path:dre04916	Melanogenesis	122	1	8	0.354156	0.001375
path:dre05168	Herpes simplex infection	157	2	9	0.107036	0.001797
path:dre04933	AGE-RAGE signaling pathway in diabetic complications	103	0	7	1	0.002225
path:dre00790	Folate biosynthesis	20	2	0	0.002246	1
path:dre00532	Glycosaminoglycan biosynthesis - chondroitin sulfate / dermatan sulfate	16	0	3	1	0.002532
path:dre03440	Homologous recombination	33	1	4	0.111081	0.002544
path:dre04150	mTOR signaling pathway	166	0	9	1	0.002629
path:dre00970	Aminoacyl-tRNA biosynthesis	34	0	4	1	0.002844
path:dre00310	Lysine degradation	59	0	5	1	0.003703
path:dre03040	Spliceosome	116	1	7	0.340039	0.004329
path:dre00983	Drug metabolism - other enzymes	28	2	1	0.004389	0.391974
path:dre04070	Phosphatidylinositol signaling system	88	0	6	1	0.004488
path:dre03420	Nucleotide excision repair	39	0	4	1	0.004712
path:dre04810	Regulation of actin cytoskeleton	222	0	10	1	0.005838
path:dre04621	NOD-like receptor signaling pathway	129	3	7	0.010642	0.007677
path:dre04920	Adipocytokine signaling pathway	72	0	5	1	0.008622
path:dre00534	Glycosaminoglycan biosynthesis - heparan sulfate / heparin	25	0	3	1	0.009262
path:dre04510	Focal adhesion	204	1	9	0.520005	0.009952

Table 3.2: KEGG pathways (FDR < 0.01) in the leptin-a rescue : leptin-a morphant contrast.

KEGG Pathway	Leptin-a Rescue : Control	N	Up	Dwn	P.Up	P.Dwn
path:dre04080	Neuroactive ligand-receptor interaction	313	30	69	7.75E-15	1.62E-21
path:dre04010	MAPK signaling pathway	257	4	60	0.659681	4.35E-20
path:dre01100	Metabolic pathways	1086	23	134	0.182348	1.55E-16
path:dre04070	Phosphatidylinositol signaling system	88	0	30	1	2.61E-15
path:dre04020	Calcium signaling pathway	216	6	47	0.174326	1.19E-14
path:dre04144	Endocytosis	273	5	46	0.518666	3E-10
path:dre00534	Glycosaminoglycan biosynthesis - heparan sulfate / heparin	25	0	12	1	7.1E-09
path:dre04060	Cytokine-cytokine receptor interaction	127	13	10	2.64E-07	0.263625
path:dre04114	Oocyte meiosis	125	0	24	1	5.44E-07
path:dre00562	Inositol phosphate metabolism	66	1	16	0.68775	1.8E-06
path:dre04012	ErbB signaling pathway	90	3	19	0.206382	1.9E-06
path:dre04261	Adrenergic signaling in cardiomyocytes	149	2	25	0.737095	4.24E-06
path:dre03020	RNA polymerase	27	6	0	5.45E-06	1
path:dre00564	Glycerophospholipid metabolism	73	1	16	0.724177	7.41E-06
path:dre00230	Purine metabolism	165	6	24	0.067742	7.52E-05
path:dre00240	Pyrimidine metabolism	91	8	7	0.000173	0.335494
path:dre00983	Drug metabolism - other enzymes	28	1	8	0.388942	0.000214
path:dre04145	Phagosome	121	9	10	0.000244	0.218107
path:dre02010	ABC transporters	32	0	8	1	0.000582
path:dre00512	Mucin type O-glycan biosynthesis	21	0	6	1	0.001351
path:dre03050	Proteasome	52	5	1	0.002	0.964738
path:dre00100	Steroid biosynthesis	17	0	5	1	0.002995
path:dre00604	Glycosphingolipid biosynthesis - ganglio series	11	0	4	1	0.003411
path:dre00590	Arachidonic acid metabolism	39	4	1	0.004504	0.918448

path:dre03460	Fanconi anemia pathway	40	4	1	0.004938	0.923538
path:dre04150	mTOR signaling pathway	166	3	19	0.555664	0.006974
path:dre04068	FoxO signaling pathway	145	6	17	0.040581	0.008243
path:dre04140	Autophagy	25	3	4	0.008964	0.065869

Table 3.3: KEGG pathways (FDR < 0.01) in the leptin-a rescue : control contrast.

DIFFERENTIALLY EXPRESSED TRANSCRIPTION FACTORS

Transcriptional regulation of the teleost leptin signal transduction pathway is poorly defined. To identify gene targets regulated by the leptin-a signaling axis, differentially expressed transcription factors (DETF) were extracted from the morphant:control contrast. From a total of 1,461 DEG [Figure 3.9], 7.7%, or 113, (putative) transcription factors were identified [Table 3.4] in leptin-a morphants. Transcription factors (TF), or DNA-binding proteins that function as repressors or activators of gene transcription, are distinguishable by the structural architecture of their DNA-binding-domains as well as the sequence motif(s) that they recognize. Members from different TF families (bHLH, homeobox, winged helix, zinc finger, c-Fos/c-Jun/AP-1, -CCAAT- enhancer-binding proteins, GATA-binding proteins, and *myb*) responded to leptin-a knockdown. Only 20 of these 113 differentially expressed transcription factors were downregulated (17.7%, or 82.3% were upregulated) relative to wild type expression [Table 3.4] which suggests that in addition to transactivation, leptin signaling also play a role in transcriptional repression.

A subset of the leptin-a morphant DEG were analogous to endocrine targets of the mammalian leptin transduction pathway including: agouti related peptide-2 (*agrp2*, -1.2 logFC), cocaine- and amphetamine- regulated transcript protein-like (*LOC557301*, 1.02 logFC), cAMP responsive element binding protein 5 (*creb5*, 1.03 logFC), CCAAT enhancer binding protein (C/EBP) beta (*cebpb*), gonadotropin releasing hormone receptor 4 (*gnrhr4*, -0.76 logFC), growth hormone releasing hormone (*ghrh*, 1.50 logFC)

and thyroid hormone receptor alpha b (*thrab*, -1.26 logFC). Notably, leptin-a (*lepa*, 1.01 logFC) and leptin receptor (*lepr*, 0.77 logFC) expression was also upregulated in morphant embryos. To elucidate homologous transcription factors that regulate zebrafish *lepa* and human *LEP* expression, transcription factors returned from the leptin-a morphant:control comparison [Table 3.4] were compared to putative *LEP* transcription factor binding sites (TFBS) derived from Qiagen's EpiTect ChIP qPCR webtool (Qiagen; Hilden, Germany) [Figure 3.17]. Figure 3.17 illustrates chr7: 127,861,331 – 127,891,3310 flanking human *LEP*. (Putative) TFBS are indicated by green hashes for each corresponding transcription factor; the scaffold spans -20kb to +10kb of the human *LEP* transcription start site (TSS, red arrow). Figure 3.17 indicates the transcription factors that respond to *lepa* knockdown [Table 3.4] also agree with (putative) ChIP peaks flanking *LEP* which together suggests that transcriptional control of the human and zebrafish leptins may be regulated by homologous factors [Figure 3.17 - red rectangles].

Biological processes regulated by the differentially expressed transcription factors [Table 3.4] were explored with the GO (PANTHER) over-representation test, and a subset are listed in Table 3.5. Parent ontologies returned from the leptin-a knockdown transcription factor enrichment analysis ($P < 0.01$) affirms dysregulation of neurogenesis, development (spinal cord, brain, nervous system, columnar/cuboidal epithelial cell), and (negative) regulation of transcription from the RNA polymerase II promoter. Notably, *fosl1a* was differentially expressed in the microarray and qPCR datasets for both contrasts (morphant:control, rescue:control) [Figures 3.14 – 3.15]. In

humans and rodents, *FOSL2* is a transcription factor that drives leptin expression in adipocytes [Wrann et al., 2014], and it belongs to the same protein family as zebrafish *fosl1a* (c-Fos). In mammals, *PPARΥ* encodes a transcription factor involved in adipogenesis while *PPARδ* activates transcription of enzymes involved in lipid metabolism. *ppardb* was differentially expressed in the qPCR dataset as was *pparg* from microarray analysis [Figure 3.16 and Table 3.4]. In summary, a subset of differentially expressed transcription factors from the leptin-a knockdown expression data are putative regulators of the preadipocyte-adipocyte transition as well as lipid metabolism. Intriguingly, zebrafish leptin-a and leptin-b are not expressed in adipocytes.

SYMBOL	(TRANSCRIPTION FACTOR) GENENAME	logFC	adj.P.Val
ascl1a	achaete-scute complex-like 1a (Drosophila)	1.639281	0.000137
ascl1b	achaete-scute complex-like 1b (Drosophila)	0.880268	0.000934
atf3	activating transcription factor 3	1.549587	0.000116
atf4b1	activating transcription factor 4b1 (tax-responsive enhancer element B67)	1.112514	0.006134
atf5a	activating transcription factor 5a	0.780766	0.00945
atf5b	activating transcription factor 5b	2.173439	0.000247
arvcfa	armadillo repeat gene deleted in velocardiofacial syndrome a	-0.63659	0.004484
ahctf1	AT hook containing transcription factor 1	0.615992	0.004927
atoh1a	atonal homolog 1a	0.882311	0.002553
atoh1b	atonal homolog 1b	1.194614	0.000195
atoh7	atonal homolog 7	1.175818	0.004727
brn1.2	brain POU domain gene 1.2	0.821051	0.00146
baz1b	bromodomain adjacent to zinc finger domain, 1B	0.850687	0.000887
LOC563263	BTB/POZ domain-containing protein 17-like	-1.21626	0.007188
cebpb	CCAAT/enhancer binding protein (C/EBP), beta	1.253994	0.001079
ENSDART00000130365	cAMP responsive element binding protein 5	1.026471	0.000174
cbx7a	chromobox homolog 7a	2.17303	0.000176
dbx1a	developing brain homeobox 1a	1.371367	0.000113
dbx1b	developing brain homeobox 1b	1.042267	0.00199
diexf	digestive organ expansion factor homolog	0.875053	0.006232
LOC571757	DNA-binding protein SATB1-like	-0.74766	0.004249
ddit3	DNA-damage-inducible transcript 3	0.697482	0.003847
foxj1a	forkhead box J1a	0.985218	0.000992
foxk2	forkhead box K2	0.890444	0.000531
foxn4	forkhead box N4	2.188575	1.01E-05
foxp1b	forkhead box P1b	0.67917	0.008807
fosl1a	FOS-like antigen 1a	2.512919	0.000113
LOC100005923	gastrula zinc finger protein XlCGF57.1-like	0.708328	0.003388
gli1	GLI-Kruppel family member 1	0.759583	0.002308
hes2.1	hairy and enhancer of split 2.1	1.608187	0.001299
hes2.2	hairy and enhancer of split 2.2	1.896599	8.85E-05
hes6	hairy and enhancer of split 6 (Drosophila)	0.566489	0.002999
her15.1	hairy and enhancer of split-related 15.1	1.370323	0.000497
her13	hairy-related 13	1.456074	0.000651
her2	hairy-related 2	1.02274	0.008525
LOC100149066	hairy-related 4.2-like	1.03035	0.001667
hoxb2a	homeo box B2a	0.582927	0.005872
hoxb4a	homeo box B4a	0.570699	0.006165
hoxb6a	homeo box B6a	0.566886	0.007204

hoxb8b	homeo box B8b	1.256222	0.000649
hoxc1a	homeo box C1a	1.376224	0.002796
LOC556898	homeobox protein MOX-2-like	-1.04643	0.003256
homez	homeodomain leucine zipper gene	1.382255	0.000608
insm1a	insulinoma-associated 1a	1.767329	3.43E-06
insm1b	insulinoma-associated 1b	1.46487	6.67E-05
irx3b	iroquois homeobox protein 3b	1.071278	0.00578
irx5b	iroquois homeobox protein 5b	0.757243	0.001768
klf5b	Kruppel-like factor 5b	-0.92814	0.004611
lbx1b	ladybird homeobox 1b	1.072177	0.000349
smad3b	MAD, mothers against decapentaplegic homolog 3b (Drosophila)	0.764496	0.008343
mkxb	mohawk homeobox b	-0.93251	0.008365
mybbp1a	MYB binding protein (P160) 1a	1.369228	0.001774
LOC100536821	myelin transcription factor 1-like	1.046164	0.00097
neurod4	neurogenic differentiation 4	1.019373	0.000444
neurod6b	neurogenic differentiation 6b	-0.88382	0.000853
neurog1	neurogenin 1	1.919667	1.38E-05
npas4a	neuronal PAS domain protein 4a	-1.36542	0.001926
nkx1.2lb	NK1 transcription factor related 2-like,b	0.630126	0.002776
nkx6.1	NK6 transcription factor related, locus 1 (Drosophila)	1.170579	0.002328
nfixa	nuclear factor I/Xa	-1.13836	0.000617
nfixb	nuclear factor I/Xb	-1.33266	0.000161
NFAT5	nuclear factor of activated T-cells 5, tonicity-responsive	-0.80653	0.007982
nfxl1	nuclear transcription factor, X-box binding-like 1	0.837558	0.002751
olig3	oligodendrocyte transcription factor 3	1.296721	0.001014
olig4	oligodendrocyte transcription factor 4	1.361349	0.000583
onecut1	one cut domain, family member 1	1.432696	5.47E-05
onecutl	one cut domain, family member, like	0.746868	0.008553
LOC100534691	oocyte zinc finger protein XlCOF6-like	0.730068	0.003669
pax2b	paired box gene 2b	1.11643	4.72E-05
pax5	paired box gene 5	1.105964	0.002491
pparg	peroxisome proliferator activated receptor gamma	-1.02615	0.004229
PHF21B	PHD finger protein 21B	1.254608	0.000166
pou2f3	POU class 2 homeobox 3	-0.86371	0.007054
pou3f1	POU class 3 homeobox 1	0.95103	0.000338
pou2f2a	POU domain, class 2, transcription factor 2a	1.60189	2.71E-06
LOC100534934	POU domain, class 2, transcription factor 2-like	0.904319	0.001331
prdm1b	PR domain containing 1b, with ZNF domain	1.681238	0.000253
LOC100003615	PR domain zinc finger protein 2-like	-0.73747	0.009637
LOC100004079	PR domain zinc finger protein 8-like	-1.378	0.009851

rfx4	regulatory factor X, 4	0.855663	0.001451
rcor2	REST corepressor 2	0.826858	0.002363
scrt2	scratch homolog 2, zinc finger protein (Drosophila)	1.030575	0.002735
slit1b	slit homolog 1b (Drosophila)	0.80692	0.001768
sp8b	sp8 transcription factor b	0.824869	0.001052
sox11b	SRY-box containing gene 11b	1.294473	0.000261
LOC100003272	storkhead-box protein 2-like	0.660256	0.003048
suz12a	suppressor of zeste 12 homolog (Drosophila) a	0.687189	0.004494
tcf4	transcription factor 4	-1.05762	0.000243
tfap4	transcription factor AP-4 (activating enhancer binding protein 4)	0.954931	0.004727
tfdp2	transcription factor Dp-2	0.964761	0.002363
LOC100332016	transcription factor SOX-8-like	-0.75394	0.004437
vezf1a	vascular endothelial zinc finger 1a	1.27925	0.000521
vsx2	visual system homeobox 2	1.274472	0.000175
mybl1	v-myb myeloblastosis viral oncogene homolog (avian)-like 1	0.867444	0.002619
mycl1a	v-myc myelocytomatosis viral oncogene homolog 1, lung carcinoma derived (avian) a	0.854331	0.000261
mycn	v-myc myelocytomatosis viral related oncogene, neuroblastoma derived (avian)	0.905871	0.001749
whsc1	Wolf-Hirschhorn syndrome candidate 1	1.007415	0.000326
zic2b	zic family member 2 (odd-paired homolog, Drosophila) b	0.975633	0.000346
zbtb18	zinc finger and BTB domain containing 18	0.655175	0.006372
znf259	zinc finger protein 259	1.323035	0.002893
LOC100334443	zinc finger protein 36, C3H1 type-like 1-like	1.423082	0.001145
znf385b	zinc finger protein 385B	-0.81349	0.003699
LOC100536867	zinc finger protein 568-like	0.760187	0.00624
LOC100538284	zinc finger protein 569-like	0.598682	0.009397
LOC100536110	zinc finger protein 658-like	0.932071	0.008289
znf804a	zinc finger protein 804A	-0.82148	0.007841
LOC100333582	zinc finger protein GLIS2-like	1.073396	0.000639
zfpm2a	zinc finger protein, multitype 2a	-0.85606	0.007019
zranb3	zinc finger, RAN-binding domain containing 3	0.654255	0.005297
zhx3	zinc fingers and homeoboxes 3	0.756545	0.003884

Table 3.4: Differentially expressed transcription factors from the leptin-a morphant : control contrast. Complementary GO enrichment is provided in Table 6.5.

GO Biological Process	Transcription Factor GO Enrichment	P.value	Fold Enrichment	Ref. List 27187	Input	Expect
GO:0006355	regulation of transcription, DNA-templated	5.21E-32	3.4	1776	11.48	39
GO:0010468	regulation of gene expression	5.26E-30	3.83	2005	10.17	39
GO:0006351	transcription, DNA-templated	5.19E-29	1.53	800	19.61	30
GO:0032774	RNA biosynthetic process	6.23E-29	1.54	805	19.48	30
GO:0016070	RNA metabolic process	1.46E-23	2.63	1377	11.77	31
GO:0010467	gene expression	1.33E-21	3.06	1602	10.12	31
GO:0006139	nucleobase-containing compound metabolic process	1.44E-18	3.88	2029	7.99	31
GO:0048856	anatomical structure development	1.79E-15	6.42	3359	5.29	34
GO:0032502	developmental process	5.39E-15	6.65	3479	5.11	34
GO:0048731	system development	6.54E-10	5.08	2656	5.12	26
GO:0006357	regulation of transcription from RNA polymerase II promoter	7.07E-09	1.08	563	13	14
GO:0007399	nervous system development	7.66E-09	2.57	1345	7.39	19
GO:0030154	cell differentiation	2.69E-08	3.15	1649	6.34	20
GO:0048869	cellular developmental process	3.34E-08	3.19	1669	6.27	20
GO:0048513	animal organ development	1.94E-07	3.52	1841	5.68	20
GO:0007417	central nervous system development	1.77E-05	1.04	542	10.61	11
GO:0021510	spinal cord development	6.26E-04	0.13	66	39.61	5
GO:0051960	regulation of nervous system development	9.61E-04	0.44	231	15.84	7
GO:0002065	columnar/cuboidal epithelial cell differentiation	3.08E-03	0.07	38	55.03	4
GO:0048699	generation of neurons	5.95E-03	1.48	776	6.74	10

Table 3.5: GO Biological process. Enrichment analysis ($P < 0.01$) using differentially expressed transcription factors from the leptin-a morphant : control comparison.

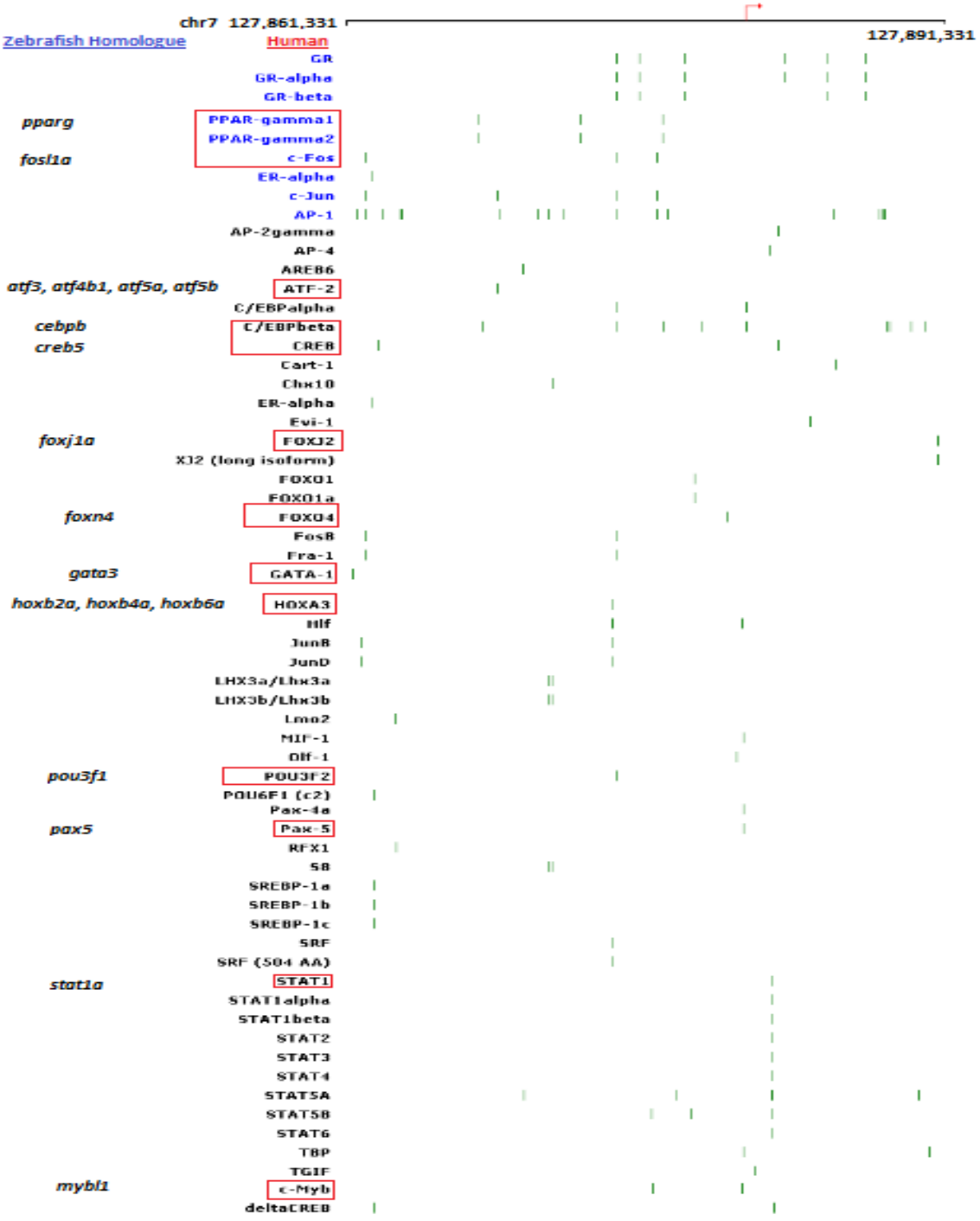

Figure 3.17: The human *LEP* transcription start site (TSS) is denoted with a red arrow. Transcription factor binding sites are indicated with green hashes. Image modified from the Qiagen Champion ChIP Transcription Factor Search Portal (SABiosciences - DECODE).

CHAPTER IV

DISCUSSION

The molecular mechanisms by which leptin signaling regulates the embryonic transcriptome are unclear and functional data available for non-mammal leptins are lagging behind their mammalian counterparts. To address this, our group is using zebrafish as a comparative analog to study the leptin signal transduction pathway in a basal vertebrate. Leptin-a morpholino oligonucleotide (MO) knockdown disrupts embryonic pigmentation as well as eye, otolith, brain, spinal cord, and pericardial cavity morphology. A partial morphological rescue of these developmental miscues was attained with co-injection of leptin-a morpholino oligonucleotides and recombinant leptin-a protein (rLEPA); leptin-a rescue was dose-dependent where embryos microinjected with increasing concentrations of rLEPA resembled control morphology [Liu et al., 2012]. Morpholino oligonucleotides (MO), directed against zebrafish leptin-a mRNA, were microinjected into 1-2 cell embryos as a means to knockdown, or repress translation, of the *lepa* gene product [Figure 3.1]. Commensurable leptin-a "rescue" microinjections were prepared with *lepa* MO's in tandem with rLEPA (1:1) as detailed previously [Liu et al., 2012]. Leptin-a "knockdown" describes the response to reduced leptin signaling on the embryonic transcriptome while leptin-a "rescue" represents a

combination of responses to both *lepa* morpholino knockdown and exogenous leptin on 48 hpf gene expression. Notably, these are the first whole-transcriptome expression data (26,046 genes) describing the role of zebrafish leptin-a at 48 hpf.

Candidate pathways and genes returned from the *lepa* morpholino knockdown and rescue expression microarray dataset correspond well to experimental observations ("Phototransduction" – reduced eye size, retinal ganglia; "Melanogenesis" – reduced pigmentation, "Adrenergic signaling in cardiomyocytes" – pericardial edema, reduced metabolic rate; "Dorso-ventral axis differentiation" – bent notochord; "Inositol phosphate" and "Glycerophospholipid" metabolism – enlarged yolk) [Liu et al., 2012; Dalman et al., 2013]. This investigation tested the null hypothesis that the zebrafish leptin-a signaling axis regulates gene targets analogous to the mammalian leptin signal transduction pathway, or adipocytokine model, including: endocrine signaling [Malendowicz et al., 2007], gonadotropin signaling [Israel et al., 2012], insulin signaling [Perez et al., 2004], lipid metabolism [Minokoshi et al., 2002], and glucose homeostasis [Hill et al., 2010]. Consistent with the null hypothesis, KEGG analyses support the notion that zebrafish leptin-a regulates "Neuroactive ligand-receptor interactions", "GnRH", as well as "Adipocytokine" signaling [Tables 3.1 – 3.3]. Additional ontologies that responded to leptin-a included: "Anatomical structure morphogenesis", "Cell differentiation", and "Neurogenesis", as well as cellular pathways related to "Animal organ", "Central nervous system", "Spinal cord", "Brain", "Epithelium", and "Chordate embryonic" development [Tables 6.2 – 6.4] which, together, may link leptin signaling to regulative development.

Zebrafish leptin-a regulates 48 hpf lipid signaling. (KEGG) Pathway enrichment in the leptin-a rescue:control contrast reveals functional elements that correspond well to the mammalian leptin adipostat model including: “MAPK”, “PI”, “Calcium signaling”, and “Glycerophospholipid metabolism” signaling as well as (long chain) “Arachidonic acid metabolism” and “Metabolic pathways” [Table 3.3]. Consistent with increased *LEP* expression in rescue arrays, acyl CoA carboxylase-b (*acacb*), which regulates a committed step of fatty acid biosynthesis, was downregulated as was pantothenate kinase-2 (*pank2*, -0.76 logFC) which similarly regulates a committed step of Co-enzymeA biosynthesis (-2.25 logFC). Sterol regulatory element binding transcription factor-2 (*srebf2*) was downregulated in rescue embryos (-0.89 logFC). Transactivation of the *SREBP1* promoter by *SREBF2*, the human homologue of zebrafish *srebf2,* induces expression of enzymes linked to sterol biosynthesis and lipid homeostasis [Eberlé et al., 2004]. Consistent with increased leptin signaling and lipid catabolism, (KEGG) “Steroid biosynthesis” was under-represented in leptin-a rescue embryos [Table 3.3]; enzymes involved in cholesterol biosynthesis pathways were downregulated (*msmo1, faxdc2*). Notably, peroxisome-proliferator activated receptor gamma (*pparg*) and its transcriptional coactivator, *ppargc1a* were both dysregulated in leptin-a rescue embryos, and *pparg* was additionally downregulated in leptin-a morphants. Many DEG from the microarray analysis were linked to lipid metabolism (diacylglycerol lipase alpha and beta, adiponectin receptor-2, apolipoprotein-F, lipoprotein lipase, fatty acid desaturase-6, perilipin-1, carnitine palmitoyl transferase, fatty acyl CoA reductase 1), glucose regulation (aldolase b, phosphofructokinase, pyruvate kinase, glucagon-like-2

peptide receptor, glucose-6-phosphatase, facilitated glucose transporters, glucose-6-phosphate dehydrogenase), and energy homeostasis (cAMP-dependent protein kinase, AMP-activated protein kinase).

Zebrafish leptin-a regulates 48 hpf endocrine physiology. (KEGG) "Neuroactive ligand-receptor interactions" were enriched in all three contrasts [Tables 3.1 – 3.3], and homologous neuropeptide targets of the human leptin signal transduction pathway were dysregulated in both leptin-a morphant and rescue embryos (agouti-related-peptide-2 (*agrp2*); cocaine-and-amphetamine-related-transcript-protein-like (*LOC557301*)). Further, catalytic cAMP-dependent kinase (*prkacaa* and *prkacab*), protein kinase cAMP-dependent regulatory type II (*prkar2aa*, *prkar2ab*), as well as AMP-activated kinase (*prkaa2*) were downregulated in leptin-a rescue embryos relative to wild type. Transcription factors involved in the regulation of cAMP secondary messaging were downregulated in both leptin-a rescue (*crebl2* and *creb3l3*) and morphant (*creb5*) embryos relative to controls. According to the Human protein atlas (http://www.proteinatlas.org/), *CREB5* has the highest density of expression in gall bladder and brain which coincides well with alterations in KEGG "Sterol biosynthesis", "Glycerophospholipid biosynthesis", "Glycosphingolipid biosynthesis", "Arachidonic acid metabolism", and "Inositol phosphate metabolism" [Table 3.3] in leptin-a rescue embryos.

The role of leptin signaling in zebrafish physiology is not well characterized due in part to the paralogous copies of the leptin gene as well as a general lack of sequence

homology with mammals [Gorissen et al., 2009]. These microarray data provide insight into the potential regulatory targets of the leptin-a signaling axis during 48 hpf teleost embryogenesis, and the suggested mechanism is described. Leptin-a signaling in the brain may stimulate endocrine hormone production (e.g. *gnrh2*) which leads to peripheral circulation of additional neuropeptides secreted from the hypothalamus, pituitary, and thyroid. The central endocrine peptide efflux, refractory to leptin receptor stimulation in the brain, facilitates hormone receptor signaling in gall bladder and liver through cAMP/Ca^{2+}/PKA secondary messaging. This system likely regulates hepatic receptivity of sterol and lipid (*apof, srebf2, pparg, prkaa2, vldlr*) through feedback loops initiated with AMPK (*prkaa2*) in the CNS. In short, the gall bladder and liver may maintain sterol and lipid homeostasis through endocrine transduction pathways that respond to leptin-a. Endocrine peptide efflux may then increase intracellular cAMP/Ca^{2+} in peripheral tissues (using hormone receptor or GCPR signaling) which activate intracellular kinases (*prkacaa, prkacab*) as well as hormone-sensitive-lipases (*dagla, daglb, lpl, LOC567728*). Consequently, many DEG were linked to adenylate cyclase (*adcy2a, adcy3l*, *adcy6a*, *adcyap1r1*, *LOC560410*), calcium signaling (*adrb1, grm1a, calm1a, camk2a, camk4, plcb4, itpr1a*), and G-coupled protein receptor signaling pathways (*grk7a, rgs7, rgs7bpa, rgs7bpb, rgs3b, rgs9b, rgs9bp*). Pathway enrichment ("Smooth muscle contraction", "Adrenergic signaling in cardiomyocytes") as well as dysregulation of adenylate cyclase 2a (*adcy2a*) and adrenergeic receptor 1 beta (*adrb1*), may also link leptin-a to muscle function through GCPR/cAMP/Ca^{2+} secondary messaging.

113 differentially expressed transcription factors (DETF) from the morphant:control comparison [Table 3.4] mapped to GO Biological Process annotations for “Central nervous system development”, “Neurogenesis”, “Regulation of transcription from the RNA pol. II promoter”, and “Epithelial cell differentiation” [Table 3.5]. Only 20/113 (17.7%) of DETF were downregulated which was interesting given that 876/1,461, or 60.0%, of all morphant:control DEG were downregulated [Figure 3.9], and one should expect 68/113 (60%) of DETF to be downregulated by equal prediction. Comparison of putative transcription factor binding sites flanking the *LEP* TSS to differentially expressed transcription factors extracted from the *lepa* knockdown dataset [Table 3.4] reveals homologous factors that are likely tied to leptin expression in zebrafish and human [Figure 3.17] (*cebpb, creb5, fosl1a, foxn4, mybl1, pax5, pou3fl1, pparg*, *stat1a*). Indications taken from this analysis suggest that a subset of factors involved in transcriptional regulation of the leptin system are conserved from teleost (lower vertebrate) to human (higher vertebrate).

Transcription factors (*foxn4, insm1a*, *neurog1, pou2f2a*), notch pathway genes (*notch1a, dla, dlb, dld*), as well as genes involved in visual perception (*gngt2b, gng3a, gng3b, arr3b, opn1lw1, prph2b*) were among the top-50 DEG in the morphant:control comparison [Figure 3.11]. Of the top-50 DEG in the rescue:control comparison [Figure 3.13], odorant receptors (*odr115-6, odr125-4, odr125-2*) were upregulated providing additional evidence in support of leptin-a as a regulator of sensory organ development. Additionally, notch is a juxtacrine signaling pathway that participates in neurogenesis, cellular differentiation, and many cancers [Wakeham 1997; Artavanis-Tsakonas et al.,

1999; Stylianou et al., 2003; Murtaugh et al., 2003]. Leptin signaling is associated with Notch1 upregulation in human and mouse breast cancer (BC) cell lines. Upregulation of the leptin/notch1 signaling axis is linked to increased murine E0771 BC cell migration. This association is enriched in diet-induced-obese mice inoculated with E0771 cells, and a leptin inhibitor downregulated Notch1 expression in this cell line [Battle et al., 2014]. "Notch signaling" was the most over-represented pathway returned from leptin-a morphant KEGG analysis [Table 3.1]. In contrast, leptin-a rescue (KEGG) "Notch signaling" was not significant ($P < 0.01$) [Table 3.3], and "Notch signaling" was under-represented in rescue (relative to morphant) embryos [Table 3.2] which affirms that the notch pathway responds to leptin-a. Further, this notion implies that zebrafish likely maintain a leptin/delta/notch axis (*lepa, lepb, lepr, notch1a, notch1b, dla, dlb, dld*) [Figure 3.11]. Notably, the leptin/notch axis may also play a facultative role in zebrafish eye development as well as regulation of the phototransduction cascade. Figure 3.11 indicates that notch versus phototransduction pathways show reciprocal trends in differential expression among the top-50 DEG between leptin-a morphants and wild type embryos. Transcriptional repression of the notch pathway in retinal progenitor cell populations, possibly through crosstalk with leptin-a, may be required for programming photoreceptor, horizontal, amacrine, and retinal ganglion cell identities.

In the top-50 leptin-a rescue:control DEG [Figure 3.13], *map3k12,* a calcium-sensitive kinase expressed in nervous tissue and regulates the activity of PKA, neurogenesis, and the retinoic acid pathway in mammals [Oetjen et al., 2016] was downregulated. Interleukin (1b, 4, 10, 11b, 12Ba, 15, 17a/f3, 26, 34), interferon (gamma

1-1, gamma 1-2, phi 1, phi2), and immunoglobin (heavy variable 4-5, 21a, 21b) members were differentially expressed in the rescue:control contrast which supports leptin signaling in teleost immune response. TGF-β is an inhibitory signaling pathway, regulated by IL-6, that modulates the activity of G_1 phase cyclin dependent kinases in mammals [Koff et al., 1993]. (KEGG) "TGF-β signaling" was under-represented in rescue arrays relative to morphants as was "Cell cycle" [Table 3.3]. *cdk11b* regulates the G2-M checkpoint of the cell cycle, and it was among the top-50 DEG in the rescue:morphant comparison [Figure 3.12]. Interestingly, activation of leptin receptor induces IL-6 expression in human fibroblast [Yang et al., 2013]. Hence, zebrafish leptin-a may similarly act as a modulator of cell cycle progression via feedback between interleukin expression and "TGF-β" signaling [Table 3.3].

"Phototransduction" and "Neuroactive ligand-receptor interaction" were enriched in the morphant:control contrast which coincides well with leptin-a knockdown phenotypes (small eyes, disrupted retinal ganglion cell morphology, dorsal brain patterning, bent notochord, and reduction of spinal nerves) [Liu et al., 2012]. Notably, visual system homeobox-2 (*vsx2*) was upregulated in both morphant (1.27 logFC) and rescue arrays (0.67 logFC) relative to wild type embryos. In mammals, null mutations within either of two conserved DNA binding domains of *VSX2* are associated with varying degrees microopthalmia, or small, non-functional eyes and hyperpigmented neural retinas [Zou and Levine 2012]. Importantly, dysregulation of *vsx2* coincides well with the leptin-a knockdown phenotype (small eyes, lack of pigmentation, reduced opsin expression) [Liu et al., 2012]. In zebrafish, *vsx2* functions

as a transcriptional repressor of other transcription factors (*vsx1*, *foxn4*, and *atoh5*) involved in ocular/retinal differentiation; dysregulation of *vsx2, foxn4*, *atoh1a, atoh1b*, *atoh7* in leptin-a morphants corroborate this notion [Table 3.4]. Zebrafish retinal progenitor- *vsx2* -expressing cell populations are restricted in their terminal cell fates (amacrine, hotizontal, retinal ganglion, photoreceptor), while retinal progenitor pools that do not express *vsx2* retain a multipotent state of differentiation [Vitorino et al., 2009]. Both *lepa* (1.01 logFC) and *vsx2* (1.27 logFC) messages are upregulated in morphant embryos. Spatial and temporal leptin-a expression in retinal progenitor cell populations may be critical to program photoreceptor, horizontal, amacrine, and retinal ganglion cell fates. In summary, oscillations in expression between leptin-a, homeobox genes (e.g. *vsx2*), and embryonic transcription factors [Table 3.5] may shape the transcriptional landscape of the developing eye, central nervous and endocrine systems, as well as the notochord.

Fourteen DEG mapped to phototransduction KEGG annotations from the leptin-a morphant:control contrast (*rho, gc3, gnat2, rgs9a, grk7a, grk1b, rcvrna, gnat1, saga, pde6a, pde6b, calm1a, calm1b, guca1b, grk1a*). In all comparisons, opsin members (*rho, opn1mw1*, *opn1sw1*, *opn1lw1*) were among the most downregulated genes in the dataset. Further, GO enrichment returned downregulation of GABA receptor activity in the morphant:control as well as rescue : control contrasts but not the rescue : morphant contrast indicating that GABA receptor activity was comparable between both knockdown and rescue. In short, there was no significant difference in GABA receptor activity between morphant or rescue embryos. The (KEGG) phototransduction pathway

was not enriched in the leptin-a rescue:control contrast at (FDR < 0.01) [Table 3.3], and KEGG phototransduction was not significant when comparing rescue arrays to morphant arrays [Table 3.2]. However, GO enrichment (FDR < 0.01) for "Visual perception" in all three contrasts suggests that rLEPA rescue was insufficient to compensate for embryonic depletion of leptin-a [Tables 6.2 – 6.4]. Dysregulation of phototransduction may stem from a transient developmental window requiring leptin signaling to, perhaps indirectly, induce expression of opsin members as well as components of the phototransduction signaling cascade in the developing zebrafish eye. Interpretations drawn from these enrichment data indicate that phototransduction (GCPR) and visual perception (opsin) as well as GABA activity (neurotransmitters) did not respond to rLEPA.

Comparison of leptin-a morphant expression data to published zebrafish morpholino knockdown datasets reveals consistent enrichment results shared between unrelated datasets which includes dysregulation of phototransduction and p53 signaling. Leptin-a morphants share extensive morphological markers comparable to unrelated zebrafish morpholino studies including: pericardial edema, enlarged yolk sac, reduced eye and otolith size, and tail curvature [Pham et al., 2007; Robu et al., 2007; Liu et al., 2012; Bagci et al., 2015; Kok et al., 2015; Kwon 2016]. Due to the similarities in developmental morphology as well as the inconsistencies between phenotypes of morphants and CRISPR/TALEN mutants [Kok et al., 2015], these data indicate that a subset of genes returned from the analysis could be a response to non-specific morpholino effects. Morpholino off-targeting obscurely promotes transcription of an N-

terminal truncated *tp53* isoform which may be associated with neuron death and cranio-facial abnormalities [Robu et al., 2007]. At adjusted P.value < 0.01 and $\log_2$ fold change < -0.5 or > 0.5, leptin-a morphant DEG mapped to upregulation of "p53 signaling" (*ccng2, sesn2, ccnd1, igf1, cdk6*) although *tp53* was not differentially expressed at this criterion [Table 3.1]. "p53 signaling" in the rescue:control contrast was not significant (P < 0.01), although TP53 dependent G2 arrest mediator candidate-a (*rprma*) was downregulated as was tumor protein p53 binding protein 2-like (*LOC793439*) hinting that leptin-a may avert apoptotic signaling. However, this observation could be related to the role of leptin signaling in cell survival through crosstalk with the MAPK cascade [Takahashi et al., 1997]. Notably, neurogenin-1 (*neurog1*), a bHLH transcription factor which regulates neurogenesis and cell differentiation, was upregulated in both morphant and rescue arrays relative to controls. However, this may be a candidate marker regulated non-specifically by morpholinos as it is reported in (unrelated) zebrafish knockdown studies featuring eye and brain defects [Leung et al., 2008; Bagci et al., 2015].

"Morphant" and commensurable "mutant" phenotypes are often inconsistent; morphants do not mimic mutant phenotypes [Kok et al., 2015; reviewed: Stainier et al., 2015; reviewed: Lawson 2016]. However, no studies have directly addressed potential discrepancies in developmental physiology or gene regulation between knockout vs. morpholino knockdown of zebrafish leptin signaling. Comparison of leptin-a knockdown expression data to morpholino literature highlighted candidate genes and pathways that may be artifacts of morpholino knockdown ("Phototransduction" and "Visual

perception", "P-53 signaling", and "ncRNA metabolic processes") [Robu et al., 2007; Leung et al., 2008; Bagci et al., 2015]. Unrelated zebrafish morphants often share combinations of morphological markers ranging from disrupted eye, ear, and brain development, irregular body/tail curvature, pericardial edema, and/or enlarged yolk [Lorent et al., 2004; Rai et al., 2007; Robu et al., 2007; Danilova et al., 2008; Ulitsky et al., 2011; Liu et al., 2012; Bagci et al., 2015; Kok et al., 2015; Kwon 2016; Pinto et al., 2016]. Non-specific *in vivo* activity of splice-blocking and translational inhibitor MO's stimulates transcription of *tp53* which is likely associated with neuron atrophy [Robu et al., 2007]. Co-knockdowns of *p53* and target mRNA's in tandem alleviate the phenotypes associated with p53 signaling activation refractory to morpholinos [Robu et al., 2007; Padanad and Riley 2011; Kwon 2016], however, the biological relevance of these approaches should be interpreted with hesitation.

CHAPTER V

CONCLUSIONS

In accord with a lack of functional, biochemical, and structural evidence, the role of the leptin signal transduction pathway in teleost physiology is not clear nor are the regulatory factors that govern expression of the zebrafish leptin paralogues (*lepa*, *lepb*) or the leptin receptor (*lepr*). Leptin is expressed in human embryos [Antczak and Van Blerkom 1997] but there is little experimental evidence that substantiates the molecular function of leptin signaling in regulative development. To address this, morpholino oligonucleotide knockdown of leptin-a elicited a potent effect on embryonic zebrafish development (small eyes/otoliths, reduced metabolic rate, pericardial edema, notochord curvature, reduced pigmentation, thinning of spinal nerves, enlarged yolk sac); embryos microinjected (1:1) with both recombinant leptin-a (rLEPA) and *lepa* morpholinos, or "leptin-a rescue" embryos, resemble wild type (48 hpf) morphology [Liu et al., 2012; Dalman et al., 2013]. Microarray KEGG and GO enrichment analyses of leptin-a "morphant" and "rescue" expression data correspond well to analogues of the mammalian leptin signal transduction pathway ("GnRH signaling", "MAPK signaling", "Adipocytokine signaling", "Phosphatidylinositol signaling", "Neuroactive ligand-receptor interaction", "Notch signaling", "mTOR signaling", "ErbB signaling", "FoxO

signaling"). Importantly, these data indicate leptin-a functions as an endocrine regulator in 48 hpf zebrafish embryos.

Gene targets analogous to the human leptin/JAK-STAT neuroendocrine axis were differentially expressed in the leptin-a microarray dataset including: agouti related peptide-2 (*agrp2*), cocaine-and amphetamine-related transcript like-1 (*cart1*), cocaine- and amphetamine-regulated transcript like-protein (*LOC557301*), neuropeptide Y receptor 8a (*npy8ar*), oxytocin receptor (*oxtr*), gonadotropin releasing hormone-2 (*gnrh2*), melanocortin 5a receptor (*mc5ra*), melanin-concentrating hormone receptor 1a (*mchr1a*), melanocortin 2 receptor accessory protein (*mrap*), thyroid stimulating hormone beta subunit (*tshb*), thyroid hormone receptor alpha b (*thrab*), prolactin releasing hormone (*prlh*), corticotropin releasing hormone receptor 1 (*crhr1*), glucocorticoid induced transcript 1 (*glcci1*), dopamine receptor D4b (*drd4b*), growth hormone releasing hormone (*ghrh*), janus kinase 2a (*jak2a*), janus kinase 2b (*jak2b*), and hippocampus abundant transcript 1a and 1b (*hiat1a, hiat1b*). A subset of transcription factors that respond to leptin-a knockdown are homologous to putative regulators of human *LEP* expression (*fosl1a, stat1a*, *pparg*, *cebpb, creb5, mybl1, foxn4*, *pax5, pouf3l1*) [Figure 3.17] which suggests that many regulatory elements of the leptin system are maintained between zebrafish and human.

KEGG "Phosphatidylinositol signaling", "Calcium signaling", "G-protein signaling", and "MAPK signaling", which likely form one signaling axis, were enriched in the leptin-a rescue:control contrast [Table 3.3]. GCPR (*gpr7, gpr18, gpr22, gpr37b, gpr39, gpr101,*

gpr176, gpr183), adrenergic receptor (*adrb1*), and hormone receptor (*esrrga, LOC100534744, glp2r, insra, igf1ra, thrab, pthr1a*) activation in gall bladder, liver, and extrahepatic tissues likely respond to endocrine peptides secreted refractory to leptin-a signaling in the brain. This system levers lipid (*pparg*) and sterol (*srebf2*) homeostasis through adenylate cyclase (*adcy2a*) and cAMP/Ca^{2+} secondary messaging. Peripheral cAMP/Ca^{2+} flux modulates the activity of protein kinases A, B, or C (*prkar1b*, *prkar2ab*, *prkacaa, prkacab, prkcba, prkcea, prkcbb*), calmodulin kinases (*camk1db, camkk2, camk4, cask*), and cAMP-sensitive transcription factors *cebpb* and *creb5*. Sterol regulatory element binding factors (e.g. *srebf2*) and peroxisome proliferator activated receptors (e.g. *pparg, ppargc1a*) may also act as intracellular lipid and sterol (*apof, srebf2, pparg, prkaa2, vldlr*) sensors in gall bladder and liver. After PKA activation through adenylate cyclase (*adcy2a, adcy3l*, *adcy6a*, *adcyap1r1*, *LOC560410*) and G-coupled protein receptor signaling pathways (*grk7a, rgs7, rgs7bpa, rgs7bpb, rgs3b, rgs9b, rgs9bp*), hormone-sensitive-lipases (*dagla, daglb, lpl, plcg1, pla2g6*), perilipin (*plin1*), and carnitine palmitoyl transferase beta (*cpt1b*) increase fatty acid transport from liver and adipose into the blood for uptake by high-respiring tissues (e.g. muscle). Together, the leptin-a/cAMP axis likely compensates for energy demand through feedback loops between leptin-a expression, endocrine hormone secretion, AMP-activated protein kinase (*prkaa2*) in the brain, and sterol/lipid metabolism in gall bladder, liver, and muscle.

Some genes from the leptin-a microarray dataset may include morpholino artifacts ("Phototransduction" and "P-53 signaling") that are irrespective of changes in leptin-a

expression. The biochemical and kinetic mechanisms underlying *in vivo* morpholino knockdown are obscure. Genes involved in intracellular RNA defense responded to leptin-a knockdown including upregulation (1.17 logFC) of protein argonaute-1-like (*LOC570775*) as well as "mRNA surveillance pathway", "ncRNA metabolism", "ncRNA processing", "RNA transport", and "RNA binding". Morpholino:mRNA double stranding could potentially activate the RISC/argonaute complex leading to the ubiquitous enrichment of "p53 signaling" in zebrafish morpholino studies [Robu et al., 2007]. As a generality, most RNA species in metazoan cells are classified as rRNA's, and ontologies associated with ribosome production were strongly dysregulated in leptin-a morphant ("Ribosome biogenesis", "rRNA processing", "rRNA metabolic process") [Table 3.1 and 6.2], but not rescue embryos [Table 3.3 and 6.4]. This suggests that pathways reliant upon (small) RNA interactions are more prone to non-specific morpholino effects than those pathways implementing fewer RNA interactions. This notion may also be true in reference to those pathways which function during early neonatal life staging (e.g. 1-2 cell) as opposed to later (e.g. 22-somite) because morpholinos have a temporal range of effectiveness where the concentration of morpholino oligonucleotide per cell decreases with every subsequent division.

The whole-transcriptome response to morpholino knockdown of leptin-a was not a complete "rescue" via recombinant leptin-a (rLEPA) which coincides with the intermediate "rescue" phenotype [Liu et al., 2012]. After comparison of the leptin-a knockdown expression data to commensurable zebrafish datasets (which targeted different mRNA's), a subset of the differentially expressed genes and pathways reported

here are similarly featured in unrelated morpholino studies. For these reasons, a concerted effort within the morpholino community describing *in vivo* morpholino action and binding kinetics, enhanced guidelines detailing MO dosage effects and "rescue" protocols, as well direct comparison to age/batch-matched bona fide mutants, when available, should be established before reliable conclusions should be drawn from zebrafish morphants. Given the practical concerns over the continued use of antisense morpholino approaches from the community [Kok et al., 2015; reviewed: Lawson 2016], and leptin-a morpholino knockdown microarray expression data featuring candidate artifacts [Robu et al., 2007], future directives should pursue alternative approaches to (antisense) morpholino technologies as a means to investigate gene function. Opting for forward/reverse genetics, namely CRISPR Cas9 genome editing in place of morpholino oligonucleotides, provides a more discernable method to elucidate the role of leptin signaling in developmental teleost physiology and gene expression.

The statistical methods used to generate this dataset were appropriate but this study has limitations. Microarray samples were subject to batch effects as 16 samples were processed on five separate scan dates. Variation in probeset signal intensity is evident between two factors of variance: both treatment and scan date [Figures 3.4 and 3.7]. Processing additional replicates for each experimental condition (n = 8 wild type, n = 4 leptin-a MO, n = 4 leptin-a Rescue) could improve the accuracy and/or precision of the results. To complement the leptin-a rescue treatment, including an additional group of embryos treated exclusively using recombinant leptin-a (rLEPA) without morpholinos would provide a more accurate measure to describe responses exclusive to

augmentation of leptin signaling. In summary, zebrafish pathways that respond to leptin-a expression participate in the development of nervous, endocrine, and sensory systems as well as fatty acyl, sterol, and glucose homeostasis. The present study cannot unequivocally assign DEG as a response specific to morpholino off-target effects or, conversely, true to changes in leptin-a expression. However, these microarray data provoke functional investigations that can be used to test additional hypothesis related to comparative leptin signaling. In conclusion, these are the first expression data describing the whole-transcriptome response to *in vivo* knockdown of embryonic zebrafish leptin signaling.

CHAPTER VI

SUPPORTING INFORMATION

Filename	Sample	Treatment	Run Date
control1.ga	control1	control	5/12/2012
control2.ga	control2	control	5/12/2012
control3.ga	control3	control	3/6/2013
control4.ga	control4	control	7/16/2013
control5.ga	control5	control	9/7/2012
control6.ga	control6	control	9/7/2012
control7.ga	control7	control	3/6/2013
control8.ga	control8	control	7/16/2013
morphant1.ga	lepa_morphant1	morphant	5/12/2012
morphant2.ga	lepa_morphant2	morphant	3/6/2013
morphant3.ga	lepa_morphant3	morphant	7/16/2013
morphant4.ga	lepa_morphant4	morphant	5/12/2012
rescue1.ga	lepa_rescue1	rescue	4/23/2014
rescue2.ga	lepa_rescue2	rescue	4/23/2014
rescue3.ga	lepa_rescue3	rescue	4/23/2014
rescue4.ga	lepa_rescue4	rescue	4/23/2014

Table 6.1: Microarray sample information.

GO ID	Leptin-a Morphant : Control	O	N	Up	Dwn	P.Up	P.Dwn
GO:0016070	RNA metabolic process	BP	1846	141	21	5.83E-36	1
GO:0005634	nucleus	CC	2362	160	28	2.7E-35	1
GO:0090304	nucleic acid metabolic process	BP	2084	147	21	9.07E-34	1
GO:0006139	nucleobase-containing compound metabolic process	BP	2387	155	37	9.98E-32	1
GO:0010467	gene expression	BP	2147	145	24	4.3E-31	1
GO:0046483	heterocycle metabolic process	BP	2461	155	38	3.56E-30	1
GO:0006725	cellular aromatic compound metabolic process	BP	2472	155	40	5.97E-30	1
GO:1901360	organic cyclic compound metabolic process	BP	2540	155	42	1.36E-28	1
GO:0034641	cellular nitrogen compound metabolic process	BP	2820	161	42	1.32E-26	1
GO:0006807	nitrogen compound metabolic process	BP	2955	161	43	2.71E-24	1
GO:0003676	nucleic acid binding	MF	2152	132	26	1.01E-23	1
GO:0007601	visual perception	BP	61	1	26	0.796674	8.97E-23
GO:0050953	sensory perception of light stimulus	BP	62	1	26	0.801926	1.5E-22
GO:0005886	plasma membrane	CC	1436	12	120	1	4E-22
GO:0071944	cell periphery	CC	1470	12	121	1	9.25E-22
GO:0044428	nuclear part	CC	692	64	2	1.64E-19	1
GO:0034660	ncRNA metabolic process	BP	215	36	0	1.88E-19	1
GO:0044260	cellular macromolecule metabolic process	BP	3745	175	73	3.12E-19	1
GO:0043231	intracellular membrane-bounded organelle	CC	3722	174	71	4.21E-19	1
GO:0043227	membrane-bounded organelle	CC	3734	174	72	6E-19	1
GO:0031981	nuclear lumen	CC	461	51	0	6.39E-19	1
GO:0005730	nucleolus	CC	132	28	0	3.43E-18	1
GO:2000112	regulation of cellular macromolecule biosynthetic process	BP	1434	94	22	3.81E-18	0.999997
GO:1901363	heterocyclic compound binding	MF	3809	174	104	5.29E-18	0.99484
GO:0010556	regulation of macromolecule biosynthetic process	BP	1445	94	22	6.35E-18	0.999998
GO:0051171	regulation of nitrogen compound metabolic process	BP	1500	96	24	7.54E-18	0.999995
GO:0034470	ncRNA processing	BP	163	30	0	1.42E-17	1

GO:0097159	organic cyclic compound binding	MF	3845	174	111	1.46E-17	0.972824
GO:0010468	regulation of gene expression	BP	1469	94	23	1.89E-17	0.999996
GO:0043170	macromolecule metabolic process	BP	4132	182	83	2.31E-17	1
GO:0031326	regulation of cellular biosynthetic process	BP	1479	94	24	2.96E-17	0.999993
GO:0009889	regulation of biosynthetic process	BP	1484	94	24	3.7E-17	0.999994
GO:0006351	transcription, DNA-templated	BP	1408	91	21	3.87E-17	0.999998
GO:0097659	nucleic acid-templated transcription	BP	1409	91	21	4.05E-17	0.999998
GO:0032774	RNA biosynthetic process	BP	1414	91	21	5.08E-17	0.999998
GO:0070013	intracellular organelle lumen	CC	535	52	0	7.8E-17	1
GO:0043233	organelle lumen	CC	536	52	0	8.45E-17	1
GO:0045202	synapse	CC	167	0	33	1	9.28E-17
GO:0043229	intracellular organelle	CC	4327	186	85	1.05E-16	1
GO:0022613	ribonucleoprotein complex biogenesis	BP	205	32	0	1.74E-16	1
GO:0019219	regulation of nucleobase-containing compound metabolic process	BP	1418	90	23	1.91E-16	0.999989
GO:0060255	regulation of macromolecule metabolic process	BP	1771	103	29	2.67E-16	0.999999
GO:0031974	membrane-enclosed lumen	CC	552	52	0	2.93E-16	1
GO:0043226	organelle	CC	4368	186	89	3E-16	1
GO:0044424	intracellular part	CC	5430	215	128	4.53E-16	1
GO:0006355	regulation of transcription, DNA-templated	BP	1337	86	21	4.94E-16	0.99999
GO:1903506	regulation of nucleic acid-templated transcription	BP	1338	86	21	5.16E-16	0.99999
GO:0016020	membrane	CC	4787	43	244	1	5.19E-16
GO:2001141	regulation of RNA biosynthetic process	BP	1340	86	21	5.65E-16	0.99999
GO:0051252	regulation of RNA metabolic process	BP	1367	87	21	6.03E-16	0.999995
GO:0080090	regulation of primary metabolic process	BP	1793	103	29	6.24E-16	0.999999
GO:0031323	regulation of cellular metabolic process	BP	1824	103	29	2E-15	1
GO:0006396	RNA processing	BP	372	41	0	2.65E-15	1
GO:0003677	DNA binding	MF	1180	78	17	3.72E-15	0.999992
GO:0044271	cellular nitrogen compound biosynthetic process	BP	2018	109	36	4.92E-15	0.999998

GO:0031224	intrinsic component of membrane	CC	4003	37	212	1	5.18E-15
GO:0034645	cellular macromolecule biosynthetic process	BP	2023	109	26	5.85E-15	1
GO:0016021	integral component of membrane	CC	3981	37	211	1	5.89E-15
GO:0034654	nucleobase-containing compound biosynthetic process	BP	1607	94	33	6.1E-15	0.999557
GO:0009059	macromolecule biosynthetic process	BP	2040	109	26	1.05E-14	1
GO:0044459	plasma membrane part	CC	825	3	73	1	1.29E-14
GO:0044425	membrane part	CC	4345	39	223	1	1.96E-14
GO:0042254	ribosome biogenesis	BP	143	25	0	2.66E-14	1
GO:0005622	intracellular	CC	5689	217	138	2.85E-14	1
GO:0030684	preribosome	CC	41	15	0	3.7E-14	1
GO:0019438	aromatic compound biosynthetic process	BP	1655	94	35	3.77E-14	0.999332
GO:0018130	heterocycle biosynthetic process	BP	1659	94	34	4.37E-14	0.999654
GO:0005488	binding	MF	6938	248	221	5.96E-14	0.860039
GO:0019222	regulation of metabolic process	BP	1937	103	31	1.07E-13	1
GO:1901362	organic cyclic compound biosynthetic process	BP	1701	94	34	1.99E-13	0.99983
GO:0044765	single-organism transport	BP	1332	16	96	0.999912	2.08E-13
GO:0005887	integral component of plasma membrane	CC	536	2	54	0.99999	3.23E-13
GO:0044237	cellular metabolic process	BP	4753	188	106	4.91E-13	1
GO:0009583	detection of light stimulus	BP	32	0	14	1	4.92E-13
GO:0044238	primary metabolic process	BP	4955	193	111	7.83E-13	1
GO:0003723	RNA binding	MF	502	44	5	8.85E-13	0.999848
GO:0005215	transporter activity	MF	878	12	72	0.995854	8.96E-13
GO:1902578	single-organism localization	BP	1393	16	97	0.999969	1.2E-12
GO:0031226	intrinsic component of plasma membrane	CC	556	3	54	0.99995	1.41E-12
GO:0006364	rRNA processing	BP	92	19	0	1.61E-12	1
GO:0007602	phototransduction	BP	23	0	12	1	1.65E-12
GO:0016072	rRNA metabolic process	BP	94	19	0	2.43E-12	1
GO:0006811	ion transport	BP	636	2	58	0.999999	2.71E-12
GO:0099536	synaptic signaling	BP	140	0	25	1	5.75E-12
GO:0007268	synaptic transmission	BP	140	0	25	1	5.75E-12
GO:0099537	trans-synaptic signaling	BP	140	0	25	1	5.75E-12
GO:0009881	photoreceptor activity	MF	25	0	12	1	5.97E-12

GO:0022838	substrate-specific channel activity	MF	271	0	35	1	6.24E-12
GO:0007154	cell communication	BP	2641	57	149	0.942904	6.48E-12
GO:0050877	neurological system process	BP	258	1	34	0.99887	7.14E-12
GO:0071704	organic substance metabolic process	BP	5115	194	114	9.99E-12	1
GO:0006810	transport	BP	1765	23	111	0.999968	1.41E-11
GO:0060089	molecular transducer activity	MF	951	10	73	0.999809	1.48E-11
GO:0004872	receptor activity	MF	951	10	73	0.999809	1.48E-11
GO:0021510	spinal cord development	BP	59	15	0	1.53E-11	1
GO:0044700	single organism signaling	BP	2575	57	145	0.911819	1.69E-11
GO:0022857	transmembrane transporter activity	MF	685	4	59	0.999985	1.84E-11
GO:0023052	signaling	BP	2581	58	145	0.890637	2.02E-11
GO:0009416	response to light stimulus	BP	74	0	18	1	2.56E-11
GO:0005216	ion channel activity	MF	258	0	33	1	3.33E-11
GO:0044249	cellular biosynthetic process	BP	2461	114	46	3.52E-11	0.999999
GO:0032040	small-subunit processome	CC	28	11	0	4.07E-11	1
GO:0022891	substrate-specific transmembrane transporter activity	MF	613	4	54	0.999923	6.2E-11
GO:0015267	channel activity	MF	294	1	35	0.999566	6.39E-11
GO:0022803	passive transmembrane transporter activity	MF	294	1	35	0.999566	6.39E-11
GO:0051234	establishment of localization	BP	1811	23	111	0.999985	7.02E-11
GO:0044452	nucleolar part	CC	37	12	0	7.27E-11	1
GO:0009582	detection of abiotic stimulus	BP	52	0	15	1	8.44E-11
GO:0009581	detection of external stimulus	BP	52	0	15	1	8.44E-11
GO:0018298	protein-chromophore linkage	BP	24	0	11	1	8.79E-11
GO:0007267	cell-cell signaling	BP	211	1	29	0.996073	9.36E-11
GO:0015075	ion transmembrane transporter activity	MF	567	2	51	0.999995	1.05E-10
GO:0007399	nervous system development	BP	996	61	30	1.55E-10	0.752989
GO:0004871	signal transducer activity	MF	980	6	72	0.999999	1.56E-10
GO:0005230	extracellular ligand-gated ion channel activity	MF	64	0	16	1	2.12E-10
GO:0007600	sensory perception	BP	235	1	30	0.99792	2.8E-10
GO:0022892	substrate-specific transporter activity	MF	734	12	59	0.968439	2.91E-10

GO:0009058	biosynthetic process	BP	2579	115	47	3.14E-10	1
GO:0022836	gated channel activity	MF	208	0	28	1	3.24E-10
GO:0038023	signaling receptor activity	MF	836	6	64	0.999987	3.57E-10
GO:0009987	cellular process	BP	8310	269	271	6.1E-10	0.760375
GO:0008066	glutamate receptor activity	MF	22	0	10	1	7.18E-10
GO:1901576	organic substance biosynthetic process	BP	2520	112	46	7.42E-10	1
GO:0007417	central nervous system development	BP	460	37	5	7.56E-10	0.999524
GO:0022834	ligand-gated channel activity	MF	101	0	19	1	8.25E-10
GO:0015276	ligand-gated ion channel activity	MF	101	0	19	1	8.25E-10
GO:0021515	cell differentiation in spinal cord	BP	47	12	0	1.63E-09	1
GO:0008328	ionotropic glutamate receptor complex	CC	19	0	9	1	3.33E-09
GO:0044767	single-organism developmental process	BP	2857	120	68	4.62E-09	0.999652
GO:0043235	receptor complex	CC	89	0	17	1	5.06E-09
GO:0044085	cellular component biogenesis	BP	828	51	18	5.11E-09	0.983648
GO:0044456	synapse part	CC	114	0	19	1	6.85E-09
GO:0032502	developmental process	BP	2883	120	68	8.04E-09	0.999757
GO:0021514	ventral spinal cord interneuron differentiation	BP	19	8	0	1.05E-08	1
GO:0009314	response to radiation	BP	105	2	18	0.756616	1.08E-08
GO:0097458	neuron part	CC	143	0	21	1	1.15E-08
GO:0016917	GABA receptor activity	MF	16	0	8	1	1.5E-08
GO:0030686	90S preribosome	CC	20	8	0	1.71E-08	1
GO:0099600	transmembrane receptor activity	MF	780	5	57	0.999991	1.95E-08
GO:0007275	multicellular organism development	BP	2537	108	65	2E-08	0.99465
GO:0051179	localization	BP	2217	35	120	0.999754	2.14E-08
GO:0000462	maturation of SSU-rRNA from tricistronic rRNA transcript (SSU-rRNA, 5.8S rRNA, LSU-rRNA)	BP	21	8	0	2.69E-08	1
GO:0004888	transmembrane signaling receptor activity	MF	749	5	55	0.999982	3.01E-08
GO:0008152	metabolic process	BP	5767	199	132	3.88E-08	1
GO:0098797	plasma membrane protein complex	CC	243	0	27	1	4.49E-08
GO:0021517	ventral spinal cord development	BP	41	10	0	6.17E-08	1
GO:0004890	GABA-A receptor activity	MF	13	0	7	1	6.45E-08

GO:0005623	cell	CC	6843	225	230	1.14E-07	0.475911
GO:0044464	cell part	CC	6843	225	230	1.14E-07	0.475911
GO:0048731	system development	BP	2150	93	56	1.4E-07	0.985895

Table 6.2: Top-150 GO terms from the leptin-a morphant : control contrast to “Dr” Gene Ontologies.

GO ID	Leptin-a Morphant : Leptin-a Rescue	O	N	Up	Dwn	P.Up	P.Dwn
GO:0004984	olfactory receptor activity	MF	102	33	0	9.72E-38	1
GO:0007608	sensory perception of smell	BP	106	32	0	1.73E-35	1
GO:0007606	sensory perception of chemical stimulus	BP	143	34	0	9.63E-34	1
GO:0004930	G-protein coupled receptor activity	MF	532	51	7	2.3E-30	0.999961
GO:0007186	G-protein coupled receptor signaling pathway	BP	632	52	6	9.48E-28	1
GO:0007600	sensory perception	BP	235	35	3	2.89E-27	0.997003
GO:0050877	neurological system process	BP	258	36	4	5.13E-27	0.99452
GO:0004888	transmembrane signaling receptor activity	MF	749	55	26	6.08E-27	0.843677
GO:0099600	transmembrane receptor activity	MF	780	55	27	4.58E-26	0.851661
GO:0038023	signaling receptor activity	MF	836	55	31	1.39E-24	0.755075
GO:0060089	molecular transducer activity	MF	951	56	36	1.09E-22	0.726725
GO:0004872	receptor activity	MF	951	56	36	1.09E-22	0.726725
GO:0050907	detection of chemical stimulus involved in sensory perception	BP	101	23	0	1.47E-22	1
GO:0009593	detection of chemical stimulus	BP	104	23	0	3.04E-22	1
GO:0004871	signal transducer activity	MF	980	56	38	4.67E-22	0.676095
GO:0044260	cellular macromolecule metabolic process	BP	3745	19	258	1	1.97E-21
GO:0050906	detection of stimulus involved in sensory perception	BP	120	23	1	9.98E-21	0.993696
GO:0051606	detection of stimulus	BP	157	24	1	3.64E-19	0.99869
GO:0003008	system process	BP	488	37	11	1.95E-18	0.991702
GO:0016070	RNA metabolic process	BP	1846	5	151	1	1.03E-17
GO:0090304	nucleic acid metabolic process	BP	2084	6	162	1	5.74E-17
GO:0043170	macromolecule metabolic process	BP	4132	28	263	0.999998	5.89E-17

GO:0019222	regulation of metabolic process	BP	1937	7	153	0.999999	1.45E-16
GO:0060255	regulation of macromolecule metabolic process	BP	1771	5	143	1	3.21E-16
GO:0031323	regulation of cellular metabolic process	BP	1824	6	145	0.999999	7.1E-16
GO:0080090	regulation of primary metabolic process	BP	1793	6	143	0.999998	9.22E-16
GO:0044767	single-organism developmental process	BP	2857	14	197	0.999999	2.59E-15
GO:0048856	anatomical structure development	BP	2636	12	185	0.999999	5.32E-15
GO:0032502	developmental process	BP	2883	14	197	1	6.74E-15
GO:0032774	RNA biosynthetic process	BP	1414	4	119	0.999995	1.09E-14
GO:0006351	transcription, DNA-templated	BP	1408	3	118	0.999999	1.96E-14
GO:0097659	nucleic acid-templated transcription	BP	1409	3	118	0.999999	2.07E-14
GO:0050794	regulation of cellular process	BP	4310	74	262	0.003151	3.42E-14
GO:0051252	regulation of RNA metabolic process	BP	1367	3	115	0.999999	3.54E-14
GO:0010556	regulation of macromolecule biosynthetic process	BP	1445	3	119	0.999999	5.19E-14
GO:0005634	nucleus	CC	2362	10	168	0.999999	5.5E-14
GO:0051171	regulation of nitrogen compound metabolic process	BP	1500	4	122	0.999998	5.62E-14
GO:0003676	nucleic acid binding	MF	2152	7	157	1	6.25E-14
GO:2000112	regulation of cellular macromolecule biosynthetic process	BP	1434	3	118	0.999999	7.22E-14
GO:0019219	regulation of nucleobase-containing compound metabolic process	BP	1418	4	117	0.999995	7.85E-14
GO:0007275	multicellular organism development	BP	2537	11	176	1	1.05E-13
GO:0006355	regulation of transcription, DNA-templated	BP	1337	3	112	0.999998	1.11E-13
GO:1903506	regulation of nucleic acid-templated transcription	BP	1338	3	112	0.999998	1.17E-13
GO:2001141	regulation of RNA biosynthetic process	BP	1340	3	112	0.999998	1.29E-13
GO:0006139	nucleobase-containing compound metabolic process	BP	2387	9	168	1	1.42E-13
GO:0010468	regulation of gene expression	BP	1469	3	119	1	1.66E-13
GO:0048731	system development	BP	2150	9	155	0.999998	2.65E-13
GO:0031326	regulation of cellular biosynthetic process	BP	1479	4	119	0.999998	2.68E-13

GO:0009889	regulation of biosynthetic process	BP	1484	4	119	0.999998	3.39E-13
GO:0006725	cellular aromatic compound metabolic process	BP	2472	12	171	0.999997	3.68E-13
GO:0050789	regulation of biological process	BP	4464	75	265	0.005303	4.36E-13
GO:1901363	heterocyclic compound binding	MF	3809	18	235	1	4.86E-13
GO:0097159	organic cyclic compound binding	MF	3845	19	235	1	1.41E-12
GO:1901360	organic cyclic compound metabolic process	BP	2540	12	172	0.999999	2.02E-12
GO:0044707	single-multicellular organism process	BP	2702	14	180	0.999997	2.07E-12
GO:0046483	heterocycle metabolic process	BP	2461	12	168	0.999997	2.1E-12
GO:0044237	cellular metabolic process	BP	4753	26	274	1	4.65E-12
GO:0034654	nucleobase-containing compound biosynthetic process	BP	1607	7	122	0.99994	7.06E-12
GO:0003677	DNA binding	MF	1180	2	98	0.999998	8.86E-12
GO:0010467	gene expression	BP	2147	6	150	1	9.18E-12
GO:0019438	aromatic compound biosynthetic process	BP	1655	9	124	0.999597	1.11E-11
GO:0005488	binding	MF	6938	41	364	1	1.7E-11
GO:0065007	biological regulation	BP	4778	76	272	0.020286	2.87E-11
GO:1901362	organic cyclic compound biosynthetic process	BP	1701	9	125	0.999743	3.32E-11
GO:0048513	animal organ development	BP	1595	7	119	0.999932	4.3E-11
GO:0005886	plasma membrane	CC	1436	50	42	4.83E-11	0.994928
GO:0018130	heterocycle biosynthetic process	BP	1659	9	122	0.999612	5.89E-11
GO:0007399	nervous system development	BP	996	4	85	0.99925	6.84E-11
GO:0004672	protein kinase activity	MF	486	3	53	0.955081	7.73E-11
GO:0044238	primary metabolic process	BP	4955	34	278	1	7.81E-11
GO:0009059	macromolecule biosynthetic process	BP	2040	8	141	0.999998	1.08E-10
GO:0071944	cell periphery	CC	1470	50	43	1.12E-10	0.995367
GO:0034645	cellular macromolecule biosynthetic process	BP	2023	8	139	0.999998	2.33E-10
GO:0007166	cell surface receptor signaling pathway	BP	858	6	75	0.970972	3.56E-10
GO:0009966	regulation of signal transduction	BP	601	5	59	0.897206	4.21E-10
GO:0006464	cellular protein modification process	BP	1429	11	107	0.983155	4.31E-10
GO:0036211	protein modification process	BP	1429	11	107	0.983155	4.31E-10
GO:0043412	macromolecule modification	BP	1500	11	110	0.990153	7.86E-10

GO:0071704	organic substance metabolic process	BP	5115	37	280	0.999999	1.15E-09
GO:0010646	regulation of cell communication	BP	650	5	61	0.93041	1.24E-09
GO:0023051	regulation of signaling	BP	651	5	61	0.930975	1.32E-09
GO:0016021	integral component of membrane	CC	3981	90	109	1.8E-09	1
GO:0031224	intrinsic component of membrane	CC	4003	90	111	2.43E-09	1
GO:0016773	phosphotransferase activity, alcohol group as acceptor	MF	566	3	55	0.980153	2.49E-09
GO:0032501	multicellular organismal process	BP	3010	50	183	0.034221	3.38E-09
GO:0016020	membrane	CC	4787	101	140	3.51E-09	1
GO:0009653	anatomical structure morphogenesis	BP	1478	3	106	1	5.9E-09
GO:0044425	membrane part	CC	4345	94	122	6.22E-09	1
GO:0006468	protein phosphorylation	BP	614	4	57	0.961749	6.71E-09
GO:0007165	signal transduction	BP	2443	64	139	7.26E-09	2.2E-05
GO:0009987	cellular process	BP	8310	96	407	0.973034	8.44E-09
GO:0048869	cellular developmental process	BP	1492	8	106	0.999343	9.83E-09
GO:0030154	cell differentiation	BP	1349	7	98	0.99913	1.32E-08
GO:0034641	cellular nitrogen compound metabolic process	BP	2820	13	171	1	1.81E-08
GO:0009790	embryo development	BP	835	2	69	0.999842	1.97E-08
GO:0044700	single organism signaling	BP	2575	65	142	2.32E-08	8.38E-05
GO:0023052	signaling	BP	2581	65	144	2.55E-08	4.08E-05
GO:0044271	cellular nitrogen compound biosynthetic process	BP	2018	10	131	0.999967	3.29E-08
GO:1902531	regulation of intracellular signal transduction	BP	303	4	35	0.560041	3.39E-08
GO:0009888	tissue development	BP	1053	1	80	0.999999	5.41E-08
GO:0050896	response to stimulus	BP	3390	77	175	6.12E-08	0.000351
GO:0007154	cell communication	BP	2641	65	142	6.31E-08	0.000276
GO:0005524	ATP binding	MF	1098	8	82	0.97822	7.61E-08
GO:0043229	intracellular organelle	CC	4327	15	237	1	8.04E-08
GO:0032559	adenyl ribonucleotide binding	MF	1105	8	82	0.979398	1E-07
GO:0030554	adenyl nucleotide binding	MF	1106	8	82	0.979562	1.04E-07
GO:0043226	organelle	CC	4368	16	238	1	1.18E-07
GO:0016301	kinase activity	MF	669	3	57	0.993422	1.35E-07
GO:0006807	nitrogen compound metabolic process	BP	2955	14	173	1	1.81E-07
GO:0044424	intracellular part	CC	5430	28	283	1	1.93E-07
GO:0043231	intracellular membrane-bounded organelle	CC	3722	15	208	1	2.02E-07

GO:0043227	membrane-bounded organelle	CC	3734	16	208	1	2.62E-07
GO:0016772	transferase activity, transferring phosphorus-containing groups	MF	771	3	62	0.997899	2.89E-07
GO:0008152	metabolic process	BP	5767	45	296	0.999999	3.43E-07
GO:0044249	cellular biosynthetic process	BP	2461	14	148	0.999968	4.28E-07
GO:0035556	intracellular signal transduction	BP	833	4	65	0.995631	4.31E-07
GO:0007417	central nervous system development	BP	460	2	43	0.984269	4.36E-07
GO:0051716	cellular response to stimulus	BP	2842	66	158	4.47E-07	1.77E-05
GO:0048583	regulation of response to stimulus	BP	764	8	61	0.785473	4.64E-07
GO:0043167	ion binding	MF	4054	24	221	1	4.88E-07
GO:0007389	pattern specification process	BP	448	1	42	0.997459	5.51E-07
GO:0022008	neurogenesis	BP	630	1	53	0.999788	5.67E-07
GO:0007420	brain development	BP	333	2	34	0.933912	1.01E-06
GO:0005622	intracellular	CC	5689	32	290	1	1.1E-06
GO:1901576	organic substance biosynthetic process	BP	2520	14	148	0.999982	1.77E-06
GO:0007167	enzyme linked receptor protein signaling pathway	BP	343	1	34	0.989508	1.97E-06
GO:0006366	transcription from RNA polymerase II promoter	BP	472	0	42	1	2.16E-06
GO:0051056	regulation of small GTPase mediated signal transduction	BP	87	1	15	0.681855	2.33E-06
GO:0060322	head development	BP	346	2	34	0.942694	2.4E-06
GO:0009058	biosynthetic process	BP	2579	15	150	0.999971	2.59E-06
GO:0048523	negative regulation of cellular process	BP	754	2	58	0.999559	2.97E-06
GO:0009968	negative regulation of signal transduction	BP	202	0	24	1	3.01E-06
GO:0035295	tube development	BP	319	0	32	1	3.07E-06
GO:0019199	transmembrane receptor protein kinase activity	MF	68	0	13	1	3.33E-06
GO:0001594	trace-amine receptor activity	MF	33	6	0	3.74E-06	1
GO:0016310	phosphorylation	BP	814	4	61	0.994674	3.77E-06
GO:0007219	Notch signaling pathway	BP	69	0	13	1	3.95E-06
GO:0043009	chordate embryonic development	BP	387	1	36	0.9942	4.31E-06
GO:0009792	embryo development ending in birth or egg hatching	BP	387	1	36	0.9942	4.31E-06
GO:0006928	movement of cell or subcellular component	BP	570	0	47	1	4.4E-06
GO:0042221	response to chemical	BP	944	30	49	4.73E-06	0.05463

GO:0023057	negative regulation of signaling	BP	208	0	24	1	5.02E-06
GO:0010648	negative regulation of cell communication	BP	210	0	24	1	5.93E-06
GO:0044267	cellular protein metabolic process	BP	1926	14	117	0.996389	6.38E-06
GO:0003002	regionalization	BP	300	1	30	0.981307	6.64E-06
GO:0048699	generation of neurons	BP	579	1	47	0.999573	6.68E-06
GO:0046872	metal ion binding	MF	2453	13	142	0.999988	6.92E-06
GO:0060429	epithelium development	BP	616	0	49	1	7.37E-06
GO:0006357	regulation of transcription from RNA polymerase II promoter	BP	431	0	38	1	8.23E-06
GO:0004674	protein serine/threonine kinase activity	MF	291	2	29	0.896114	1.01E-05

Table 6.3: Top-150 GO terms generated from the leptin-a rescue : leptin-a morphant contrast.

GO ID	Leptin-a Rescue : Control	O	N	Up	Dwn	P.Up	P.Dwn
GO:0007606	sensory perception of chemical stimulus	BP	143	56	2	7.31E-38	1
GO:0004930	G-protein coupled receptor activity	MF	532	100	59	4.26E-35	0.798683
GO:0007608	sensory perception of smell	BP	106	47	1	6.47E-35	0.999999
GO:0004984	olfactory receptor activity	MF	102	46	0	1.32E-34	1
GO:0007186	G-protein coupled receptor signaling pathway	BP	632	106	81	1.14E-32	0.32246
GO:0004888	transmembrane signaling receptor activity	MF	749	109	118	4.65E-28	0.001661
GO:0050907	detection of chemical stimulus involved in sensory perception	BP	101	40	1	1.53E-27	0.999998
GO:0099600	transmembrane receptor activity	MF	780	110	124	3.96E-27	0.000907
GO:0009593	detection of chemical stimulus	BP	104	40	1	5.86E-27	0.999999
GO:0007600	sensory perception	BP	235	58	38	7.2E-27	0.04037
GO:0050906	detection of stimulus involved in sensory perception	BP	120	41	6	2.98E-25	0.997706
GO:0050877	neurological system process	BP	258	58	45	1.28E-24	0.007852
GO:0038023	signaling receptor activity	MF	836	109	141	5.26E-24	2.5E-05
GO:0060089	molecular transducer activity	MF	951	115	162	1.47E-22	3.35E-06
GO:0004872	receptor activity	MF	951	115	162	1.47E-22	3.35E-06
GO:0051606	detection of stimulus	BP	157	41	23	2.79E-20	0.199259
GO:0004871	signal transducer activity	MF	980	110	168	4.9E-19	1.46E-06

GO:0045202	synapse	CC	167	2	65	0.996603	7.6E-19
GO:0023052	signaling	BP	2581	154	450	0.000205	2.15E-18
GO:0044700	single organism signaling	BP	2575	154	447	0.000183	6.87E-18
GO:0007154	cell communication	BP	2641	156	456	0.000299	7.68E-18
GO:0098772	molecular function regulator	MF	532	13	133	0.996804	7.89E-17
GO:0071944	cell periphery	CC	1470	89	280	0.003751	5.91E-16
GO:0005216	ion channel activity	MF	258	7	79	0.955196	1.68E-15
GO:0003008	system process	BP	488	66	75	1.7E-15	0.018753
GO:0022836	gated channel activity	MF	208	4	68	0.987651	4.35E-15
GO:0044765	single-organism transport	BP	1332	35	256	0.999958	4.59E-15
GO:0005886	plasma membrane	CC	1436	89	271	0.001922	6.42E-15
GO:0022838	substrate-specific channel activity	MF	271	7	80	0.968469	1.08E-14
GO:1902578	single-organism localization	BP	1393	36	263	0.999981	1.67E-14
GO:0044459	plasma membrane part	CC	825	28	175	0.966937	2.55E-14
GO:0035556	intracellular signal transduction	BP	833	21	175	0.99946	6.39E-14
GO:0006811	ion transport	BP	636	17	143	0.995791	6.49E-14
GO:0015075	ion transmembrane transporter activity	MF	567	12	131	0.999492	9.41E-14
GO:0031226	intrinsic component of plasma membrane	CC	556	16	129	0.985819	1.06E-13
GO:0016773	phosphotransferase activity, alcohol group as acceptor	MF	566	12	130	0.999476	1.87E-13
GO:0007601	visual perception	BP	61	1	31	0.943495	1.99E-13
GO:0050953	sensory perception of light stimulus	BP	62	1	31	0.9461	3.51E-13
GO:0005887	integral component of plasma membrane	CC	536	16	124	0.978016	4.06E-13
GO:0099536	synaptic signaling	BP	140	2	50	0.989524	4.22E-13
GO:0007268	synaptic transmission	BP	140	2	50	0.989524	4.22E-13
GO:0099537	trans-synaptic signaling	BP	140	2	50	0.989524	4.22E-13
GO:0015267	channel activity	MF	294	7	81	0.983522	4.64E-13
GO:0022803	passive transmembrane transporter activity	MF	294	7	81	0.983522	4.64E-13
GO:0044456	synapse part	CC	114	2	44	0.96991	4.79E-13
GO:0007165	signal transduction	BP	2443	152	404	2.77E-05	1.4E-12
GO:0016301	kinase activity	MF	669	13	144	0.99994	1.91E-12
GO:0006810	transport	BP	1765	43	308	1	2.48E-12
GO:0004672	protein kinase activity	MF	486	12	113	0.995027	3.33E-12
GO:0034702	ion channel complex	CC	111	2	42	0.966093	3.52E-12
GO:0008066	glutamate receptor activity	MF	22	0	17	1	3.76E-12
GO:0022891	substrate-specific transmembrane transporter activity	MF	613	12	133	0.999874	7.85E-12

GO:0051179	localization	BP	2217	54	369	1	7.92E-12
GO:0051234	establishment of localization	BP	1811	45	312	1	8.7E-12
GO:0022857	transmembrane transporter activity	MF	685	13	144	0.999964	1.22E-11
GO:0009416	response to light stimulus	BP	74	0	32	1	2.08E-11
GO:0005085	guanyl-nucleotide exchange factor activity	MF	114	2	41	0.96991	4.19E-11
GO:0007267	cell-cell signaling	BP	211	5	61	0.968133	4.2E-11
GO:0001594	trace-amine receptor activity	MF	33	14	0	5.87E-11	1
GO:1902495	transmembrane transporter complex	CC	125	2	43	0.980665	7.51E-11
GO:0046873	metal ion transmembrane transporter activity	MF	269	4	71	0.998635	1.11E-10
GO:0044699	single-organism process	BP	7562	324	1042	0.971955	1.48E-10
GO:1990351	transporter complex	CC	128	2	43	0.982881	1.79E-10
GO:0097060	synaptic membrane	CC	61	2	27	0.776874	4.05E-10
GO:0022892	substrate-specific transporter activity	MF	734	21	146	0.994376	5.67E-10
GO:0065007	biological regulation	BP	4778	244	695	0.020801	5.67E-10
GO:0097458	neuron part	CC	143	0	45	1	7.67E-10
GO:0005230	extracellular ligand-gated ion channel activity	MF	64	3	27	0.56843	1.5E-09
GO:0044763	single-organism cellular process	BP	6118	281	859	0.512576	1.7E-09
GO:0006464	cellular protein modification process	BP	1429	38	246	0.99997	2.43E-09
GO:0036211	protein modification process	BP	1429	38	246	0.99997	2.43E-09
GO:0009583	detection of light stimulus	BP	32	0	18	1	2.73E-09
GO:0051056	regulation of small GTPase mediated signal transduction	BP	87	2	32	0.91377	2.98E-09
GO:0005215	transporter activity	MF	878	23	165	0.999276	3.35E-09
GO:0022834	ligand-gated channel activity	MF	101	4	35	0.68749	3.45E-09
GO:0015276	ligand-gated ion channel activity	MF	101	4	35	0.68749	3.45E-09
GO:0050789	regulation of biological process	BP	4464	234	647	0.007232	7.83E-09
GO:0009582	detection of abiotic stimulus	BP	52	1	23	0.913592	8.17E-09
GO:0009581	detection of external stimulus	BP	52	1	23	0.913592	8.17E-09
GO:0050794	regulation of cellular process	BP	4310	227	627	0.006693	8.8E-09
GO:0006468	protein phosphorylation	BP	614	16	123	0.996391	9.03E-09
GO:0005096	GTPase activator activity	MF	114	0	37	1	9.59E-09
GO:0016772	transferase activity, transferring phosphorus-containing groups	MF	771	21	147	0.997568	9.76E-09

GO:0030695	GTPase regulator activity	MF	124	0	39	1	1.04E-08
GO:0009314	response to radiation	BP	105	3	35	0.866554	1.1E-08
GO:0016917	GABA receptor activity	MF	16	0	12	1	1.15E-08
GO:0034703	cation channel complex	CC	65	0	26	1	1.17E-08
GO:0051716	cellular response to stimulus	BP	2842	170	435	7.26E-05	1.32E-08
GO:0060589	nucleoside-triphosphatase regulator activity	MF	127	1	39	0.997513	2.19E-08
GO:0006793	phosphorus metabolic process	BP	1206	32	209	0.999884	2.73E-08
GO:0006796	phosphate-containing compound metabolic process	BP	1181	32	205	0.99979	3.32E-08
GO:0022890	inorganic cation transmembrane transporter activity	MF	344	6	77	0.998791	5.69E-08
GO:1902531	regulation of intracellular signal transduction	BP	303	11	70	0.827512	6.18E-08
GO:0022843	voltage-gated cation channel activity	MF	98	1	32	0.990172	8.05E-08
GO:0005261	cation channel activity	MF	180	5	48	0.92081	8.16E-08
GO:0016020	membrane	CC	4787	250	680	0.006152	8.5E-08
GO:0043412	macromolecule modification	BP	1500	42	248	0.999927	8.58E-08
GO:0098794	postsynapse	CC	62	2	24	0.784546	8.96E-08
GO:0008227	G-protein coupled amine receptor activity	MF	62	15	7	9.02E-08	0.64183
GO:0051704	multi-organism process	BP	235	31	26	1.14E-07	0.727924
GO:0016310	phosphorylation	BP	814	19	149	0.999807	1.16E-07
GO:0008047	enzyme activator activity	MF	161	4	44	0.94172	1.31E-07
GO:0009628	response to abiotic stimulus	BP	205	9	52	0.602777	1.39E-07
GO:0004890	GABA-A receptor activity	MF	13	0	10	1	1.4E-07
GO:0009617	response to bacterium	BP	102	19	7	1.62E-07	0.971925
GO:0009881	photoreceptor activity	MF	25	0	14	1	1.78E-07
GO:0004970	ionotropic glutamate receptor activity	MF	16	0	11	1	2.04E-07
GO:0072583	clathrin-mediated endocytosis	BP	19	0	12	1	2.24E-07
GO:0008328	ionotropic glutamate receptor complex	CC	19	0	12	1	2.24E-07
GO:0006952	defense response	BP	195	27	16	2.82E-07	0.970642
GO:0046578	regulation of Ras protein signal transduction	BP	79	2	27	0.883533	2.89E-07
GO:0042742	defense response to bacterium	BP	43	12	1	3.28E-07	0.996254
GO:0007602	phototransduction	BP	23	0	13	1	4.29E-07
GO:0023051	regulation of signaling	BP	651	16	122	0.998592	4.89E-07
GO:0005234	extracellular-glutamate-gated ion channel activity	MF	17	0	11	1	5.14E-07
GO:0050896	response to stimulus	BP	3390	208	495	1.08E-06	5.77E-07

GO:0019905	syntaxin binding	MF	46	1	19	0.885326	6.01E-07
GO:0098797	plasma membrane protein complex	CC	243	12	57	0.440054	6.06E-07
GO:0005244	voltage-gated ion channel activity	MF	117	1	34	0.996004	7.33E-07
GO:0030001	metal ion transport	BP	280	7	63	0.975442	7.5E-07
GO:0010646	regulation of cell communication	BP	650	16	121	0.998555	7.81E-07
GO:0045211	postsynaptic membrane	CC	51	2	20	0.686266	8.26E-07
GO:0018298	protein-chromophore linkage	BP	24	0	13	1	8.32E-07
GO:1902711	GABA-A receptor complex	CC	12	0	9	1	8.92E-07
GO:1902710	GABA receptor complex	CC	12	0	9	1	8.92E-07
GO:0022832	voltage-gated channel activity	MF	120	1	34	0.996534	1.39E-06
GO:0008324	cation transmembrane transporter activity	MF	410	10	83	0.992128	1.58E-06
GO:0098542	defense response to other organism	BP	67	14	3	1.65E-06	0.991258
GO:0043207	response to external biotic stimulus	BP	152	22	12	1.67E-06	0.965899
GO:0051707	response to other organism	BP	152	22	12	1.67E-06	0.965899
GO:0006955	immune response	BP	255	30	19	2.15E-06	0.994833
GO:0016192	vesicle-mediated transport	BP	384	6	78	0.999702	2.85E-06
GO:0098590	plasma membrane region	CC	140	3	37	0.958704	3.05E-06
GO:0046903	secretion	BP	124	2	34	0.979866	3.13E-06
GO:0030276	clathrin binding	MF	30	0	14	1	3.21E-06
GO:0009607	response to biotic stimulus	BP	158	22	13	3.22E-06	0.956302
GO:0032940	secretion by cell	BP	119	2	33	0.97537	3.33E-06
GO:0000786	nucleosome	CC	44	11	3	3.37E-06	0.916519
GO:0030234	enzyme regulator activity	MF	392	11	79	0.973907	3.37E-06
GO:0015085	calcium ion transmembrane transporter activity	MF	74	0	24	1	3.77E-06
GO:0015079	potassium ion transmembrane transporter activity	MF	94	2	28	0.934026	4.02E-06
GO:0051260	protein homooligomerization	BP	56	1	20	0.928454	4.58E-06
GO:0016247	channel regulator activity	MF	31	0	14	1	5.2E-06
GO:0007215	glutamate receptor signaling pathway	BP	14	0	9	1	6.45E-06
GO:0048488	synaptic vesicle endocytosis	BP	14	0	9	1	6.45E-06
GO:0098793	presynapse	CC	53	0	19	1	7.41E-06
GO:0072509	divalent inorganic cation transmembrane transporter activity	MF	97	1	28	0.989696	7.85E-06
GO:0031224	intrinsic component of membrane	CC	4003	227	564	9.17E-05	7.86E-06
GO:0044815	DNA packaging complex	CC	48	11	3	8.39E-06	0.942418

GO:0019199	transmembrane receptor protein kinase activity	MF	68	0	22	1	9.91E-06

Table 6.4: Top-150 GO terms generated from the leptin-a rescue : control contrast to "Dr" Gene Ontologies.

BIBLIOGRAPHY

Angotzi, A.R., Stefansson, S.O., Nilsen, T.O., Øvrebø, J.I., Andersson, E., Taranger, G.L., Rønnestad, I., 2016. Identification of a novel leptin receptor duplicate in Atlantic salmon: Expression analyses in different life stages and in response to feeding status. Gen. Comp. Endocrinol. 235, 108–119.

Angotzi, A.R., Stefansson, S.O., Nilsen, T.O., Rathore, R.M., Rønnestad, I., 2013. Molecular cloning and genomic characterization of novel leptin-like genes in salmonids provide new insight into the evolution of the Leptin gene family. Gen. Comp. Endocrinol. 187, 48–59.

Antczak, M., Van Blerkom, J., 1997. Oocyte influences on early development: the regulatory proteins leptin and STAT3 are polarized in mouse and human oocytes and differentially distributed within the cells of the preimplantation stage embryo. Mol. Hum. Reprod. 3, 1067–1086.

Antonell, A., Lladó, A., Altirriba, J., Botta-Orfila, T., Balasa, M., Fernández, M., Ferrer, I., Sánchez-Valle, R., Molinuevo, J.L., 2013. A preliminary study of the whole-genome expression profile of sporadic and monogenic early-onset Alzheimer's disease. Neurobiol. Aging 34, 1772–1778.

Artavanis-Tsakonas, S., Rand, M.D., Lake, R.J., 1999. Notch signaling: cell fate control and signal integration in development. Science 284, 770–776.

Ashburner, M., Ball, C.A., Blake, J.A., Botstein, D., Butler, H., Cherry, J.M., Davis, A.P., Dolinski, K., Dwight, S.S., Eppig, J.T., 2000. Gene Ontology: tool for the unification of biology. Nat. Genet. 25, 25–29.

Bagci, E., Heijlen, M., Vergauwen, L., Hagenaars, A., Houbrechts, A.M., Esguerra, C.V., Blust, R., Darras, V.M., Knapen, D., 2015. Deiodinase knockdown during early

zebrafish development affects growth, development, energy metabolism, motility and phototransduction. PloS One 10, e0123285.

Bahrenberg, G., Behrmann, I., Barthel, A., Hekerman, P., Heinrich, P.C., Joost, H.-G., Becker, W., 2002. Identification of the critical sequence elements in the cytoplasmic domain of leptin receptor isoforms required for Janus kinase/signal transducer and activator of transcription activation by receptor heterodimers. Mol. Endocrinol. 16, 859–872.

Barbazuk, W.B., Korf, I., Kadavi, C., Heyen, J., Tate, S., Wun, E., Bedell, J.A., McPherson, J.D., Johnson, S.L., 2000. The syntenic relationship of the zebrafish and human genomes. Genome Res. 10, 1351–1358.

Battle, M., Gillespie, C., Quarshie, A., Lanier, V., Harmon, T., Wilson, K., Torroella-Kouri, M., Gonzalez-Perez, R.R., 2014. Obesity induced a leptin-Notch signaling axis in breast cancer. Int. J. Cancer 134, 1605–1616.

Baumann, H., Morella, K.K., White, D.W., Dembski, M., Bailon, P.S., Kim, H., Lai, C.F., Tartaglia, L.A., 1996. The full-length leptin receptor has signaling capabilities of interleukin 6-type cytokine receptors. Proc. Natl. Acad. Sci. 93, 8374–8378.

Bazan, J.F., 1990. Structural design and molecular evolution of a cytokine receptor superfamily. Proc. Natl. Acad. Sci. 87, 6934–6938.

Benjamini, Y., Hochberg, Y., 1995. Controlling the false discovery rate: a practical and powerful approach to multiple testing. J. R. Stat. Soc. Ser. B Methodol. 289–300.

Bjørbæk, C., Uotani, S., da Silva, B., Flier, J.S., 1997. Divergent signaling capacities of the long and short isoforms of the leptin receptor. J. Biol. Chem. 272, 32686–32695.

Bolstad, B.M., Irizarry, R.A., Åstrand, M., Speed, T.P., 2003. A comparison of normalization methods for high density oligonucleotide array data based on variance and bias. Bioinformatics 19, 185–193.

Boulay, J.-L., O'shea, J.J., Paul, W.E., 2003. Molecular phylogeny within type I cytokines and their cognate receptors. Immunity 19, 159–163.

Bradford, Y., Conlin, T., Dunn, N., Fashena, D., Frazer, K., Howe, D.G., Knight, J., Mani, P., Martin, R., Moxon, S.A., 2011. ZFIN: enhancements and updates to the Zebrafish Model Organism Database. Nucleic Acids Res. 39, D822–D829.

Brazma, A., Hingamp, P., Quackenbush, J., Sherlock, G., Spellman, P., Stoeckert, C., Aach, J., Ansorge, W., Ball, C.A., Causton, H.C., 2001. Minimum information about a microarray experiment (MIAME)—toward standards for microarray data. Nat. Genet. 29, 365–371.

Burden, C.J., 2008. Understanding the physics of oligonucleotide microarrays: the Affymetrix spike-in data reanalysed. Phys. Biol. 5, 016004.

Campfield, L.A., Smith, F.J., Guisez, Y., Devos, R., Burn, P., 1995. Recombinant mouse OB protein: evidence for a peripheral signal linking adiposity and central neural networks. Science 269, 546.

Carlson, M., 2016. org.Dr.eg.db: Genome wide annotation for Zebrafish. R Package V 3.3.0.

Carpenter, B., Hemsworth, G.R., Wu, Z., Maamra, M., Strasburger, C.J., Ross, R.J., Artymiuk, P.J., 2012. Structure of the human obesity receptor leptin-binding domain reveals the mechanism of leptin antagonism by a monoclonal antibody. Structure 20, 487–497.

Carvalho, B.S., 2015. pd.zebgene.1.1.st: Platform Design Info for Affymetrix ZebGene-1_1-st. R Package Version 3120.

Carvalho, B.S., Irizarry, R.A., 2010. A framework for oligonucleotide microarray preprocessing. Bioinformatics 26, 2363–2367.

Cervero, A., Domínguez, F., Horcajadas, J.A., Quiñonero, A., Pellicer, A., Simón, C., 2006. The role of the leptin in reproduction. Curr. Opin. Obstet. Gynecol. 18, 297–303.

Chen, H., Charlat, O., Tartaglia, L.A., Woolf, E.A., Weng, X., Ellis, S.J., Lakey, N.D., Culpepper, J., More, K.J., Breitbart, R.E., 1996. Evidence that the diabetes gene

encodes the leptin receptor: identification of a mutation in the leptin receptor gene in db/db mice. Cell 84, 491–495.

Chisada, S., Kurokawa, T., Murashita, K., Rønnestad, I., Taniguchi, Y., Toyoda, A., Sakaki, Y., Takeda, S., Yoshiura, Y., 2014. Leptin receptor-deficient (knockout) medaka, *Oryzias latipes*, show chronical up-regulated levels of orexigenic neuropeptides, elevated food intake and stage specific effects on growth and fat allocation. Gen. Comp. Endocrinol. 195, 9–20.

Chu, D.L.H., Li, V.W.T., Yu, R.M.K., 2010. Leptin: clue to poor appetite in oxygen-starved fish. Mol. Cell. Endocrinol. 319, 143–146.

Chua Jr, S.C., Chung, W.K., Wu-Peng, S., Zhang, Y., 1996. Phenotypes of mouse diabetes and rat fatty due to mutations in the OB (leptin) receptor. Science 271, 994.

Chung, W.K., Belfi, K., Chua, M., Wiley, J., Mackintosh, R., Nicolson, M., Boozer, C.N., Leibel, R.L., 1998. Heterozygosity for Lep ob or Lepr db affects body composition and leptin homeostasis in adult mice. Am. J. Physiol.-Regul. Integr. Comp. Physiol. 274, R985–R990.

Cioffi, J.A., Van Blerkom, J., Antczak, M., Shafer, A., Wittmer, S., Snodgrass, H.R., 1997. The expression of leptin and its receptors in pre-ovulatory human follicles. Mol. Hum. Reprod. 3, 467–472.

Clement, K., Vaisse, C., Lahlou, N., Cabrol, S., Pelloux, V., Cassuto, D., Gourmelen, M., Dina, C., Chambaz, J., Lacorte, J.-M., 1998. A mutation in the human leptin receptor gene causes obesity and pituitary dysfunction. Nature 392, 398–401.

Cohen, P., Zhao, C., Cai, X., Montez, J.M., Rohani, S.C., Feinstein, P., Mombaerts, P., Friedman, J.M., 2001. Selective deletion of leptin receptor in neurons leads to obesity. J. Clin. Invest. 108, 1113–1121.

Coleman, D.L., 1978. Obese and diabetes: two mutant genes causing diabetes-obesity syndromes in mice. Diabetologia 14, 141–148.

Coleman, D.L., 1973. Effects of parabiosis of obese with diabetes and normal mice. Diabetologia 9, 294–298.

Considine, R.V., Sinha, M.K., Heiman, M.L., Kriauciunas, A., Stephens, T.W., Nyce, M.R., Ohannesian, J.P., Marco, C.C., McKee, L.J., Bauer, T.L., 1996. Serum immunoreactive-leptin concentrations in normal-weight and obese humans. N. Engl. J. Med. 334, 292–295.

Consoli, L., Lefevre, A., Zivy, M., De Vienne, D., Damerval, C., 2002. QTL analysis of proteome and transcriptome variations for dissecting the genetic architecture of complex traits in maize. Plant Mol. Biol. 48, 575–581.

Copeland, D.L., Duff, R.J., Liu, Q., Prokop, J., Londraville, R.L., 2011. Leptin in teleost fishes: an argument for comparative study. Front. Physiol. 2, 26.

Crespi, E.J., Denver, R.J., 2006. Leptin (ob gene) of the South African clawed frog *Xenopus laevis*. Proc. Natl. Acad. Sci. 103, 10092–10097.

Dalman, M.R., Liu, Q., King, M.D., Bagatto, B., Londraville, R.L., 2013. Leptin expression affects metabolic rate in zebrafish embryos (*D. rerio*). Front. Physiol. 4, 160.

Danilova, N., Sakamoto, K.M., Lin, S., 2008. Ribosomal protein S19 deficiency in zebrafish leads to developmental abnormalities and defective erythropoiesis through activation of p53 protein family. Blood 112, 5228–5237.

Darnell Jr, J.E., Kerr, I.M., Stark, G.R., 1994. Jak-STAT pathways and transcriptional activation in response to IFNs and other extracellular signaling proteins. Sci.-AAAS-Wkly. Pap. Ed.- Guide Sci. Inf. 264, 1415–1420.

De Rosa, V., Procaccini, C., Calì, G., Pirozzi, G., Fontana, S., Zappacosta, S., La Cava, A., Matarese, G., 2007. A key role of leptin in the control of regulatory T cell proliferation. Immunity 26, 241–255.

Devos, R., Guisez, Y., Van der Heyden, J., White, D.W., Kalai, M., Fountoulakis, M., Plaetinck, G., 1997. Ligand-independent dimerization of the extracellular domain

of the leptin receptor and determination of the stoichiometry of leptin binding. J. Biol. Chem. 272, 18304–18310.

Eberlé, D., Hegarty, B., Bossard, P., Ferré, P., Foufelle, F., 2004. SREBP transcription factors: master regulators of lipid homeostasis. Biochimie 86, 839–848.

Elias, C.F., Purohit, D., 2013. Leptin signaling and circuits in puberty and fertility. Cell. Mol. Life Sci. 70, 841–862.

Elmquist, J.K., Bjørbæk, C., Ahima, R.S., Flier, J.S., Saper, C.B., 1998. Distributions of leptin receptor mRNA isoforms in the rat brain. J. Comp. Neurol. 395, 535–547.

Farooqi, I.S., Jebb, S.A., Langmack, G., Lawrence, E., Cheetham, C.H., Prentice, A.M., Hughes, I.A., McCamish, M.A., O'rahilly, S., 1999. Effects of recombinant leptin therapy in a child with congenital leptin deficiency. N. Engl. J. Med. 341, 879–884.

Farooqi, I.S., Matarese, G., Lord, G.M., Keogh, J.M., Lawrence, E., Agwu, C., Sanna, V., Jebb, S.A., Perna, F., Fontana, S., 2002. Beneficial effects of leptin on obesity, T cell hyporesponsiveness, and neuroendocrine/metabolic dysfunction of human congenital leptin deficiency. J. Clin. Invest. 110, 1093–1103.

Farooqi, I.S., Wangensteen, T., Collins, S., Kimber, W., Matarese, G., Keogh, J.M., Lank, E., Bottomley, B., Lopez-Fernandez, J., Ferraz-Amaro, I., 2007. Clinical and molecular genetic spectrum of congenital deficiency of the leptin receptor. N. Engl. J. Med. 356, 237–247.

Gardner, R.L., 1997. The early blastocyst is bilaterally symmetrical and its axis of symmetry is aligned with the animal-vegetal axis of the zygote in the mouse. Development 124, 289–301.

Gentleman, R.C., Carey, V.J., Bates, D.M., Bolstad, B., Dettling, M., Dudoit, S., Ellis, B., Gautier, L., Ge, Y., Gentry, J., 2004. Bioconductor: open software development for computational biology and bioinformatics. Genome Biol. 5, R80.

Ghilardi, N., Ziegler, S., Wiestner, A., Stoffel, R., Heim, M.H., Skoda, R.C., 1996. Defective STAT signaling by the leptin receptor in diabetic mice. Proc. Natl. Acad. Sci. 93, 6231–6235.

Gibson, W.T., Farooqi, I.S., Moreau, M., DePaoli, A.M., Lawrence, E., O'rahilly, S., Trussell, R.A., 2004. Congenital leptin deficiency due to homozygosity for the Δ133G mutation: report of another case and evaluation of response to four years of leptin therapy. J. Clin. Endocrinol. Metab. 89, 4821–4826.

Gong, Y., Ishida-Takahashi, R., Villanueva, E.C., Fingar, D.C., Münzberg, H., Myers, M.G., 2007. The long form of the leptin receptor regulates STAT5 and ribosomal protein S6 via alternate mechanisms. J. Biol. Chem. 282, 31019–31027.

Gorissen, M., Bernier, N.J., Nabuurs, S.B., Flik, G., Huising, M.O., 2009. Two divergent leptin paralogues in zebrafish (*Danio rerio*) that originate early in teleostean evolution. J. Endocrinol. 201, 329–339.

Haakansson, M.-L., Meister, B. rn, 1998. Transcription factor STAT3 in leptin target neurons of the rat hypothalamus. Neuroendocrinology 68, 420–427.

Håkansson, M.-L., Brown, H., Ghilardi, N., Skoda, R.C., Meister, B., 1998. Leptin receptor immunoreactivity in chemically defined target neurons of the hypothalamus. J. Neurosci. 18, 559–572.

Halaas, J.L., Gajiwala, K.S., Maffei, M., Cohen, S.L., 1995. Weight-reducing effects of the plasma protein encoded by the obese gene. Science 269, 543.

Hasenkrug, K.J., 2007. The leptin connection: regulatory T cells and autoimmunity. Immunity 26, 143–145.

Heasman, J., Kofron, M., Wylie, C., 2000. βCatenin Signaling Activity Dissected in the Early *Xenopus* Embryo: A Novel Antisense Approach. Dev. Biol. 222, 124–134.

Heymsfield, S.B., Greenberg, A.S., Fujioka, K., Dixon, R.M., Kushner, R., Hunt, T., Lubina, J.A., Patane, J., Self, B., Hunt, P., 1999. Recombinant leptin for weight loss in

obese and lean adults: a randomized, controlled, dose-escalation trial. Jama 282, 1568–1575.

Hill, J.W., Elias, C.F., Fukuda, M., Williams, K.W., Berglund, E.D., Holland, W.L., Cho, Y.-R., Chuang, J.-C., Xu, Y., Choi, M., 2010. Direct insulin and leptin action on pro-opiomelanocortin neurons is required for normal glucose homeostasis and fertility. Cell Metab. 11, 286–297.

Howe, K., Clark, M.D., Torroja, C.F., Torrance, J., Berthelot, C., Muffato, M., Collins, J.E., Humphray, S., McLaren, K., Matthews, L., 2013. The zebrafish reference genome sequence and its relationship to the human genome. Nature 496, 498–503.

Hu, Y., Smyth, G.K., 2009. ELDA: extreme limiting dilution analysis for comparing depleted and enriched populations in stem cell and other assays. J. Immunol. Methods 347, 70–78.

Huising, M.O., Geven, E.J., Kruiswijk, C.P., Nabuurs, S.B., Stolte, E.H., Spanings, F.T., Verburg-van Kemenade, B.L., Flik, G., 2006. Increased leptin expression in common carp (*Cyprinus carpio*) after food intake but not after fasting or feeding to satiation. Endocrinology 147, 5786–5797.

Irizarry, R.A., Bolstad, B.M., Collin, F., Cope, L.M., Hobbs, B., Speed, T.P., 2003a. Summaries of Affymetrix GeneChip probe level data. Nucleic Acids Res. 31, e15–e15.

Irizarry, R.A., Hobbs, B., Collin, F., Beazer-Barclay, Y.D., Antonellis, K.J., Scherf, U., Speed, T.P., 2003b. Exploration, normalization, and summaries of high density oligonucleotide array probe level data. Biostatistics 4, 249–264.

Irizarry, R.A., Wu, Z., Jaffee, H.A., 2005. Comparison of Affymetrix GeneChip expression measures.

Ishikawa, M., Kitayama, J., Nagawa, H., 2006. Expression pattern of leptin and leptin receptor (OB-R) in human gastric cancer. World J. Gastroenterol. 12, 5517.

Ishikawa, M., Kitayama, J., Nagawa, H., 2004. Enhanced expression of leptin and leptin receptor (OB-R) in human breast cancer. Clin. Cancer Res. 10, 4325–4331.

Israel, D.D., Sheffer-Babila, S., De Luca, C., Jo, Y.-H., Liu, S.M., Xia, Q., Spergel, D.J., Dun, S.L., Dun, N.J., Chua Jr, S.C., 2012. Effects of leptin and melanocortin signaling interactions on pubertal development and reproduction. Endocrinology 153, 2408–2419.

Jaillon, O., Aury, J.-M., Brunet, F., Petit, J.-L., Stange-Thomann, N., Mauceli, E., Bouneau, L., Fischer, C., Ozouf-Costaz, C., Bernot, A., 2004. Genome duplication in the teleost fish *Tetraodon nigroviridis* reveals the early vertebrate proto-karyotype. Nature 431, 946–957.

Johnson, R.M., Johnson, T.M., Londraville, R.L., 2000. Evidence for leptin expression in fishes. J. Exp. Zool. 286, 718.

Kielar, D., Clark, J.S.C., Ciechanowicz, A., Kurzawski, G., Sulikowski, T., Naruszewicz, M., 1998. Leptin receptor isoforms expressed in human adipose tissue. Metabolism 47, 844–847.

Kimmel, C.B., Ballard, W.W., Kimmel, S.R., Ullmann, B., Schilling, T.F., 1995. Stages of embryonic development of the zebrafish. Dev. Dyn. 203, 253–310.

Kloosterman, W.P., Lagendijk, A.K., Ketting, R.F., Moulton, J.D., Plasterk, R.H., 2007. Targeted inhibition of miRNA maturation with morpholinos reveals a role for miR-375 in pancreatic islet development. PLoS Biol 5, e203.

Koff, A., Ohtsuki, M., Polynak, K., Roberts, J.M., Massague, J., 1993. Negative regulation of G1 in mammalian cells: inhibition of cyclin E-dependent kinase by TGF-beta. Science 260, 536–540.

Kok, F.O., Shin, M., Ni, C.-W., Gupta, A., Grosse, A.S., van Impel, A., Kirchmaier, B.C., Peterson-Maduro, J., Kourkoulis, G., Male, I., 2015. Reverse genetic screening reveals poor correlation between morpholino-induced and mutant phenotypes in zebrafish. Dev. Cell 32, 97–108.

Kurokawa, T., Murashita, K., 2009. Genomic characterization of multiple leptin genes and a leptin receptor gene in the Japanese medaka, *Oryzias latipes*. Gen. Comp. Endocrinol. 161, 229–237.

Kurokawa, T., Uji, S., Suzuki, T., 2005. Identification of cDNA coding for a homologue to mammalian leptin from pufferfish, *Takifugu rubripes*. Peptides 26, 745–750.

Kwon, H.-J., 2016. Vitamin D receptor signaling is required for heart development in zebrafish embryo. Biochem. Biophys. Res. Commun. 470, 575–578.

La Cava, A., Alviggi, C., Matarese, G., 2004. Unraveling the multiple roles of leptin in inflammation and autoimmunity. J. Mol. Med. 82, 4–11.

Lahlou, N., Clement, K., Carel, J.-C., Vaisse, C., Lotton, C., Le Bihan, Y., Basdevant, A., Lebouc, Y., Froguel, P., Roger, M., 2000. Soluble leptin receptor in serum of subjects with complete resistance to leptin: relation to fat mass. Diabetes 49, 1347–1352.

Lawson, N.D., 2016. Reverse genetics in zebrafish: mutants, morphants, and moving forward. Trends Cell Biol. 26, 77–79.

Lee, G.-H., Proenca, R., Montez, J.M., Carroll, K.M., 1996. Abnormal splicing of the leptin receptor in diabetic mice. Nature 379, 632.

Leung, Y.F., Ma, P., Link, B.A., Dowling, J.E., 2008. Factorial microarray analysis of zebrafish retinal development. Proc. Natl. Acad. Sci. 105, 12909–12914.

Licinio, J., Caglayan, S., Ozata, M., Yildiz, B.O., De Miranda, P.B., O'Kirwan, F., Whitby, R., Liang, L., Cohen, P., Bhasin, S., 2004. Phenotypic effects of leptin replacement on morbid obesity, diabetes mellitus, hypogonadism, and behavior in leptin-deficient adults. Proc. Natl. Acad. Sci. U. S. A. 101, 4531–4536.

Liongue, C., Ward, A.C., 2007. Evolution of class I cytokine receptors. BMC Evol. Biol. 7, 120.

Liu, Q., Chen, Y., Copeland, D., Ball, H., Duff, R.J., Rockich, B., Londraville, R.L., 2010. Expression of leptin receptor gene in developing and adult zebrafish. Gen. Comp. Endocrinol. 166, 346–355.

Liu, Q., Dalman, M., Chen, Y., Akhter, M., Brahmandam, S., Patel, Y., Lowe, J., Thakkar, M., Gregory, A.-V., Phelps, D., 2012. Knockdown of leptin A expression dramatically alters zebrafish development. Gen. Comp. Endocrinol. 178, 562–572.

Lord, G.M., Matarese, G., Howard, J.K., Baker, R.J., Bloom, S.R., Lechler, R.I., 1998. Leptin modulates the T-cell immune response and reverses starvation-induced immunosuppression. Nature 394, 897–901.

Lorent, K., Yeo, S.-Y., Oda, T., Chandrasekharappa, S., Chitnis, A., Matthews, R.P., Pack, M., 2004. Inhibition of Jagged-mediated Notch signaling disrupts zebrafish biliary development and generates multi-organ defects compatible with an Alagille syndrome phenocopy. Development 131, 5753–5766.

MacDonald, J.W., 2008. Affycoretools: Functions useful for those doing repetitive analyses with Affymetrix GeneChips. R Package Version 1.

Maffei, M., Halaas, J., Ravussin, E., Pratley, R.E., Lee, G.H., Zhang, Y., Fei, H., Kim, S., Lallone, R., Ranganathan, S., 1995. Leptin levels in human and rodent: measurement of plasma leptin and ob RNA in obese and weight-reduced subjects. Nat. Med. 1, 1155–1161.

Malendowicz, L.K., Rucinski, M., Belloni, A.S., Ziolkowska, A., Nussdorfer, G.G., 2007. Leptin and the regulation of the hypothalamic–pituitary–adrenal axis. Int. Rev. Cytol. 263, 63–102.

Michel, M., Page-McCaw, P.S., Chen, W., Cone, R.D., 2016. Leptin signaling regulates glucose homeostasis, but not adipostasis, in the zebrafish. Proc. Natl. Acad. Sci. 201513212.

Minokoshi, Y., Kim, Y.-B., Peroni, O.D., Fryer, L.G., Müller, C., Carling, D., Kahn, B.B., 2002. Leptin stimulates fatty-acid oxidation by activating AMP-activated protein kinase. Nature 415, 339–343.

Montague, C.T., Farooqi, I.S., Whitehead, J.P., Soos, M.A., 1997. Congenital leptin deficiency is associated with severe early-onset obesity in humans. Nature 387, 903.

Münzberg, H., Flier, J.S., Bjørbæk, C., 2004. Region-specific leptin resistance within the hypothalamus of diet-induced obese mice. Endocrinology 145, 4880–4889.

Murtaugh, L.C., Stanger, B.Z., Kwan, K.M., Melton, D.A., 2003. Notch signaling controls multiple steps of pancreatic differentiation. Proc. Natl. Acad. Sci. 100, 14920–14925.

Nasevicius, A., Ekker, S.C., 2000. Effective targeted gene “knockdown”in zebrafish. Nat. Genet. 26, 216–220.

Newman, M., Verdile, G., Martins, R.N., Lardelli, M., 2011. Zebrafish as a tool in Alzheimer’s disease research. Biochim. Biophys. Acta BBA-Mol. Basis Dis. 1812, 346–352.

Oetjen, E., Lemcke, T., 2016. Dual leucine zipper kinase (MAP3K12) modulators: a patent review (2010–2015). Expert Opin. Ther. Pat. 26, 607–616.

Ogata, H., Goto, S., Sato, K., Fujibuchi, W., Bono, H., Kanehisa, M., 1999. KEGG: Kyoto encyclopedia of genes and genomes. Nucleic Acids Res. 27, 29–34.

Padanad, M.S., Riley, B.B., 2011. Pax2/8 proteins coordinate sequential induction of otic and epibranchial placodes through differential regulation of foxi1, sox3 and fgf24. Dev. Biol. 351, 90–98.

Pages, H., Aboyoun, P., Gentleman, R., DebRoy, S., 2009. String objects representing biological sequences, and matching algorithms. R Package Version 2.

Pages, H., Carlson, M., Falcon, S., Li, N.A., AnnotationDbi, P.R.S., SQLForge, P.R.S., 2008. Annotation Database Interface. R Package Version 1.

Paolucci, M., Rocco, M., Varricchio, E., 2001. Leptin presence in plasma, liver and fat bodies in the lizard *Podarcis sicula*: fluctuations throughout the reproductive cycle. Life Sci. 69, 2399–2408.

Peelman, F., Iserentant, H., De Smet, A.-S., Vandekerckhove, J., Zabeau, L., Tavernier, J., 2006. Mapping of binding site III in the leptin receptor and modeling of a hexameric leptin· leptin receptor complex. J. Biol. Chem. 281, 15496–15504.

Pelleymounter, M.A., Cullen, M.J., Baker, M.B., Hecht, R., 1995. Effects of the obese gene product on body weight regulation in ob/ob mice. Science 269, 540.

Pérez, C., Fernández-Galaz, C., Fernández-Agulló, T., Arribas, C., Andrés, A., Ros, M., Carrascosa, J.M., 2004. Leptin impairs insulin signaling in rat adipocytes. Diabetes 53, 347–353.

Pfaffl, M.W., 2001. A new mathematical model for relative quantification in real-time RT–PCR. Nucleic Acids Res. 29, e45–e45.

Pfundt, B., Sauerwein, H., Mielenz, M., 2009. Leptin mRNA and protein immunoreactivity in adipose tissue and liver of rainbow trout (*Oncorhynchus mykiss*) and immunohistochemical localization in liver. Anat. Histol. Embryol. 38, 406–410.

Pham, V.N., Lawson, N.D., Mugford, J.W., Dye, L., Castranova, D., Lo, B., Weinstein, B.M., 2007. Combinatorial function of ETS transcription factors in the developing vasculature. Dev. Biol. 303, 772–783.

Pinto, C.L., Kalasekar, S.M., McCollum, C.W., Riu, A., Jonsson, P., Lopez, J., Swindell, E.C., Bouhlatouf, A., Balaguer, P., Bondesson, M., 2016. Lxr regulates lipid metabolic and visual perception pathways during zebrafish development. Mol. Cell. Endocrinol. 419, 29–43.

Pollack, J.R., Sørlie, T., Perou, C.M., Rees, C.A., Jeffrey, S.S., Lonning, P.E., Tibshirani, R., Botstein, D., Børresen-Dale, A.-L., Brown, P.O., 2002. Microarray analysis reveals

a major direct role of DNA copy number alteration in the transcriptional program of human breast tumors. Proc. Natl. Acad. Sci. 99, 12963–12968.

Prokop, J.W., Duff, R.J., Ball, H.C., Copeland, D.L., Londraville, R.L., 2012. Leptin and leptin receptor: analysis of a structure to function relationship in interaction and evolution from humans to fish. Peptides 38, 326–336.

Prokop, J.W., Schmidt, C., Gasper, D., Duff, R.J., Milsted, A., Ohkubo, T., Ball, H.C., Shawkey, M.D., Mays Jr, H.L., Cogburn, L.A., 2014. Discovery of the elusive leptin in birds: identification of several “missing links” in the evolution of leptin and its receptor. PloS One 9, e92751.

Rai, K., Chidester, S., Zavala, C.V., Manos, E.J., James, S.R., Karpf, A.R., Jones, D.A., Cairns, B.R., 2007. Dnmt2 functions in the cytoplasm to promote liver, brain, and retina development in zebrafish. Genes Dev. 21, 261–266.

Rau, H., Reaves, B.J., O’rahilly, S., Whitehead, J.P., 1999. Truncated Human Leptin (Δ133) Associated with Extreme Obesity Undergoes Proteasomal Degradation after Defective Intracellular Transport 1. Endocrinology 140, 1718–1723.

Rays, M., Chen, Y., Su, Y.A., 1996. Use of a cDNA microarray to analyse gene expression patterns in human cancer. Nat. Genet. 14.

Rhodes, D.R., Yu, J., Shanker, K., Deshpande, N., Varambally, R., Ghosh, D., Barrette, T., Pander, A., Chinnaiyan, A.M., 2004. ONCOMINE: a cancer microarray database and integrated data-mining platform. Neoplasia 6, 1–6.

Ritchie, M.E., Phipson, B., Wu, D., Hu, Y., Law, C.W., Shi, W., Smyth, G.K., 2015. limma powers differential expression analyses for RNA-sequencing and microarray studies. Nucleic Acids Res. gkv007.

Robu, M.E., Larson, J.D., Nasevicius, A., Beiraghi, S., Brenner, C., Farber, S.A., Ekker, S.C., 2007. p53 activation by knockdown technologies. PLoS Genet 3, e78.

Rønnestad, I., Nilsen, T.O., Murashita, K., Angotzi, A.R., Moen, A.-G.G., Stefansson, S.O., Kling, P., Björnsson, B.T., Kurokawa, T., 2010. Leptin and leptin receptor genes in

Atlantic salmon: cloning, phylogeny, tissue distribution and expression correlated to long-term feeding status. Gen. Comp. Endocrinol. 168, 55–70.

Rozwarski, D.A., Diederichs, K., Hecht, R., Boone, T., Karplus, P.A., 1996. Refined crystal structure and mutagenesis of human granulocyte-macrophage colony-stimulating factor. PROTEINS Struct. Funct. Genet. 26, 304–313.

Savan, R., Sakai, M., 2006. Genomics of fish cytokines. Comp. Biochem. Physiol. Part D Genomics Proteomics 1, 89–101.

Schena, M., Shalon, D., Davis, R.W., Brown, P.O., 1995. Quantitative monitoring of gene expression patterns with a complementary DNA microarray. Science 270, 467.

Schena, M., Shalon, D., Heller, R., Chai, A., Brown, P.O., Davis, R.W., 1996. Parallel human genome analysis: microarray-based expression monitoring of 1000 genes. Proc. Natl. Acad. Sci. 93, 10614–10619.

Schulz, L.C., Widmaier, E.P., 2006. Leptin receptors, in: Leptin. Springer, pp. 11–31.

Seth, A., Stemple, D.L., Barroso, I., 2013. The emerging use of zebrafish to model metabolic disease. Dis. Model. Mech. 6, 1080–1088.

Smyth, G., McCarthy, D., n.d. Empirical Bayes Statistics for Differential Expression.

Smyth, G.K., 2004. Linear models and empirical bayes methods for assessing differential expression in microarray experiments. Stat Appl Genet Mol Biol 3, 3.

Stainier, D.Y., Kontarakis, Z., Rossi, A., 2015. Making sense of anti-sense data. Dev. Cell 32, 7–8.

Strobel, A., Issad, T., Camoin, L., Ozata, M., Strosberg, A.D., 1998. A leptin missense mutation associated with hypogonadism and morbid obesity. Nat. Genet. 18, 213–215.

Stylianou, S., Clarke, R.B., Brennan, K., 2006. Aberrant activation of notch signaling in human breast cancer. Cancer Res. 66, 1517–1525.

Subramanian, A., Tamayo, P., Mootha, V.K., Mukherjee, S., Ebert, B.L., Gillette, M.A., Paulovich, A., Pomeroy, S.L., Golub, T.R., Lander, E.S., 2005. Gene set enrichment analysis: a knowledge-based approach for interpreting genome-wide expression profiles. Proc. Natl. Acad. Sci. 102, 15545–15550.

Summerton, J., 1999. Morpholino antisense oligomers: the case for an RNase H-independent structural type. Biochim. Biophys. Acta BBA-Gene Struct. Expr. 1489, 141–158.

Summerton, J., WELLER, D., 1997. Morpholino antisense oligomers: design, preparation, and properties. Antisense Nucleic Acid Drug Dev. 7, 187–195.

Summerton, J.E., 2007. Morpholino, siRNA, and S-DNA compared: impact of structure and mechanism of action on off-target effects and sequence specificity. Curr. Top. Med. Chem. 7, 651–660.

Swerdloff, R.S., Batt, R.A., Bray, G.A., 1976. Reproductive hormonal function in the genetically obese (ob/ob) mouse. Endocrinology 98, 1359–1364.

Takahashi, Y., Okimura, Y., Mizuno, I., Iida, K., Takahashi, T., Kaji, H., Abe, H., Chihara, K., 1997. Leptin induces mitogen-activated protein kinase-dependent proliferation of C3H10T1/2 cells. J. Biol. Chem. 272, 12897–12900.

Tang, Y., Yu, J., Li, H., Xu, P., Li, J., Ren, H., 2013. Molecular cloning, characterization and expression analysis of multiple leptin genes in Jian carp (*Cyprinus carpio* var. Jian). Comp. Biochem. Physiol. B Biochem. Mol. Biol. 166, 133–140.

Taouis, M., Chen, J.-W., Daviaud, C., Dupont, J., Derouet, M., Simon, J., 1998. Cloning the chicken leptin gene. Gene 208, 239–242.

Tartaglia, L.A., 1997. The leptin receptor. J. Biol. Chem. 272, 6093–6096.

Tartaglia, L.A., Dembski, M., Weng, X., Deng, N., Culpepper, J., Devos, R., Richards, G.J., Campfield, L.A., Clark, F.T., Deeds, J., 1995. Identification and expression cloning of a leptin receptor, OB-R. Cell 83, 1263–1271.

Team, R.C., 2014. R: A language and environment for statistical computing. R Foundation for Statistical Computing, Vienna, Austria. 2013.

Tessier, D.R., Ferraro, Z.M., Gruslin, A., 2013. Role of leptin in pregnancy: consequences of maternal obesity. Placenta 34, 205–211.

Tinoco, A.B., Nisembaum, L.G., Isorna, E., Delgado, M.J., de Pedro, N., 2012. Leptins and leptin receptor expression in the goldfish (*Carassius auratus*). Regulation by food intake and fasting/overfeeding conditions. Peptides 34, 329–335.

Tong, Q., Dalgin, G., Xu, H., Ting, C.-N., Leiden, J.M., Hotamisligil, G.S., 2000. Function of GATA transcription factors in preadipocyte-adipocyte transition. Science 290, 134–138.

Ulitsky, I., Shkumatava, A., Jan, C.H., Sive, H., Bartel, D.P., 2011. Conserved function of lincRNAs in vertebrate embryonic development despite rapid sequence evolution. Cell 147, 1537–1550.

Vaisse, C., Halaas, J.L., Horvath, C.M., Darnell, J.E., Stoffel, M., Friedman, J.M., 1996. Leptin activation of Stat3 in the hypothalamus of wild–type and ob/ob mice but not db/db mice. Nat. Genet. 14, 95–97.

Vegusdal, A., Sundvold, H., Gjøen, T., Ruyter, B., 2003. An in vitro method for studying the proliferation and differentiation of Atlantic salmon preadipocytes. Lipids 38, 289–296.

Vitorino, M., Jusuf, P.R., Maurus, D., Kimura, Y., Higashijima, S., Harris, W.A., 2009. Vsx2 in the zebrafish retina: restricted lineages through derepression. Neural Develop. 4, 14.

Wang, B., Charukeshi Chandrasekera, P., J Pippin, J., 2014. Leptin-and leptin receptor-deficient rodent models: relevance for human type 2 diabetes. Curr. Diabetes Rev. 10, 131–145.

Weinstein, J.N., Collisson, E.A., Mills, G.B., Shaw, K.R.M., Ozenberger, B.A., Ellrott, K., Shmulevich, I., Sander, C., Stuart, J.M., Network, C.G.A.R., 2013. The cancer genome atlas pan-cancer analysis project. Nat. Genet. 45, 1113–1120.

White, D.W., Kuropatwinski, K.K., Devos, R., Baumann, H., Tartaglia, L.A., 1997. Leptin receptor (OB-R) signaling Cytoplasmic domain mutational analysis and evidence for receptor homo-oligomerization. J. Biol. Chem. 272, 4065–4071.

Won, E.T., Baltzegar, D.A., Picha, M.E., Borski, R.J., 2012. Cloning and characterization of leptin in a Perciform fish, the striped bass (*Morone saxatilis*): Control of feeding and regulation by nutritional state. Gen. Comp. Endocrinol. 178, 98–107.

Wrann, C.D., Eguchi, J., Bozec, A., Xu, Z., Mikkelsen, T., Gimble, J., Nave, H., Wagner, E.F., Ong, S.-E., Rosen, E.D., 2012. FOSL2 promotes leptin gene expression in human and mouse adipocytes. J. Clin. Invest. 122.

Wu, Z., Irizarry, R.A., 2004. Preprocessing of oligonucleotide array data. Nat. Biotechnol. 22, 656–658.

Yang, W.-H., Liu, S.-C., Tsai, C.-H., Fong, Y.-C., Wang, S.-J., Chang, Y.-S., Tang, C.-H., 2013. Leptin induces IL-6 expression through OBRl receptor signaling pathway in human synovial fibroblasts. PloS One 8, e75551.

Yang, Y.-J., Cao, Y.-J., Bo, S.-M., Peng, S., Liu, W.-M., Duan, E.-K., 2006. Leptin-directed embryo implantation: leptin regulates adhesion and outgrowth of mouse blastocysts and receptivity of endometrial epithelial cells. Anim. Reprod. Sci. 92, 155–167.

Zhang, F., Basinski, M.B., Beals, J.M., Briggs, S.L., 1997. Crystal structure of the obese protein leptin-E100. Nature 387, 206.

Zhang, F., Chen, Y., Heiman, M., DiMarchi, R., 2005. Leptin: structure, function and biology. Vitam. Horm. 71, 345–372.

Zhang, Huixian, Chen, H., Zhang, Y., Li, S., Lu, D., Zhang, Haifa, Meng, Z., Liu, X., Lin, H., 2013. Molecular cloning, characterization and expression profiles of multiple

leptin genes and a leptin receptor gene in orange-spotted grouper (*Epinephelus coioides*). Gen. Comp. Endocrinol. 181, 295–305.

Zhang, Y., Proenca, R., Maffei, M., Barone, M., Leopold, L., Friedman, J.M., 1994. Positional cloning of the mouse obese gene and its human homologue. Nature 372, 425.

Zhao, Y., Sun, R., You, L., Gao, C., Tian, Z., 2003. Expression of leptin receptors and response to leptin stimulation of human natural killer cell lines. Biochem. Biophys. Res. Commun. 300, 247–252.

Zhou, B.O., Yue, R., Murphy, M.M., Peyer, J.G., Morrison, S.J., 2014. Leptin-receptor-expressing mesenchymal stromal cells represent the main source of bone formed by adult bone marrow. Cell Stem Cell 15, 154–168.

Zhou, Y., Rui, L., 2013. Leptin signaling and leptin resistance. Front. Med. 7, 207–222.

Zou, C., Levine, E.M., 2012. Vsx2 controls eye organogenesis and retinal progenitor identity via homeodomain and non-homeodomain residues required for high affinity DNA binding. PLoS Genet 8, e1002924.